MODELLING AND CONTROL OF GRID CONNECTED SOLAR PHOTOVOLTAIC (SPV) SYSTEM

A DISSERTATION

submitted in partial fulfillment of the requirement for the degree of

Master of Technology

in

Electrical Engineering (Power Systems)

By

Ravi Nath Tripathi

(2k11/PSY/15)

Under the esteemed guidance of

Dr. Alka Singh

Electrical Engineering Department

Delhi Technological University

(Formerly Delhi College of Engineering)

Shahbad daulatpur, Bawana road

Delhi- 110042

Department of Electrical Engineering

Delhi Technological University

(Formerly Delhi College of Engineering)

CERTIFICATE

This is to certify that the project entitled, "**MODELLING AND CONTROL OF GRID CONNECTED SOLAR PHOTOVOLTAIC (SPV) SYSTEM**", submitted by **Mr. Ravi Nath Tripathi**, University Roll No. 2k11/PSY/15, student of Master of Technology (Power Systems) in Electrical Engineering department from Delhi Technological University (Formerly Delhi college of Engineering), is a dissertation work carried out by him under my guidance during session 2012-2013 towards the partial fulfillment of the requirements for the award of the degree of Master of Technology in Power system.

I wish him all the best in his endeavours.

Date: July 2013

Dr. ALKA SINGH
ASSOCIATE PROFESSOR,
Electrical Engineering Department
Delhi Technological University
Shahbad daulatpur, Bawana road
Delhi- 110042

ACKNOWLEDGEMENT

I would like to thank my honourable guide Dr. ALKA SINGH, Associate Professor, Department of Electrical Engineering, Delhi Technological University (formerly Delhi College of Engineering). It would have never been possible for me to take this project to completion without his innovative ideas and his relentless support, encouragement and patience. I consider myself fortunate to have had a chance to work under her supervision. In spite of his hectic schedule she was always approachable and took his time to discuss my problems and give his advice and encouragement.

I would also like to thank Dr. MADHUSUDHAN, Head of the Department, Electrical Engineering Department, Delhi Technological University (formerly Delhi College of Engineering) for providing better facilities and constant support.

I am also very thankful to the entire faculty and staff members of the electrical engineering department and Mr. Anil Butola (Lab assistant, Simulation Lab) for their help and cooperation.

I wish to thank all my fellow students Mr. Shankar Rao , Bhavna, Swati for their support throughout the project work.

I wish to thank Ph.D scholars Manoj Badoni, Arun Verma (IIT-D), Ramesh Singh and Amritesh Kumar, for the invaluable knowledge they imparted to me during course work.

Finally my greatest thank to my family and friends for their continuous support.

Date: July 2013

Ravi Nath Tripathi

Roll no. 2k11/PSY/15

M.tech (Power Systems)

DECLARATION

I, hereby declare that the work being presented in this Project Report entitled **"Modelling and Control of Grid Connected Solar Photovoltaic (SPV) System"** is an original piece of work and an authentic report of our own work carried out during the period of 4th Semester as a part of our major project. The data presented in this report was generated & collected from various sources during the above said period and is being utilized by us for the submission of our Major Project Report to complete the requirements of Master's Degree of Examination in Power System Engineering, as per Delhi Technological University curriculum.

ABSTRACT

The demand of energy is increasing rapidly year by year worldwide & the whole world is looking for the alternative source of energy. The most populous alternative source of energy is renewable energy. Among, various available renewable energy sources, solar photovoltaic (SPV) energy is considered to be most reliable, environment friendly, pollution free and it's unlimited amount of availability in nature. The solar energy is directly converted into electrical energy by solar cell/ module. The characteristics of PV depend upon irradiation and temperature. The temperature and the irradiation of the solar cell depend on the atmospheric conditions. Hence, it is essential to track the MPP in any conditions to assure that the maximum available power is obtained from the PV panel. In stand-alone mode PV can feed power to fixed loads & lower power rating loads only and the storage support is also required for stand-alone mode. The grid interconnected mode of PV operation offers infinite storage. When PV is interfaced to the grid power quality problems arises due to use of power electronic devices.

Solar PV is modelled using single diode electrical equivalent circuit of solar cell and the characteristics of PV module are generated. The different maximum power point tracking (MPPT) algorithm is studied. Incremental conductance and perturbation and observation (P&O) is modelled and implemented. The maximum power point (MPP) is obtained using MPPT and dc-dc boost converter. The complete evacuation of generated and tracked maximum power is need of the entire system to improve the efficiency.

The model of Solar PV system connected to the utility grid is modelled and simulated in MATLAB/Simulink environment. Solar PV system is controlled and synchronised to grid using synchronous reference frame theory (SRFT) algorithm and power balance theory (PBT) algorithm. To handle the power quality problems the system is run under unity power factor (UPF) and zero voltage regulation mode (ZVR). UPF is obtained on the ac mains/grid side for grid voltage and grid current and zero voltage regulation is obtained for the terminal voltage of point of common coupling (PCC) voltage.

TABLE OF CONTENTS

LIST OF FIGURES

LIST OF TABLES

ACRONYMS

SPVA	Solar Photovoltaic Array
DC	Direct Current
AC	Alternating current
FF	Fill Factor
MPT	Maximum Power Tracking
MPPT	Maximum Power Point Tracking
MPP	Maximum Power Point
P&O	Perturbation and Observation
IC	Incremental Conductance
RCC	Ripple Co-relation Control
NN	Neural Network
SRFT	Synchronous Reference Frame Theory
DER	Distributed Energy Resource
VSC	Voltage Source Converter
VSI	Voltage Source Inverter
CSI	Current Source Inverter
DG	Distributed Generation
PWM	Pulse Width Modulation
HCC	Hysteresis Current Control
IGBT	Insulated Gate Bipolar Transistor
IRPT	Instantaneous Real Power Theory
KVA	Kilo Volt Ampere
THD	Total Harmonic Distortion
SVPWM	Space Vector Pulse Width Modulation
UPF	Unity Power Factor
PCC	Point of Common Coupling
ZVR	Zero Voltage Regulation
PBT	Power Balance Theory
PI	Proportional Plus Integral
PLL	Phase Locked Loop
PF	Power Factor
PWM-VSI	Pulse Width Modulated Voltage Source Inverter

SPWM	Sinusoidal Pulse Width Modulation
SRF	Synchronous Reference Frame

CHAPTER 1

INTRODUCTION AND LITERATURE REVIEW

1.1 GENERAL:

Global warming problem is increasing day by day and will have serious scenario effects on the whole Universe (World) and also prices for crude oil is been increasing very rapidly. To handle the energy and power crisis situation in global market each country is focusing on alternate source of energy or Renewable Energy Sources**.** Renewable energy is the energy that comes from resources which are continually replenished such as sunlight, wind, rain, tides, waves and geothermal heat. Approximately 16% of global energy consumption comes is met renewable resources, with 10% of all energy from traditional biomass, and 3.4% from hydroelectricity. New renewable (small hydro, modern biomass, wind, solar, geothermal, and biofuels) account for another 3% and are growing very rapidly [1]. In this chapter solar energy generation in world, types of material used for solar cell is discussed and system brief literature survey is explained about grid connected solar photovoltaic (SPV) system.

1.2 SOLAR IN WORLD AND INDIA

In recent years generation of power through solar energy is been increased significantly over the world and especially in developing countries like India and China.

Top ten nations in the solar production (MWs) are given in the Table below [2-4]

COUNTRIES	**2011**	**2010**	**2009**	**2008**	**2007**
ITALY	9284	2326	712	338	58
GERMANY	7485	7408	3806	1809	1271
CHINA	2200	520	228	45	20
UNITED STATES	1855	878	477	342	207
FRANCE	1671	719	185	58	13
JAPAN	1296	991	480	230	210
BELGIUM	974	417	519	81	23
UNITED KINGDOM	784	62	7	6	4
AUSTRALIA	774	387	79	12	6
GREECE	426	150	36	10	1
INDIA	**300**	**60**	**30**	**40**	**20**

Table 1.1: List of countries and their year-wise solar energy production

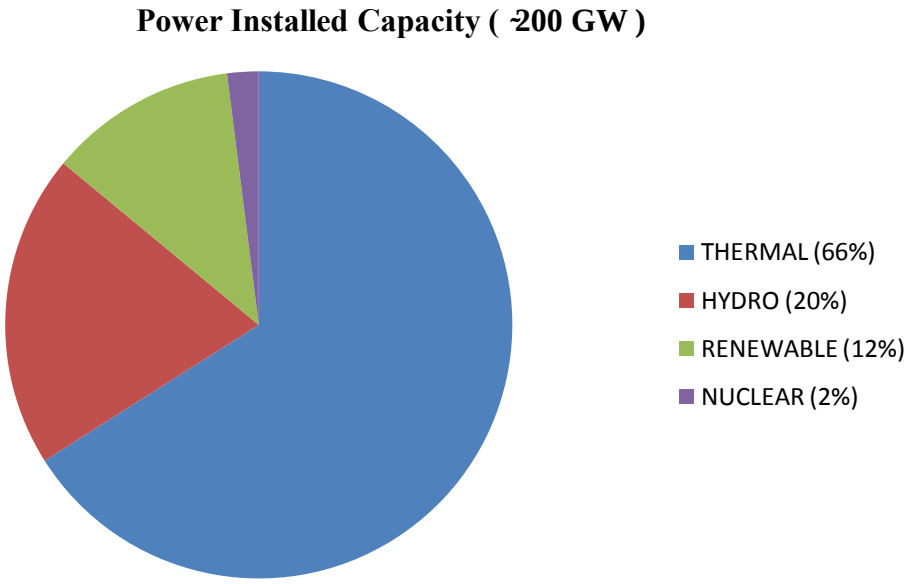

Figure 1.1: Breakup of energy consumption in India

THERMAL	HYDRO	RENEWABLE	NUCLEAR
1,31,353 MW	38,990 MW	24,915 MW	4,780 MW

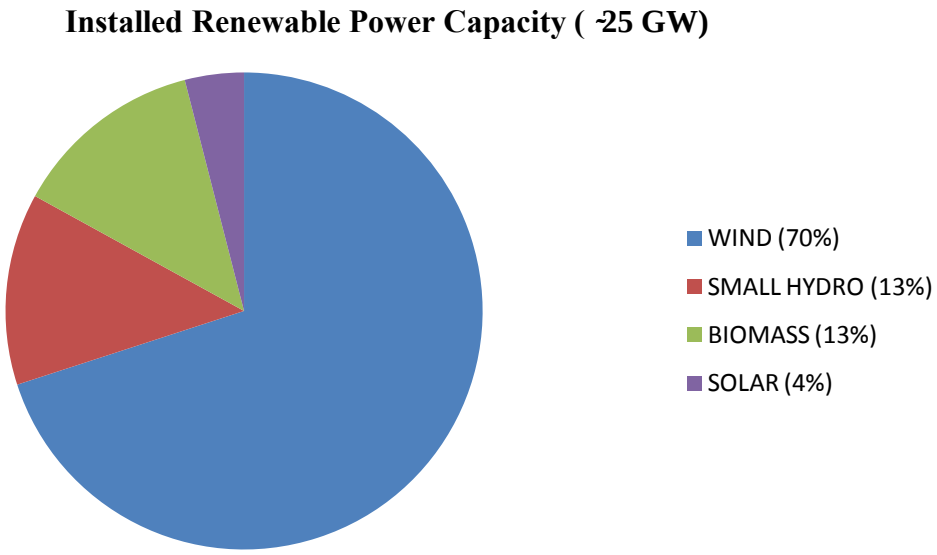

Figure 2: Distribution of renewable power capacity in India

WIND	SMALL HYDRO	BIOMASS	SOLAR
17,353 MW	3,396 MW	3,225 MW	905 MW

Solar energy production in Indian States (2012)[3,4]

S.No.	States	Megawatt power (MW)	Percentage of total production in India (%)
1	Gujarat	654.8	66.90
2	Rajasthan	197.5	20.20
3	Andhra Pradesh	21.8	2.20
4	Maharashtra	20.0	2.00
5	Tamil Nadu	15.0	1.50
6	Orissa	13.0	1.30
7	Uttar Pradesh	12.0	1.20
8	Karnataka	9.0	0.90
9	Punjab	9.0	0.90
10	Haryana	7.8	0.80
11	Uttarakhand	5.0	0.50
12	Chhattisgarh	4.0	0.40
13	Jharkhand	4.0	0.40
14	Delhi	2.5	0.30
15	Madhya Pradesh	2.0	0.20
16	West Bengal	2.0	0.20

Table 2:State-wise solar power production for the year 2012

1.3 SOLAR CELL (PV)

Solar power generation is the phenomenon of conversion of sunlight into electricity and it can be done by two ways

1. Direct conversion using Solar Photovoltaic cell
2. Indirect method of using Concentrated Solar Power.

A material or device that is capable of converting the energy contained in photons of light into an electrical voltage and current is said to be photovoltaic. The driving force to power photovoltaic comes from the sun, and it is interesting to note that the surface of the earth receives something like 6000 times as much solar energy as our total energy demand. Photovoltaic (PV) is the most direct way to convert solar radiation into electricity and is based on the photovoltaic effect. Practically all photovoltaic devices incorporate a pn junction in a semiconductor across which the photo-voltage is developed. These devices are also known as solar cells [5, 6].

1.3.1 Operating Principle

Solar cells are the basic components of photovoltaic panels and the term photovoltaic means that direct conversion of sunlight into electricity. Solar cells take advantage of the photoelectric effect: the ability of some semiconductors to convert

electromagnetic radiation directly into electrical current. Semiconductor materials such as silicon (Si), gallium arsenide (GaAs), cadmiumtelluride (CdTe) or copper indium diselenide (CIS) are used in these solar cells. The charged particles generated by the incident radiation are separated conveniently to create an electrical current by an appropriate design of the solar cell [5-6].

To understand the function of semiconductor devices and thus of solar cells, a precise understanding of the processes within a p-n junction is crucial If a p doped and n doped materials are brought together and merges into the same lattice then a p-n (positive-negative) junction is formed and it creates the region with free charge carriers [5-8].In case of p-type material atoms have one less valence electron, are known as acceptors and in case n-type material, with one more valence electron, referred as donors.

When two layers of different materials are joined together, near the interface the free electrons of the n-layer get diffused to the p-side, leaving behindan area positively charged by the donors and the free holes in the p-layer are diffused to the n-side, leaving behind a region negatively charged by the acceptors. Therefore, an electric field is created between the two sides which opposes the flow (movement) of carriers and is responsible for potential barrier to further flow of charge carriers. This electric field pulls the carriers i.e. electron and holes in opposite directions to cause the flow of current in one direction, electrons can move from the p-side to the n-side and the holes in the opposite direction. Metallic contacts are added at both sides to collect the electrons and holes so the current can flow [5-8].

If the Solar Cell (p-n semiconductor) is exposed to light, photons are absorbed by the electrons. Three different cases can happen: some of the photons are reflected from the top surface of the cell and metal fingers. Those that are not reflected penetrate in the substrate. Some of them, usually the ones with less energy, pass through the cell without causing any effect. Only those with energy level above the band gap of the silicon can create an electron-hole pair. These pairs are generated at both sides of the p-n junction. The minority charges (electrons in the p-side, holes in the n-side) are diffused to the junction and swept away in opposite directions (electrons towards the n-side, holes towards the p-side) by the electric field, generating a current in the cell, which is collected by the metal contacts at both sides. The whole process of generation of electric current through absorption of photons due to sunlight is known

as Photovoltaic effect and the light generated current depends upon the irradiance and also the temperature of the solar cell.

1.3.2 Types of Solar Cell

Over the past decades, silicon has been almost the only material used for manufacturing solar cells. Although other materials and techniques have been developed, silicon is used in more than the 80% of the production [9]. Silicon is so popular because it is one of the most abundant materials in the earth's crust, in the form of silicon dioxide, and it is not toxic. Monocrystalline and polycrystalline silicon solar cells are the two major types of silicon solar cells. There is a third type, amorphous silicon, but its efficiency is worse than the previous types so it is less used. Other new solar cells are made of copper indium gallium diselenide (CIGS) or cadmium telluride (CdTe). Much research and development (R&D) effort is being made to develop new materials, but now-a-days there are no commercial substitutes to the above types of solar cells.

One of the most important characteristics of solar cells is the efficiency, which is the percentage of solar radiation that is transformed into electricity. It is measured under Standard Test Conditions (STC), irradiance of 1000 W/m², air mass coefficient (it characterizes the solar spectrum after the solar radiation has travelled through the atmosphere) A.M 1.5, and a cell junction temperature of 25°C. The higher efficiency, the smaller surface is needed for a given power. This is important because in some applications the space is limited and other costs and parameters of the installation depend on the installed PV surface.

1.2.2.1 Monocrystalline silicon

Monocrystalline silicon solar cells are the most efficient ones. They are made fromwafers (very thin slices) of single crystals obtained from pure molten silicon. Thesesingle crystal wafers have uniform and predictable properties as the structure of thecrystal is highly ordered. However the manufacturing process must be really careful and voccurs at high temperatures, which is expensive. The efficiency of these cells is around 15-18% and the surface needed to get 1 kW in STC is about 7 m^2 [5-6].

1.2.2.2 Polycrystalline silicon

These cells are also made from wafers of pure molten silicon. However, the crystalstructure is random: as the silicon cools, it crystallizes simultaneously in many different points producing an irregular structure: crystals of random sizes, shapes and orientation. These structures are not as ideal as in the monocrystalline cells so the efficiency is lower, around 11-15% However the manufacturing process is less expensive, so the lower efficiency is compensated in some way. The surface needed to obtain 1 kW in STC is about $8m^2$. [5-6]

1.2.2.3 Amorphous and thin-film silicon

Amorphous silicon is the non-crystalline form of the silicon and it can be deposited as thin-films onto different substrates. The deposition can be made at low temperatures. The manufacturing process is simpler, easier and cheaper than in the crystalline cells. The weak point of these cells is their lower efficiency, around 6-8% [5-6]. This efficiency is measured under STC. However, the performance under weaker or diffuse irradiation, such as that in cloudy days, can be higher than in crystalline cells and their temperature coefficient is smaller [9]. Amorphous silicon is also a better light absorber than crystalline, so despite having low efficiency, the thin film is a competitive and promising technology. The first solar cells were of thin-film technology. They have been used since the 1980s in consumer electronics applications, such as calculators. In recent years used in high power applications due to the characteristics mentioned above. The main advantages of thin film technologies are the ease of manufacturing at lowtemperatures using inexpensive substrates and continuous production methods, avoidingthe need for mounting individual wafers and the potential for lightweight and flexiblesolar cells. These advantages are common to most of the thin-film solar cells, not onlythe ones made from amorphous silicon.Over recent years, one more type of silicon has been developed, microcrystalline silicon [9]. It can also be deposited as thin-films onto different substrates, minimizing thequantities of crystalline silicon needed and improving the efficiency of amorphoussilicon. However, the light absorption of microcrystalline silicon compared toamorphous silicon is poor. The solution can be an effective light trapping to keep theincident light within the film. This type of silicon is not a commercial technology yetand more R&D is needed for commercial product development.

1.2.2.4 Other cells and materials

As was mention in the beginning of this chapter, there are other materials apart from silicon that can be used for manufacturing solar cells. These compounds are also thinfilmdeposited, so they have the same advantages as the silicon thin film solar cells but have a better efficiency. Among these compounds, two are already used in commercialsolar cells. They are CIGS and CdTe. The efficiency is around 10-13% [5-6] and it is likely to increase in the following years as the technologies are improved. It is commonly said thatthin film technology is the way to achieve the grid parity, i.e. the point at which the costof generating electricity is equal, or cheaper than grid power [9].The main disadvantages of these technologies are the toxicity of some of thecompounds and the shortage of some of the elements used. In the case of the CIGS,indium is used. This element is not as abundant as silicon in the Earth's crust and it is inhigh demand for other electronics products such as liquid-crystal display(LCD)monitors, which has generated a shortage and consequently a high price rise in the recent years. Moreover, to create the p-n junction, CIGS is interfaced with cadmium sulphide (CdS), another semiconductor. The problem is that cadmium is a heavy metalwhich is cumulatively poisonous. In the case of CdTe, the other compound used incommercial thin film solar cells, it is not as toxic as its individual components, but someprecautions must be taken during the manufacturing process.

Gallium Arsenide (GaAs) has been used for space applications mainly for two reasons. Firstly, it is less susceptible to suffer damage from the space radiation than silicon, andsecondly, due to its direct band gap of 1.42 eV, it can take advantage of a greater part ofthe solar spectrum. Despite being a more expensive material, space projects can afford itas cost is not the most important factor to decide the components. Nowadays it is beinginvestigated to be used in terrestrial PV applications using light concentrators (mirror orlenses) to focus the light onto small cells, reducing the price as less material is required. Triple junction GaAs cells have already passed 40% efficiency in the laboratory using light concentrators [9]. The main handicap at present for this technology is thatconcentration systems are expensive as they have to track the Sun along the day.One other technology that is being actively researched is dye-sensitized cells [9]. Thesecells are made from artificial organic materials and are seen as part of the *"*third generation*"* of solar cells. The efficiency of these cells is above that of amorphous silicon and within the thin-film ones. The main advantage is that they work well under low and diffuse light and their temperature coefficients are

lower. The materials use dare non-toxic and abundant and their manufacturing processes are relatively simple. Flexible modules can easily be made using flexible substrates and they can be used for building integrated PV: roofs, windows, as they can be manufactured in many shapes, sizes and design criteria. They are non-commercial technologies yet, but it is expected that in the following years they will become competitive and will be also used, increasing the possibilities of PV power generation. The silicon and thin film solar cells described before are currently the technologies used in commercial PV applications.

Nevertheless, the different solar cells presented above have similar non-linear voltage-current characteristics and are affected by irradiation and temperature in a similar way. The only difference is that different type of cells have different levels of sensitivity, nevertheless the same algorithms can be used to track the MPP.

1.3 PHOTOVOLTAIC ARRAY (PVA) POWER SYSTEM

Solar cells produce direct current (DC) power which fluctuates with the sunlight's intensity. For practical use this usually requires conversion to certain desired voltages or alternating current (AC), through the use of inverters. Multiple solar cells are connected inside modules. Modules are wired together to form arrays, then tied to an inverter, which produces power at the desired voltage, and for AC, the desired frequency/phase [10].Photovoltaic (PV) systems can be grouped into stand-alone systems and grid connected systems. In stand-alone systems the solar energy yield is matched to the energy demand. Since the solar energy yield often does not coincide in time with the energy demand from

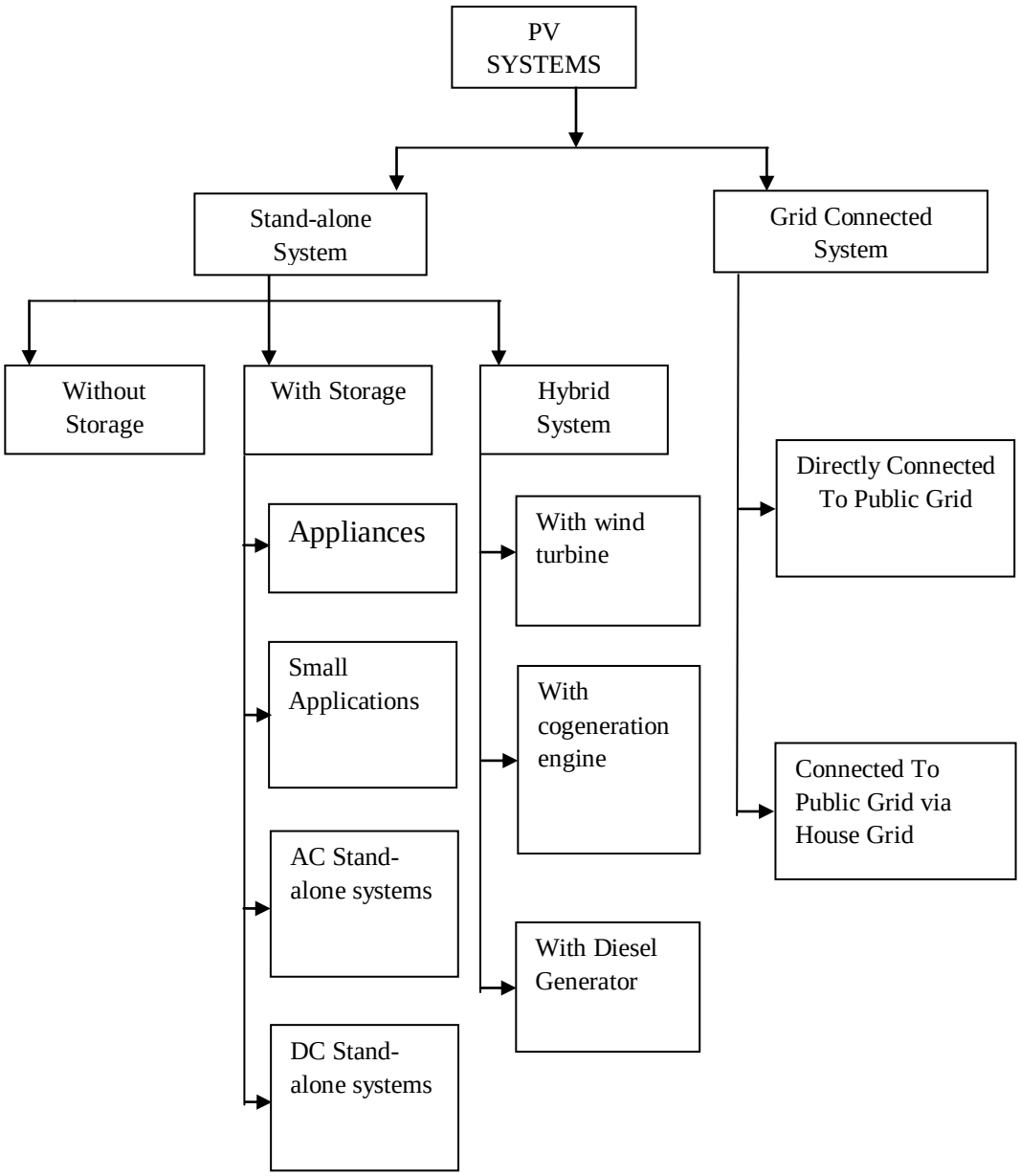

Figure 1.3: Different types of interconnection of solar Photovoltaic (SPV) power generating system to grid

the connected loads, additional storage systems (batteries) are generally used. If the PV system is supported by an additional power source – for example, a wind or diesel generator - this is known as a photovoltaic hybrid system. In grid-connected systems the public electricity grid functions as an energy store. In Germany, most PV systems are connected to the grid. Because of the premium feed-in tariff for solar electricity in Germany, all of the energy they generate is fed into the public electricity grid [7].

Grid-connected PV systems always have a connection to the public electricity grid via a suitable inverter, because a PV module delivers only dc power. Normally there are almost no effects of the PV systems on the grid affecting power quality, load-on lines,

and transformers, etc. However, for a larger share of PV in low-voltage grids, as in solar settlements, these aspects need to be taken into account. From a technical point of view, there will be no difficulty in integrating as much PV into low-voltage grids as the peak load of the respective segment.

1.4 CONCLUSION:

Growth in the generation of solar PV energy in world and in India is very rapid and different type of solar cell materials is researched and used to improve the efficiency of the solar PV system. The operating principle of solar cell and different types of material of solar cell is studied. The PV array system can be used in different modes like stand-alone mode, grid connected mode and also under various type sub modes under stand-alone and grid connected mode.

CHAPTER 2

SOLAR PHOTOVOLTAIC ARRAY (SPVA)

2.1 GENERAL:

Solar PV is modelled using electrical equivalent circuit of solar cell and the related mathematical equation is changed with equivalent model. In this chapter different types of equivalent models is been discussed and the characteristics of PV array is shown and the effects of parameters of PV on its characteristics is obtained and the design of module and array is shown.

2.2 EQUIVALENT (ELECTRICAL) CIRCUIT OF SOLAR CELL AND EQUATIONS

There are many types of electrical equivalent models for solar cell modelling and each model will yield different types of mathematical equation due to different number of components in the circuit of solar cell. Four types of the different PV cell models are shown:

2.2.1 Double diode model (Double exponential model): This model is called as double diode model and also termed as generalized model because it is most ideal model to give approximately ideal characteristics. It consists of two diodes D_1 and D_2 and two resistances i.e. series resistance (R_{se}) and parallel resistance (R_{sh}) and equation (2.1) shows the output current of solar cell.

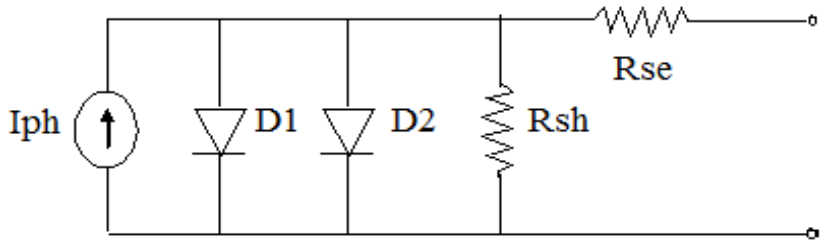

Figure 2.1: Double diode model of Solar cell

$$I = I_{ph} - I_{s1}\left(e^{V+IR_{se}/NV_t}\right) - I_{s2}\left(e^{V+IR_{se}/NVt}\right) - \frac{V+IR_{se}}{R_{sh}} \qquad (2.1)$$

2.2.2 Single diode model (General Model): It is called as single diode model and also known as general model because it is the commonly used model for the purpose of research. It consists of single diode but consists of both resistances i.e. series

resistance (R_{se}) and parallel resistance (R_{sh}) and equation (2.2) shows the output current of solar cell.

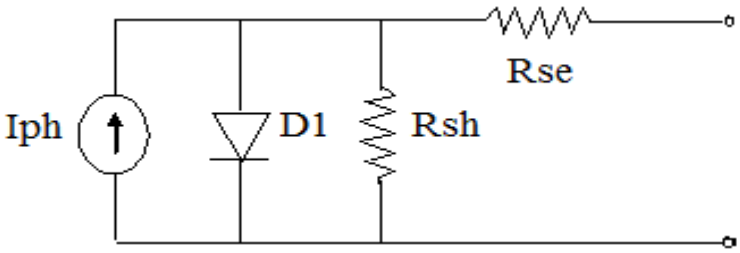

Figure 2.2: Single diode model of Solar Cell

$$I = I_{ph} - I_s\left(e^{V+IR_{se}/NV_t}\right) - \frac{V+IR_{se}}{R_{sh}} \quad (2.2)$$

2.2.3 Appropriate model: This one is the appropriate model of photovoltaic model consisting of only one diode D and one series resistance (R_{se}) and equation (2.3) shows the output current of solar cell.

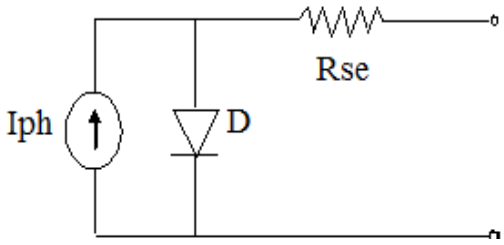

Figure 2.3: Appropriate model of Solar cell

$$I = I_{ph} - I_s\left(e^{V+IR_{se}/NV_t}\right) \quad (2.3)$$

2.2.4 Simplified model: The most simplified model of solar cell is shown with a current source and a diode in parallel and equation (2.4) shows the output current of solar cell.

where I and V are the solar cell output current and voltage respectively, I_{ph} is the light generated current, I_{s1} and I_{s2} are the dark saturation current, q is the charge of an electron, N is the diode quality (ideality) factor, V_t is thermal voltage and given by V_t=kT/q; k is the Boltzmann constant, T is the absolute temperature and R_{se} and R_{sh} are the series and shunt resistances of the solar cell.

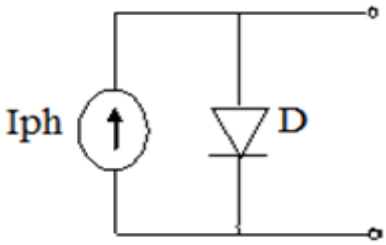

Figure 2.4: SPV from Cell to Module

(2.4)

2.3 MATLAB MODEL

The matlab model of Solar photovoltaic system (SPV) is modelled on the basis of single diode model of solar cell electrical equivalent circuit. PV is modelled as controlled current source. The two subsystems I_m & I_o shown in matlab model of PV which includes equations 2.5-2.7 on which PV is being modelled.

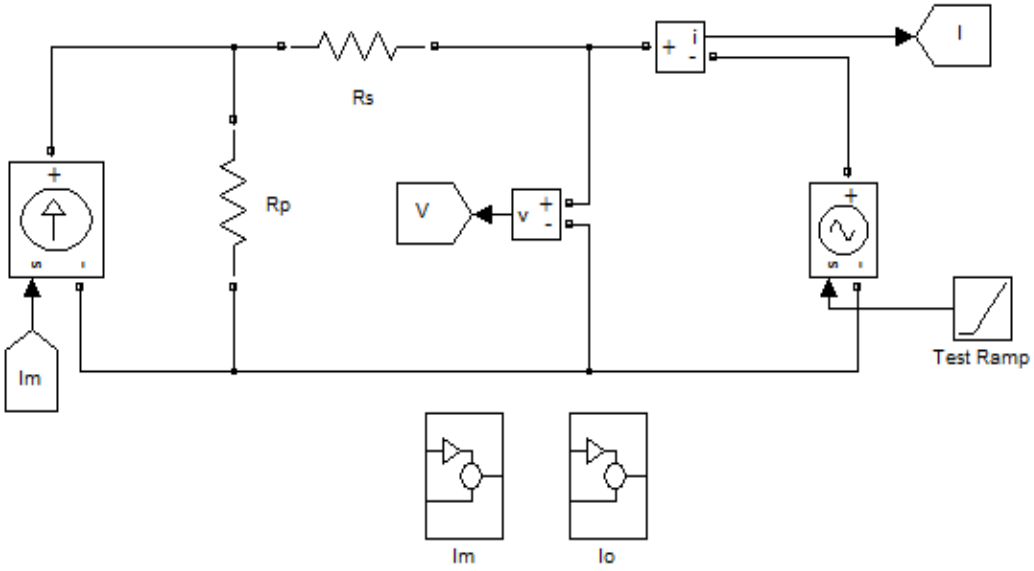

Figure 2.5: MATLAB model of PV

The equation 2.2 for the solar photovoltaic (SPV) will be modified depending upon the number of series (N_s)and parallel (N_p) modules (cells) shown in equation 2.5.

$$I = N_p I_{ph} - N_p I_s \left[e^{(V+IR_{se})/NV_{tN_s}} - 1 \right] - \frac{V + IR_{se}}{R_{sh}} \quad (2.5)$$

and subsequently the series and parallel resistance get altered also shown in equation 2.6

$$R_{se} = R_{se}\left(\frac{Ns}{Np}\right), R_{sh} = R_{sh}\left(\frac{Ns}{Np}\right) \quad (2.6)$$

Series module (cells) increases the output voltage of PVA and the parallel module increases the output current of the PVA, equation 2.7 incorporates the effect of irradiance and temperature.

$$I_{SC} = I_{SCref}\left(\frac{S}{S_{ref}}\right)[1 + (T - T_{ref})K] \quad (2.7)$$

2.4 OPEN CIRCUIT VOLTAGE AND SHORT CIRCUIT CURRENT

Two important points of the current-voltage characteristic must be pointed out: the open circuit voltage V_{OC} and the short circuit current I_{SC}. At both points, the power generated is zero. V_{OC} can be approximated from (1) when the output current of the cell is zero, i.e. I =0 and the shunt resistance R_{sh} is neglected. The short circuit current I_{SC} is the current at V=0 and is approximately equal to the light generated current I_{ph} [5

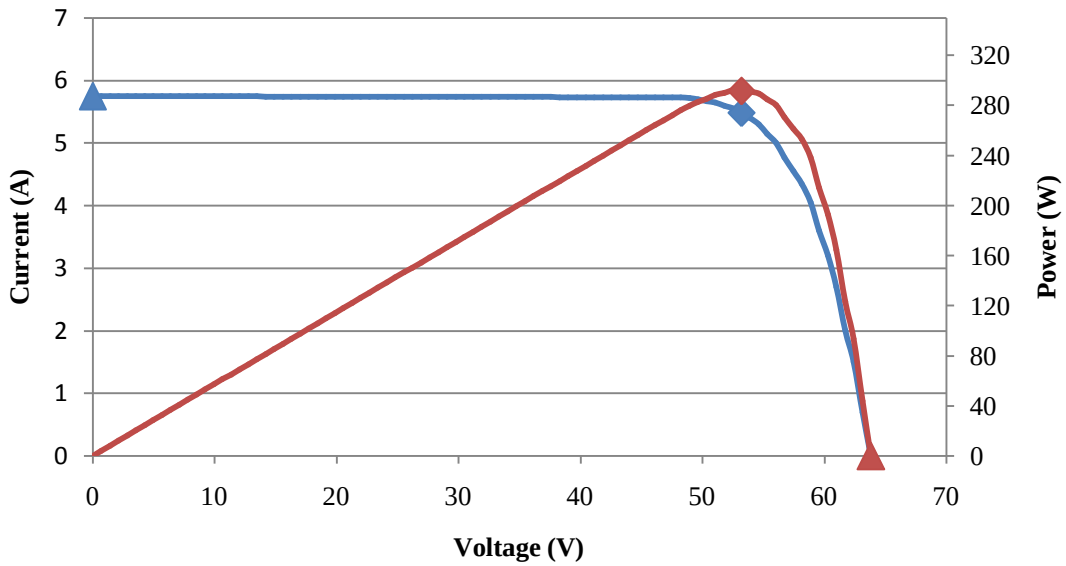

Figure 2.6a: V-I and P-V characteristic with MPP and I_{SC} and V_{OC}

The maximum power is generated by the solar cell at a point of the current-voltage (I-V) characteristic where the product voltage and current will be maximum. This point is known as the maximum power point (MPP) and is unique.

2.5 FILL FACTOR:

Using the MPP current and voltage, I_{MPP} and V_{MPP}, the open circuit voltage (V_{OC}) and the short circuit current (I_{SC}), the fill factor (FF) can be defined as:

$$FF = \frac{I_{MPP}\, V_{MPP}}{I_{SC} V_{SC}} \qquad (2.8)$$

It is a widely used measure of the solar cell overall quality [9]. It is the ratio of the actual maximum power ($I_{MPP}V_{MPP}$) to the theoretical one ($I_{SC}V_{SC}$), which is actually not obtainable. The reason for that is that the MPP voltage and current are always below the open circuit voltage and the short circuit current respectively, because of the series and shunt resistances and the diode depicted in Figure 2. The typical fill factor for commercial solar cells is usually over 0.70.

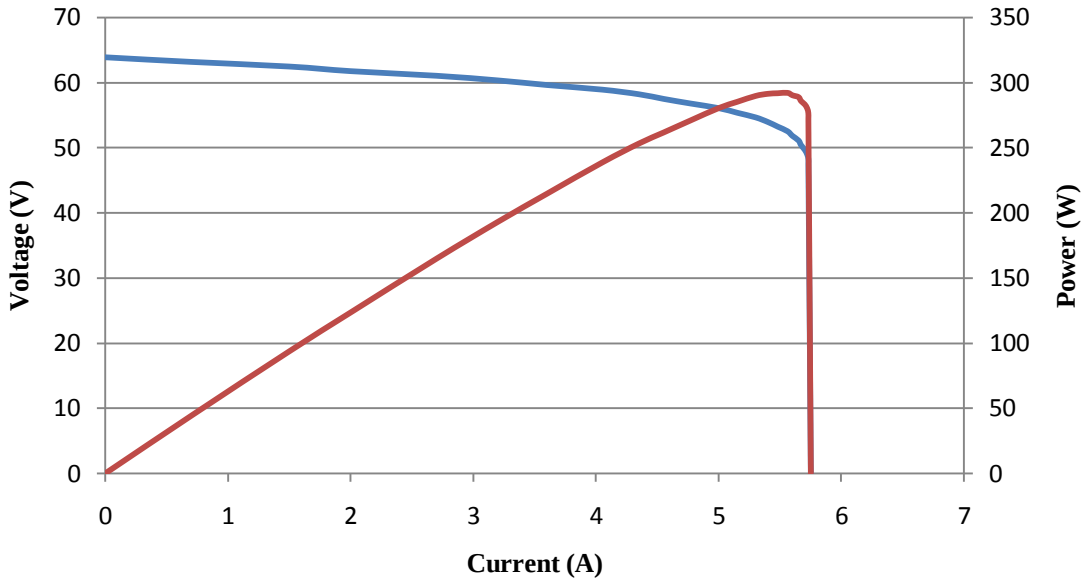

Figure 2.6b: I-V and P-I characteristic of

2.6 SOLAR CELL, MODULE AND ARRAY

Since an individual cell produces only about 0.5-0.7V, it is a rare application for which just a single cell is of any use. Instead, the basic building block for PV applications is a module consisting of a number of pre-wired cells in series, all encased in tough, weather-resistant packages. The PV system normally uses solar panels, which is in arrays. There are many types of PV system, starting from a cell up to array [6, 7].

2.6.1 From Cells to Module

When photovoltaic are wired in series, they all carry the same current, and at any given current their voltages add. Multiple modules, in turn, can be wired in series to increase voltage and in parallel to increase current, the product of which is power. An important element in PV system design is deciding how many modules should be

connected in series and how many in parallel to deliver whatever energy is needed [11, 12].

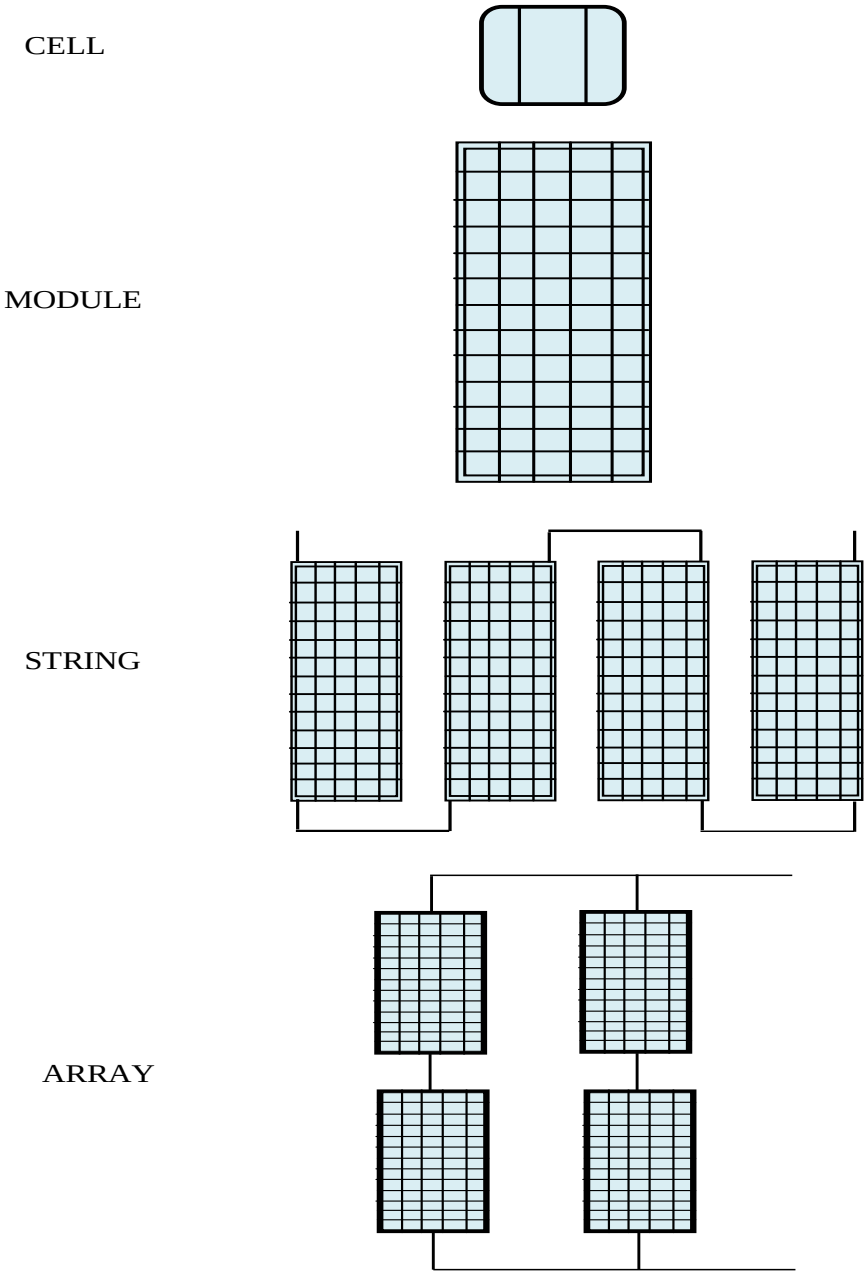

Figure 2.7: SPV from Cell to Array

2.6.2 From Module to Array

Modules can be wired in series to increase voltage, and in parallel to increase current. Arrays are made up of some combination of series and parallel modules to increase power [11,12].For modules in series, the I–V curves are simply added along the voltage axis. For modules in parallel, the same voltage is across each module and the total current is the sum of the currents. When high power is needed, the array will

usually consist of a combination of series and parallel modules for which the total I – V curve is the sum of the individual module I –V curves [6].

2.7 TEMPERATURE AND IRRADIANCE EFFECTS

Two important factors that affect the characteristics of solar modules are the irradiation and the temperature and have to be taken into account. Due to irradiation and the temperature changes throughout the day, the maximum power point (MPP) varies during the day and that is the main reason why the MPP must be constantly tracked. This will also ensure that the maximum available power is obtained from the panel.

The effect of the irradiance on the voltage-current (V-I), voltage-power (V-P) and current-power (I-P) characteristics is depicted in Figure 2.7-2.9. As was previously mentioned, the photo-generated current is directly proportional to the irradiance level, so an increment in the irradiation leads to a higher photo-generated current. Moreover, the short circuit current is directly proportional to the photo-generated current; therefore it is directly proportional to the irradiance. When the operating point is not the short circuit, in which no power is generated, the photo-generated current is also the main factor in the PV current, as is expressed by equations 2.1- 2.4. For this reason the voltage-current characteristic varies with the irradiation. In contrast, the effect in the open circuit voltage is relatively small, as the dependence of the light generated current is logarithmic, as is shown in equation 2.1-2.4 [12,13]

From figures 2.7, 2.8 and 2.9, it shows that the change in the current is greater than in the voltage due to change in irradiance. In practice, the voltage dependency on the irradiation is often neglected [11]. As the effect on both the current and voltage is positive, i.e. both increase when the irradiation rises, the effect on the power is also positive: hence under more irradiation, higher power is generated [12, 13]. The figure 2.7 shows the effect of irradiance on V-I characteristic of PV. The effect of irradiance significantly changes the short circuit current (I_{SC}) of PV and it also affects the open circuit voltage (V_{OC}) but not very significantly. Figure 2.8 shows the effect of change of irradiance on P-V characteristic of PV and as the irradiance ir-radiance decreases the power is decreasing. Figure 2.9 shows the effect of change of irradiance on P-I characteristic and as irradiance decreases I_{SC} decreases and hence power also decreases.

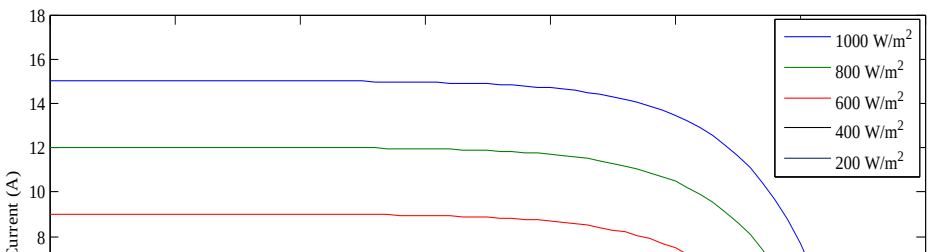

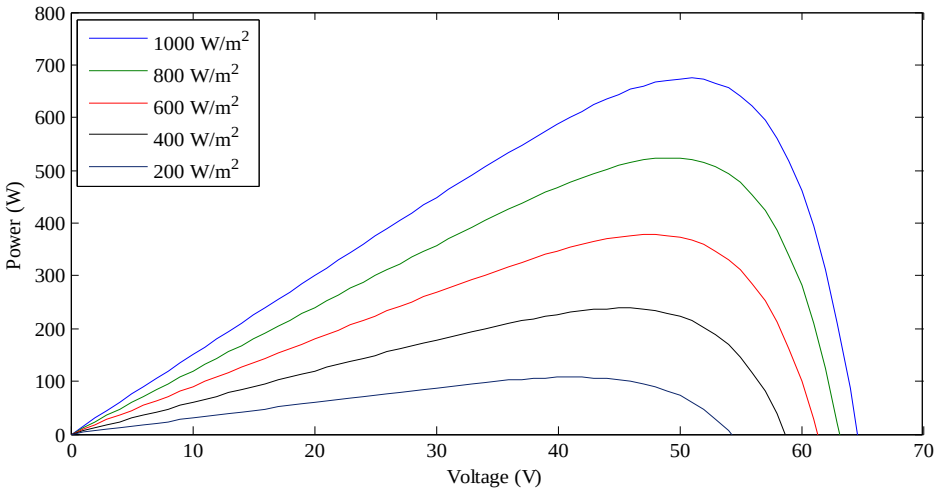

Figure 2.9: V-P characteristic of PV for different irradiance levels

The temperature, on the other hand, affects mostly the voltage. The open circuit voltage is linearly dependent on the temperature, as shown in the following equation:

$$V_{oc}(T) = V_{oc}^{STC} + \frac{K_V}{100}(T - 273.5) \tag{2.9}$$

According to equation, the effect of the temperature on V_{OC} is negative, because K_V is negative, i.e. when the temperature rises, the voltage decreases. The current increases with the temperature but very little and it does not compensate the decrease in the voltage

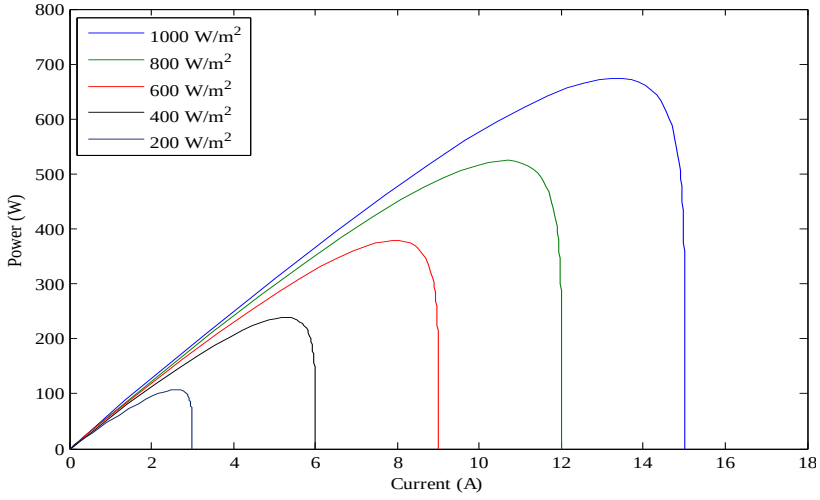

Figure 2.10: P-I characteristic of PV for different irradiance levels

caused by a given temperature rise.. As the effect of the temperature on the current is really small, it is usually neglected [11] and it can be seen in figure 2.11 and 2.13. Figure 2.11-2.13 shows how the voltage-current (V-I), the voltage-power (V-P) and current-power (I-P) characteristics change with temperature. The figure 2.10 shows the effect of temperature on V-I characteristic of PV. The effect of temperature significantly changes open circuit voltage (V_{OC}) and as the temperature increases voltages decreases. Figure 2.11 shows the effect of change of temperature on P-V characteristic of PV and as

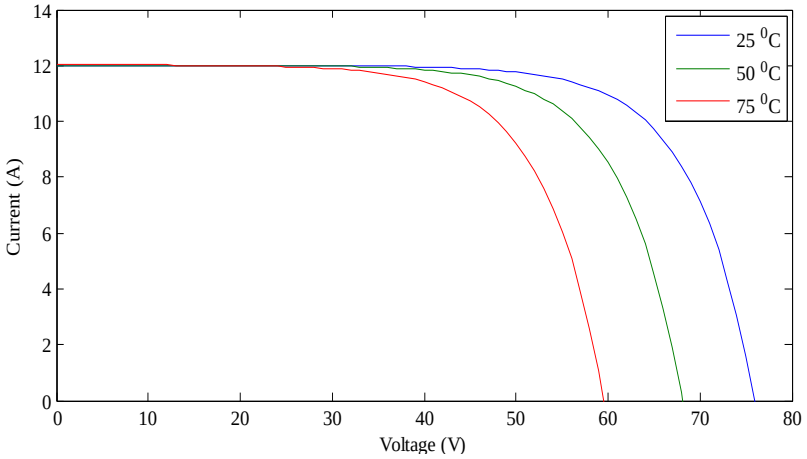

Figure 2.11: V-I characteristic of PV for different temperature

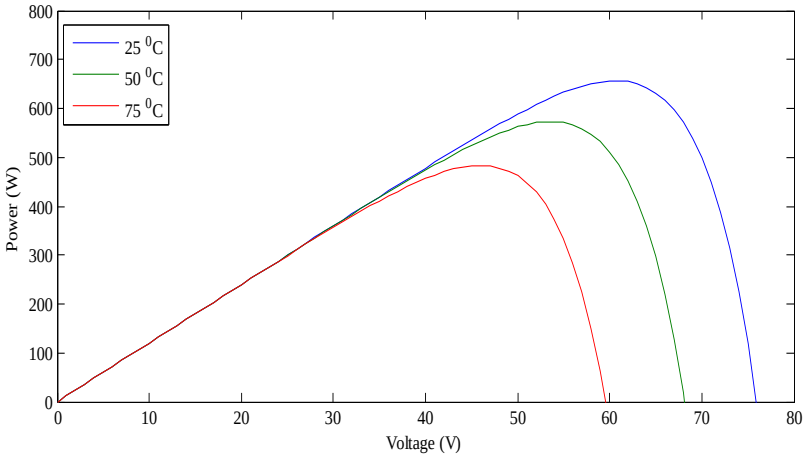

Figure 2.12: V-P characteristic of PV for different temperature

the temperature increases the power is decreasing. Figure 2.9 shows the effect of change of temperature on P-I characteristic and as temperature increases V_{OC} decreases and hence power also decreases.

It is known that the temperature and the irradiation depend on the atmospheric conditions, which are not constant during the year and not even during a single day; they can vary rapidly due to fast changing conditions such as clouds. This causes the MPP to move constantly, depending on the irradiation and temperature conditions. If the operating point is not close to the MPP, great power losses occur. Hence, it is essential to track the MPP in any conditions to assure that the maximum available power is obtained from the PV panel. In a modern solar power converter, this task is entrusted to the MPPT algorithms.

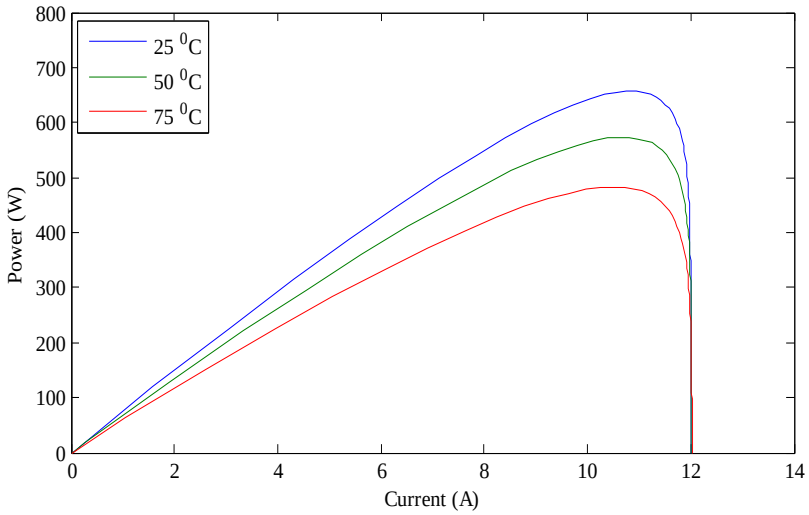

Figure 2.13: V-I characteristic of PV for different temperature

2.7 CONCLUSION:

Solar photovoltaic (SPV) system is modelled based on the equation of solar PV cell and tested using ramp signal successfully in MATLAB/Simulink environment. The characteristics of PV i.e. current-voltage, power-voltage and power-current have been successfully obtained for different conditions of irradiation and temperature levels and the effect of change of irradiance and temperature on characteristics SPV system is studied and verified. Different electrical equivalent models of solar cell and design of modules, string and array is been studied successfully.

CHAPTER 3

MAXIMUM POWER POINT TRACKING (MPPT) TECHNIQUES AND DESIGN OF BOOST CONVERTER

3.1 GENERAL:

A typical solar panel converts only 30 to 40 percent of the incident solar irradiation into electrical energy. Maximum power point tracking technique is used to improve the efficiency of the solar panel. According to Maximum Power Transfer theorem, the power output of a circuit is maximum when the thevenin impedance of the circuit (source impedance) matches with the load impedance. Hence our problem of tracking the maximum power point reduces to an impedance matching problem. In order to extract the maximum amount of energy, the PV system must be capable of tracking the solar panel unique maximum power point that varies with irradiance and temperature.

Tracking the maximum power point (MPP) of a photovoltaic (PV) array is usually an essential part of a PV system. As such, many MPP tracking (MPPT) methods have been developed and implemented. The methods vary in complexity, sensors required, convergence speed, cost, range of effectiveness, implementation hardware, popularity, and in other respects. They range from the almost obvious (but not necessarily ineffective) to the most creative (not necessarily most effective. In fact, so many methods have been developed [14] that it has become difficult to adequately determine which method, newly proposed or existing, is most appropriate for a given PV system.

A MPPT is a power electronic DC/DC converter inserted between the PV module and load to achieve optimum matching. By using an intelligent algorithm, it ensures that the PV module always operates at its maximum power point. MPPT optimizes the power output of the solar cell by constantly tracking the varying maximum power operating point and adjusts the solar panel operating voltage [14-15]. In this chapter different MPPT methods are discussed and design of boost converter is shown.

3.2 DIFFERENT MPPT TECHNIQUES

There are different MPPT techniques employed to track maximum power generated by the PV array in different environmental condition. MPPT techniques vary according to their different working algorithm, parameters and equations used. There are several MPPT methods that have been studied and researched [14-21]. The

following are the few MPPT techniques which have been introduced here and among all these techniques the most commonly used technique is Hill Climbing/ Perturbation and Observation (P & O).

3.2.1 Hill climbing / P & O

The most commonly used MPPT algorithm is the P&O, due to its simplicity of implementation in its basic form. However, it has some drawbacks, like oscillations around the MPP in steady state operation, slow response due to the change of the solar irradiance [16]. The P&O algorithm is also called "hill-climbing", but both names refer to the same algorithm depending on how it is implemented. Hill-climbing involves a perturbation in the duty cycle of the power converter and P&O a perturbation in the operating voltage of the DC link between the PV array and the power converter [14]. It is based on the calculation of PV output power and the change in power due to a change in voltage and current by sensing voltage and current. The summary of algorithm for Hill climbing/P & O is given below in Table 3.1 below.

Perturbation	Change in Power	Next Perturbation
Positive	Positive	Positive
Positive	Negative	Negative
Negative	Positive	Negative
Negative	Negative	Positive

Table 3.1: Summary of P&O algorithm

It can be observed from the summary of algorithm shown in Table 3.1 that incrementing (decrementing) the voltage increases (decreases) the power when operating on the left of the MPP and decreases (increases) the power when on the right of the MPP. Therefore, if there is an increase in power, the subsequent perturbation should be kept the same to reach the MPP and if there is a decrease in power, the perturbation should be reversed. The process is repeated periodically until the MPP is reached. The system then oscillates about the MPP. The oscillation can be minimized by reducing the perturbation step size. However, a smaller perturbation

size slows down the MPPT. Hill climbing and P&O methods may fail under rapidly changing atmospheric conditions.

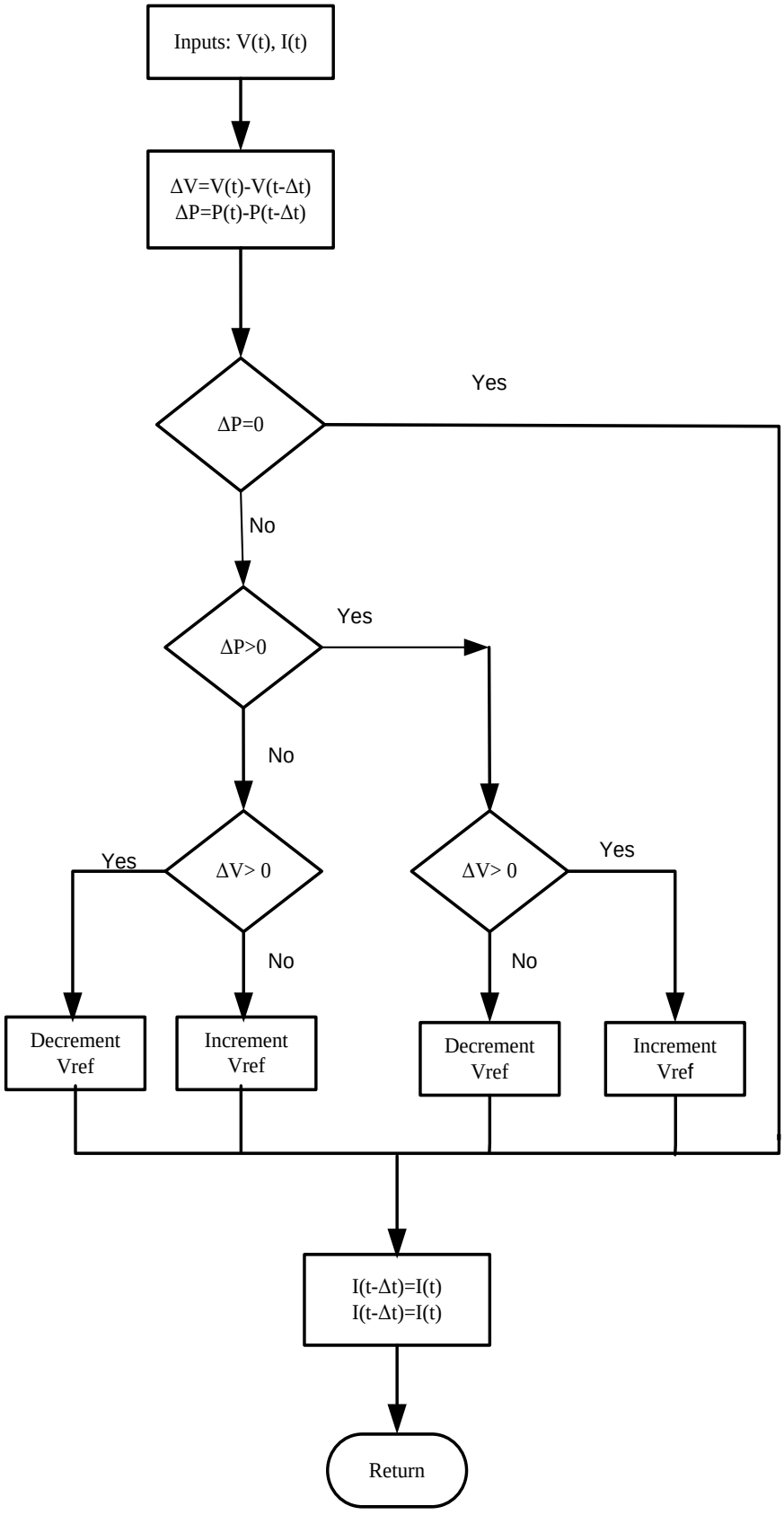

Figure 3.1: Flow chart for P & O algorithm

3.2.2 Incremental Conductance (IC):

The incremental conductance algorithm is based on the fact that the slope of the power curve vs. voltage (current) of the PV module is zero at the MPP, positive

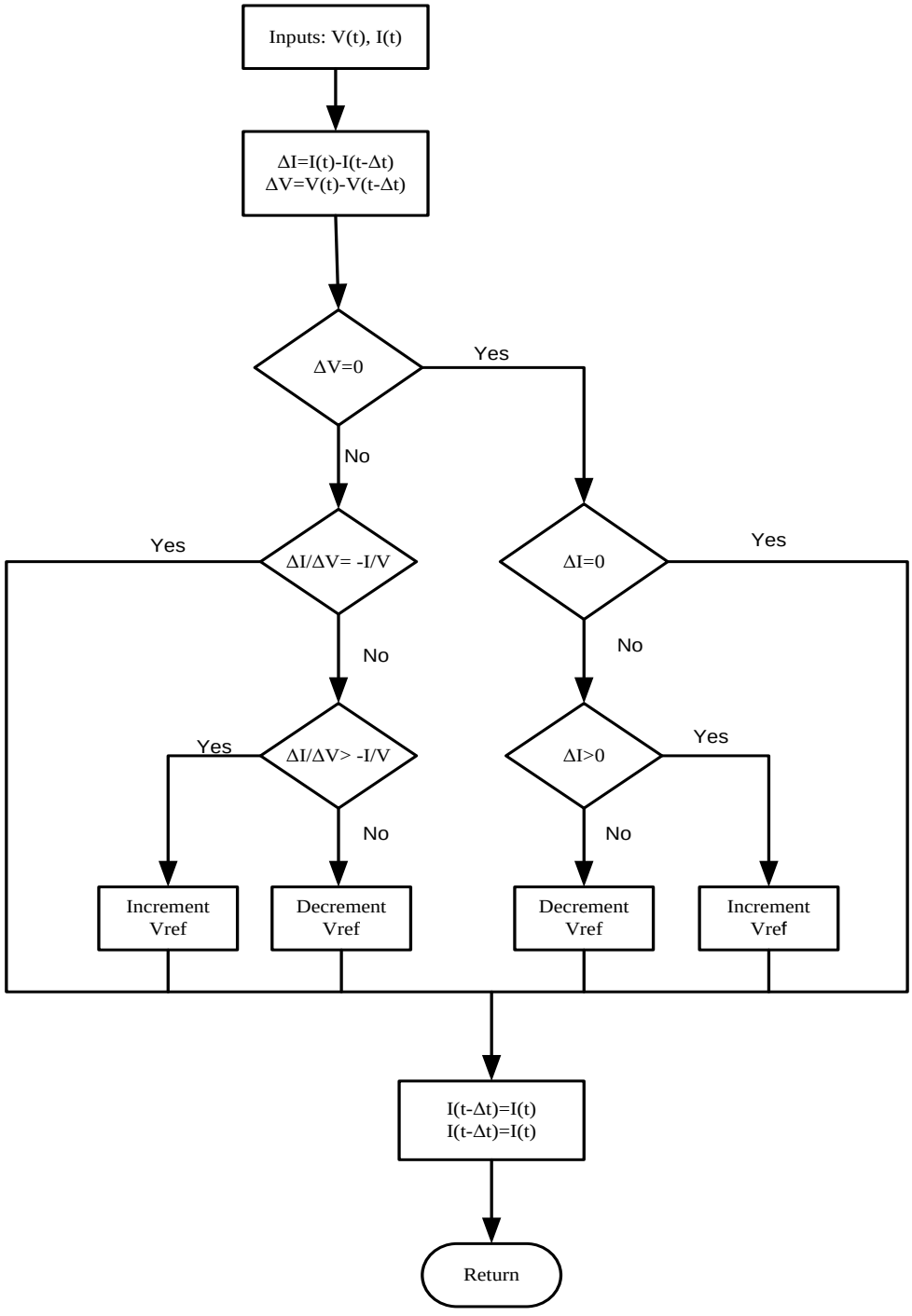

Figure 3.2: Flow chart for incremental conductance algorithm

(negative) on the left of MPP and negative (positive) on the right of MPP, given as

- dP/dV = 0 at MPP
- dP/dV > 0 left of MPP

- dP/dV < 0 right of MPP

But

$$\frac{dP}{dV} = I + V\frac{dI}{dV} \approx I + V\frac{\Delta I}{\Delta V} \tag{3.1}$$

and therefore by differentiating power with respect to voltage we will get the new condition given

$$\begin{aligned} \Delta I/\Delta V &= -I/V && \text{at MPP} \\ \Delta I/\Delta V &> -I/V && \text{left of MPP} \\ \Delta I/\Delta V &< -I/V && \text{right of MPP} \end{aligned} \tag{3.2}$$

Hence MPP can be tracked by comparison of incremental conductance and instantaneous conductance. In both P & O and incremental conductance methods, the speed of response of MPP depends upon the size of the increment of the reference voltage [14]. The drawback of both the methods is that it is unable to track maximum power point (MPP) if there are rapid changes in parameters i.e. irradiance and temperature. The other drawback of both the methods is that the oscillation occurs at the point of MPP which results in oscillations in voltage and current at MPP level. The size of the oscillations depends on the size of the rate of change of the reference voltage. The greater it is, the higher is the amplitude of the oscillations. However, how fast the MPP is reached also depends on this rate of change and this dependence is inversely proportional to the size of the voltage increments. The traditional solution is a trade-off: if the increment is small so that the oscillations decrease, then the MPP is reached slowly and vice versa, so a compromise solution has to be found.

To overcome these drawbacks some solutions have been published in recent years [15-19]. Related to the reduction of oscillations around the MPP in steady state, a variable perturbation step for the P&O algorithm has been proposed in [16, 17]. This modified P&O method also determines if the operating point is near to or far from the MPP and adjusts the size of the perturbation accordingly i.e. if the operating point is near the MPP, the perturbation size is reduced and if the point is far away, then it is increased. This technique improves the convergence speed and reduces the oscillation around the MPP.

Regarding the rapid change in the irradiation conditions, Sera et al. published in [19] and [20] an improved P&O method, called “dP-P&O”, in which an additional measurement is performed without perturbation in the voltage and current. In this

way, for every three consecutive samples the effect of the perturbation in the voltage (current) and the effect of the change in the atmospheric conditions can be evaluated so that the increment in the power used in the algorithm only contains the effect caused purely by the MPPT algorithm. Then, the correct decision about the direction of the next perturbation can be taken. The efficiency of the tracking is improved by this method.

3.2.3 Other Hill climbing MPPT Methods

Some more techniques of MPPT are summarized in [14]. These can be grouped under Hill climbing algorithm like: ripple correlation control (RCC), dP/dV or dP/dI Feedback control and slide control. RCC uses the ripple imposed by the power converter on the PV array to track the MPP. It correlates dp/dt with di/dt or dv/dt, to drive the power gradient to zero, which happens when the MPP is reached. $\frac{dP}{dT} \cdot \frac{dI}{dT}$ and $\frac{dP}{dT} \cdot \frac{dV}{dT}$ are positive to the left of the MPP, negative to the right and zero at the MPP. Actually the same criteria is used by the Incremental conductance (IC) algorithm but expressed in a different form, thus it will suffer the same problems. In fact, it has been only tested with irradiation steps, which are not appropriate to test the dynamic performance. Besides, it needs low switching frequencies to have enough ripple so the correct decisions can be made and it is an analog technique.

dP/dV or dP/dI Feedback control is a technique which computes the slope of the P-V or P-I characteristic curve and feeds it back to the controller in order to drive it to zero, as they are zero at the MPP. Again, this is another implementation of the IC algorithm, so it has the same advantages and disadvantages.

Finally, in the slide control, the switching function used is again dP/dV, thus the same problems as with the Incremental Conductance (IC) algorithm can be expected under changing irradiation. To summarise, the last three MPPT methods are based on the same principles as the P&O and the IC algorithms, so they have the same advantages and disadvantages. All hill-climbing MPPT methods depend on the PV array's V-P or I-P characteristics, which vary with temperature and irradiation, therefore these MPPT methods can be confused when the irradiation or temperature are changing, as it is explained in [19]. Finally, the other hill-climbing MPPT methods do not offer any improvement to the original P&O and IC algorithms.

3.2.4 Fractional Open circuit Voltage

This method uses the approximately linear relationship between the MPP voltage (V_{MPP}) and the open circuit voltage (V_{OC}), which varies with the irradiance and temperature [14]: (3.3)

$$V_{MPP} \approx k_1 V_{OC}$$

where k_1 is a constant depending on the characteristics of the PV array and it has to be determined beforehand by determining the V_{MPP} and V_{OC} for different levels of irradiation and different temperatures. According to [14] the constant k_1 has been reported to be between 0.71 and 0.78.

Once the constant of proportionality, k_1, is known, the MPP voltage V_{MPP} can be determined periodically by measuring V_{OC}. To measure V_{OC}, the power converter has to be shut down momentarily so in each measurement a loss of power occurs. Another problem of this method is that it is incapable of tracking the MPP under irradiation slopes, because the determination of V_{MPP} is not continuous. One more disadvantage is that the MPP reached is not the real one because the relationship is only an approximation.

To overcome these drawbacks, some solutions have been proposed, as is reported in [14]. For example, pilot cells can be used to obtain V_{OC}. They are solar cells that represent the PV array's cells and which are not used to produce electricity but to obtain characteristics parameters such as V_{OC} without interfering with the power converters. These pilot cells have to be carefully chosen and placed to represent the PV array characteristics and the irradiation conditions. One drawback of using these pilot cells is that the cost of the system is increased.

Depending on the application, this technique can be used because it is very easy to implement and it is cheap - it does not require DSP or microcontroller control and just one voltage sensor is used [14]. However, according to [14] this method is not valid under partial shading of the PV array because then the constant k_1 changes. To update then k_1 a voltage sweep is proposed though this increases the complexity of the system, the cost increases and there are more power losses during the sweep.

3.2.5 Fractional Short circuit Current

As in the fractional open circuit voltage method, there is a relationship, under varying atmospheric conditions, between the short circuit current I_{SC} and the MPP current, I_{MPP}, as is shown by:

$$I_{MPP} \approx k_2 I_{SC} \quad (3.4)$$

The coefficient of proportionality k_2 has to be determined according to each PV array, as in the previous method happened with k_1. According to [14] the constant k_2 has been reported to be between 0.78 and 0.92.

Measuring the short circuit current while the system is operating is a problem. It usually requires adding an additional switch to the power converter to periodically short the PV array and measure ISC. Most of the literature using this MPPT technique uses a DSP as controller [14].

3.2.6 Fuzzy Logic

The use of fuzzy logic control has become popular over the last decade because it can deal with imprecise inputs, does not need an accurate mathematical model and can handle nonlinearity. Microcontrollers have also helped in the popularization of fuzzy logic control.

The fuzzy logic consists of three stages: fuzzification, inference system and defuzzification. Fuzzification comprises the process of transforming numerical crisp inputs into linguistic variables based on the degree of membership to certain sets [24, 25]. Membership functions, like the ones in Figure 3.3, are used to associate a grade to each linguistic term.

The number of membership functions used depends on the accuracy of the controller. In Figure 3.3 seven fuzzy levels are used: NB (Negative Big), NM (Negative Medium), NS (Negative Small), ZE (Zero), PS (Positive Small), PM (Positive Medium) and PB (Positive Big). The values *a*, *b* and *c* are based on the range values of the numerical variable. In some cases the membership functions are chosen less symmetric or even optimized for the application for better accuracy [14].

The inputs of the fuzzy controller are usually an error, E, and the change in the error, ΔE [23, 24]. The error can be chosen by the designer, but usually it is chosen as ΔP/ΔV because it is zero at the MPP. Then E and ΔE are shown in equation 3.5 and 3.6 respectively.

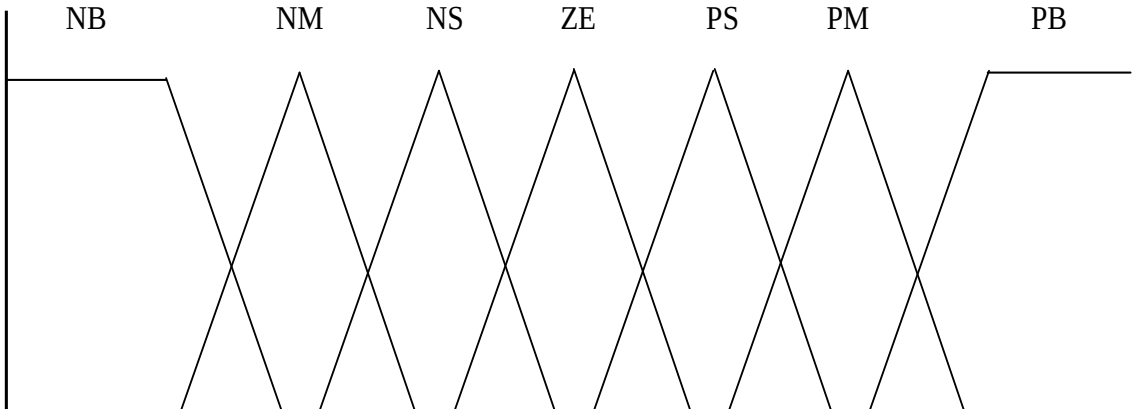

Figure 3.3: Membership function

$$E = \frac{P(k)-P(k-1)}{V(k)-V(k-1)} \tag{3.5}$$

$$\Delta E = E(k) - E(k-1) \tag{3.6}$$

The output of the fuzzy logic converter is usually a change in the duty ratio of the power converter, ΔD, or a change in the reference voltage of the DC-link, ΔV. The rule base, also known as rule base lookup table or fuzzy rule algorithm, associates the fuzzy output to the fuzzy inputs based on the power converter used and on the knowledge of the user.

Table 3.2 shows the rules for a three phase inverter, where the inputs are E and ΔE, as defined in equation (3.4) and (3.5), and the output is a change in the DC-link voltage, ΔV. For example, if the operating point is far to the right of the MPP, E is NB, and ΔE is zero, then to reach the MPP the reference voltage should decrease, so ΔV should be NB (Negative) to move the operating point towards the MPP.

The last stage of the fuzzy logic control is the defuzzification. In this stage the output is converted from a linguistic variable to a numerical crisp one again using membership functions as those in Figure 3.3**.** The advantages of these controllers, besides dealing with imprecise inputs, not needing an accurate mathematical model and handling nonlinearity, are fast convergence and minimal oscillations around the MPP. Furthermore, they have been shown to perform well under step changes in the irradiation. However, no evidence was found that they perform well under irradiation ramps. Furthermore, they have been shown to perform well under step changes in the irradiation.

E/dE	**NB**	**NM**	**NS**	**ZE**	**PS**	**PM**	**PB**
NB	NB	NB	NB	NB	NM	NS	ZE
NM	NB	NB	NB	NM	NS	ZE	PS

NS	NB	NB	NM	NS	ZE	PS	PM
ZE	NB	NM	NS	ZE	PS	PM	PB
PS	NM	NS	ZE	PS	PM	PB	PB
PM	NS	ZE	PS	PM	PB	PB	PB
PB	ZE	PS	PM	PB	PB	PB	PB

TABLE 3.2: Rule Base

Furthermore, they have been shown to perform well under step changes in the irradiation. However, no evidence was found that they perform well under irradiation ramps. The disadvantage of this method is that their effectiveness depends a lot on the skills of the designer; not only on choosing the right error computation, but also in coming up with an appropriate rule base [14].

3.1.7 Neural Network

Another MPPT method well adapted to microcontrollers is Neural Networks [14]. The simplest example of a Neural Network (NN) has three layers called the input layer, hidden layer and output layer as shown in Figure 3.4. More complicated NN's are built adding more hidden layers. The number of layers and the number of nodes in each layer as well as the function used in each layer vary and depend on the user knowledge. The input variables can be parameters of the PV array such as V_{OC} and I_{SC}, atmospheric data as irradiation and temperature or a combination of these. The output is usually one or more reference signals like the duty cycle or the DC-link reference voltage.

The performance of the NN depends on the functions used by the hidden layer and how well the neural network has been trained. The links between the nodes are all weighted. In Figure 3.4 the weight between the nodes *i* and *j* is labelled as w_{ij}. The weights are adjusted in the training process. To execute this training process, data of the patterns between inputs and outputs of the neural network are recorded over a lengthy period of time, so that the MPP can be tracked accurately.

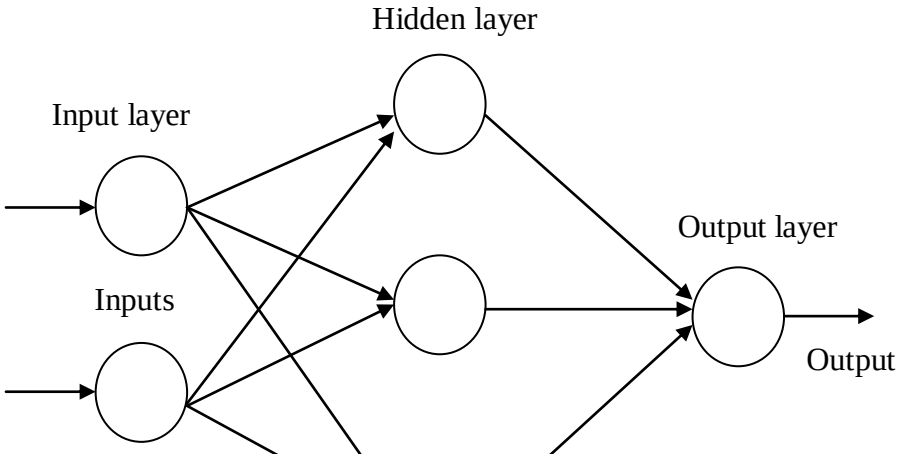

The main disadvantage of this MPPT technique is the fact that the data needed for the training process has to be specifically acquired for every PV array and location, as the characteristics of the PV array vary depending on the model and the atmospheric conditions depend on the location. These characteristics also change with time, so the neural network has to be periodically trained.

3.3 DESIGN OF DC-DC BOOST CONVERTER

The IGBT based DC-DC boost converter is modeled in the MATLAB/Simulink based design as shown in Fig. 3. The maximum power point for voltage and current is tracked using incremental conductance method of MPPT. The voltage at the load terminal of PV array system is boosted according to the change in load by using MPPT and DC-DC boost converter. The current and voltage is modulated at the load side but the power remains constant at a particular level even with the change in load. The value of inductor and capacitor is designed and calculated according to desired output levels. The design of Boost converter is given in [26]-[28].

$$L = \frac{V_{pv} D}{2\Delta i_1 f_{sh}} \tag{3.7}$$

$$C = \frac{I_d D}{\Delta V f_{sh}} \tag{3.8}$$

where V_{pv} = Output voltage on PV side

D = Duty cycle of converter

Δi_1 = Input current (PV side) ripple

I_d = Output current on load side

ΔV = Output voltage (load side) ripple

f_{sh} = Switching frequency

where, Δi_1 is known as input current ripple on the PV side and it is taken as 10% of the input current and ΔV is known as the output voltage ripple and is taken as the 5% of the output voltage on the load side and

The duty cycle (D) of the DC-DC boost converter is given by equation

$$D = 1 - \frac{V_{in}}{V_b} \tag{3.8}$$

Where V_{in} is the input voltage for converter from PV side and it is same as V_{pv} and V_b is the output voltage of the converter and is same as load voltage.

3.4: MATLAB/Simulink MODEL:

The matlab model shown in figure 3.5 consists of solar photovoltaic (SPV) array model and the dc-dc boost converter with resistive load at its output side. Perturbation and observation (P & O) and incremental conductance algorithm is modelled in MATLAB/Simulink and MPPT block is shown.

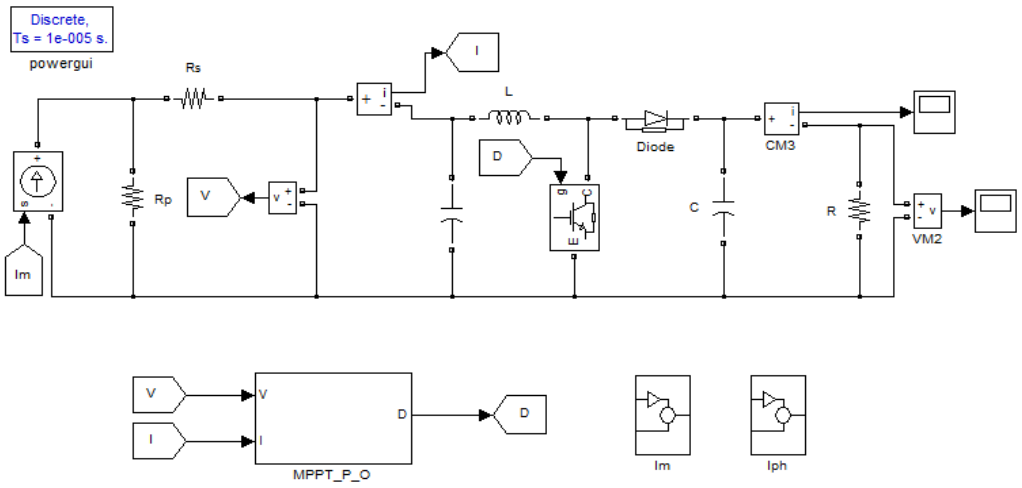

Figure 3.5: MATLAB/Simulink model of PV system with MPPT and boost

3.5 RESULTS AND DISCUSSION:

The SPV is modelled for 305 watts with open circuit voltage of 64.2 V and short circuit of 5.96 A for the verification of MPPT results. Figure 3.6-3.8 shows the results of MPPT and the outputs at the load side of the dc-dc converter.

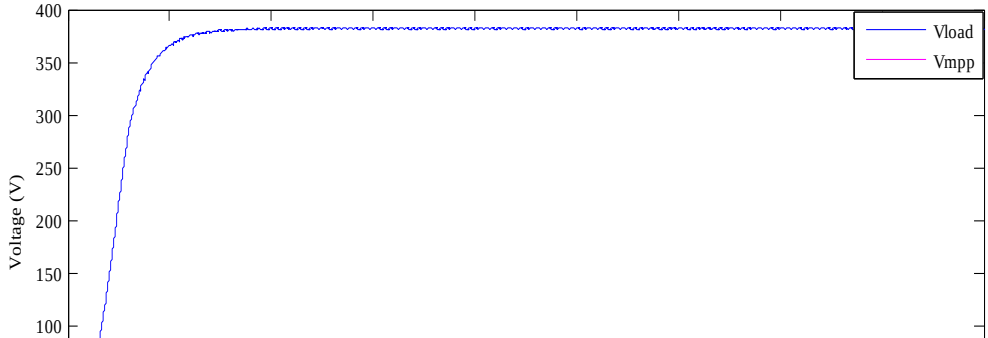

Figure 3.6 shows the output of voltage at MPP tracked by MPPT and the output voltage at the load side boosted by the dc-dc boost converter. The voltage level at the load side is boosted through boost converter if the load is increased. Figure 3.7 shows the output of current at MPP tracked by MPPT and the output current at the load side of the dc-dc boost converter. As the voltage is been boosted through boost converter the value of current is decreased because the power at the input of converter i.e. tracked MPP power and the load side of the converter must be same.

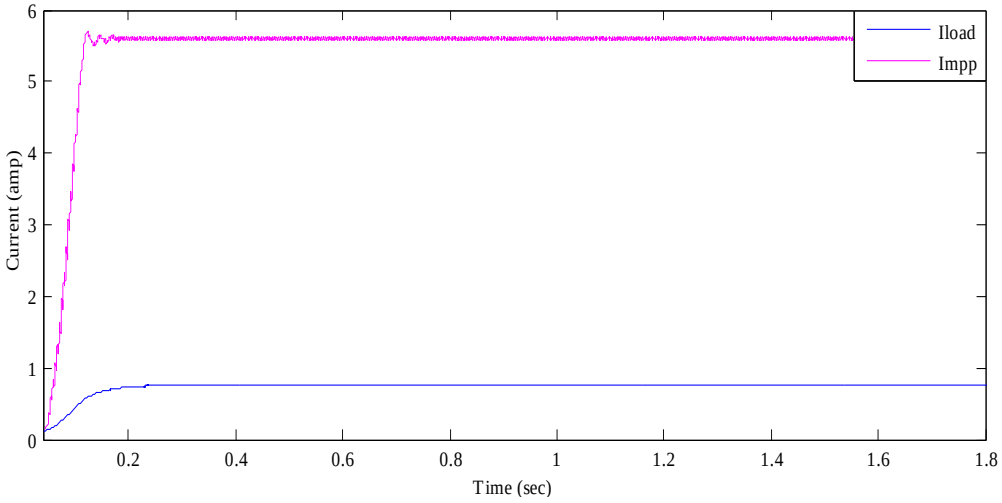

Figure 3.7: Output current of MPPT and load

Figure 3.8 shows the output power at MPP tracked by MPPT and the output power at the load side of the dc-dc boost converter. As shown in the result the power approximately remains same at the input of converter (which is maximum power tracked) and power at load side of converter. There is small difference at the load side because of the switching losses and other losses.

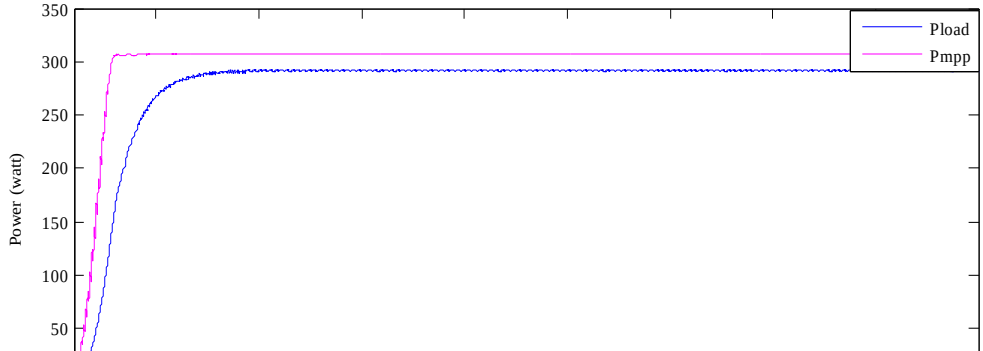

The MPP voltage tracked is 54.6 V and the MPP current tracked is 5.58 A for the open circuit voltage of 64.2 V and short circuit of 5.96 A. Power at the load side is approximately 298 watts and the power at MPP is 305 watts.

3.6 CONCLUSION

Different MPPT algorithms have been studied. Incremental conductance and P & O algorithm of MPPT is modelled and simulated successfully in MATLAB/Simulink environment. The maximum power point (MPP) for PV array voltage and current is achieved and so the maximum power is obtained. Boost converter is designed successfully for MPPT algorithm and constant power is maintained at the input and output side of the converter with slight variation due to switching losses and irrespective of the load change.

CHAPTER 4

GRID CONNECTED SOLAR PHOTOVOLTAIC (SPV) SYSTEM USING SRF CONTROL ALGORITHM

4.1 GENERAL:

The energy demand is increasing & to meet this demand, distributed energy resources (DERs) can be integrated to the grid. In this chapter, SPV power generating system is integrated to the grid as a DER. There are different techniques to control and synchronize the SPV system to the grid and this chapter focuses on synchronous reference frame theory (SRFT) based algorithm. Design and selection of different components ratings used for integration is presented in this chapter. The simulation results for grid integrated SPV system are obtained for different ambient and load conditions such as linear load, non-linear load, unbalanced load and dynamic changes in load.

4.2 GRID CONNECTED SOLAR PHOTOVOLTAIC (SPV) SYSTEM

The cost of PV modules is quite high so there is need for maximum power tracking and its complete evacuation form PV modules for maximizing the system efficiency. Often the PV based generation is tied with the grid which has lowest failure rate so that evacuated power could be effectively utilized based on its availability. PV system could be used for Maximum power point (MPP) applications in standalone mode only when storage support is available whereas, grid connected mode offer infinite storage [29].

The general structure of grid connected PV inverter system, contains two main parts:
- the Plant part (hardware components) such as the PV arrays, PV inverter and the grid utility; the Control using algorithms such as the Maximum-Power-Point-Tracker (MPPT), dc voltage controller, current controller etc. The block diagram representation of grid connected Solar PV array is shown in Figure (4.1).

There are different techniques to control the grid connected photovoltaic (PV) system to synchronize the PV system with utility grid. The grid-following power export control strategy is often used to control the Distributed Energy Resource DER (in this case PV) output power within the voltage and frequency limits as determined by the micro-grid or utility grid. The grid-following approach is employed when direct control of voltage and/or frequency is not required [30]

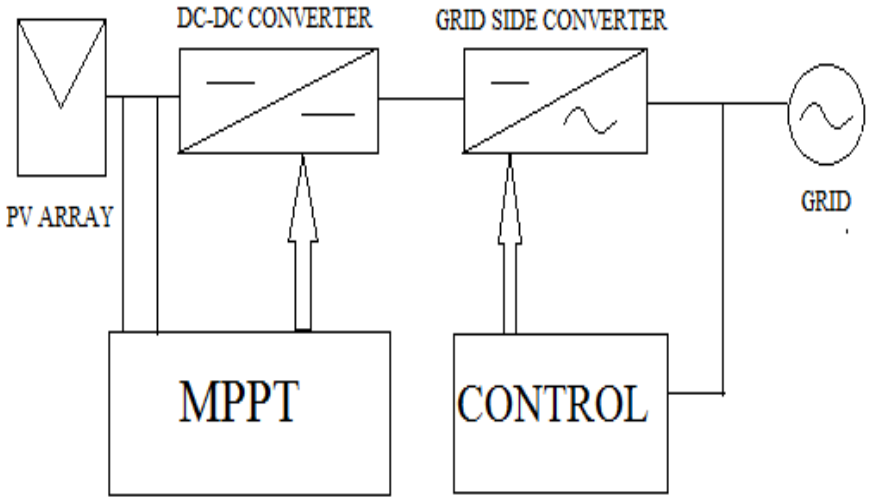

Figure 4.1: Block diagram of grid connected PV system

The integration of solar PV generation to the grid causes some very important technical issues and challenges that affect the quality of power. These include voltage fluctuations, harmonics, reactive power, low power factor (PF), load management etc. and therefore an integration of renewable energy source to the electric grid should fulfil standards of power quality and power quality requirements [31]. Solar PV generation is mainly developed in standalone mode or isolated mode and the main drawback of the isolated mode is that it is limited to very low rating of power generation. Also, it requires very large storage capacity; but in recent years the focus is also shifting to grid connected solar PV generation to augment the grid capacity.

The current source option for PV grid interfacing has been advocated as a means of improving the effectiveness of maximum power tracking (MPT), as the number of series-connected PV in each string is reduced. This reduces the impact of partial shading, and increases system efficiency by using one conversion stage instead of two stages, thereby benefiting from the voltage boost capability of the CSI (lower dc-link voltage and higher ac-side voltage). This approach may not be viable for high-power medium-voltage PV systems, since CSIs usually have higher semiconductor losses compared to VSIs of similar rating, switching frequency, and ac-side voltage. This is because the CSI has twice the semiconductors in the conduction path at any instant, compared to the VSI. Additionally, CSI ability to meet strict grid codes, such as fault ride-through, is doubtful. The use of VSIs as interfacing units for grid integration of PV systems has been investigated extensively in the last five years. This includes the

use of two-level and multilevel VSIs. Two-level VSI is widely used for grid-connected PV systems, regardless of the disadvantages such as high switching losses and relative low-quality output voltage waveforms [32].

The rapid growth and research in solar industry has led to the development of PV systems which are more reliable and efficient, especially for utility power in distributed generation (DG) at medium and low voltages power systems. Several research projects dealing with smart grids are increasingly being carried out in India and abroad. Implementing distributed energy resources (DER) into interconnected grids could be part of the solution to meet the rising electricity demand [30- 33].

In general, a photovoltaic grid-connected system can be seen as a two stage grid-connected inverter. The first stage is a dc-dc converter which is controlled so that the photovoltaic system operates in optimal condition i.e. seeking maximum power point tracking (MPPT). The second stage is a dc-ac converter that is controlled in a way that allows PV to be grid connected. Control is achieved for unity power factor (PF) correction, which means that the output current (entering the grid) must be sinusoidal and in phase with the grid voltage. The dc-dc and dc-ac converters operate independently making the entire control system easier [33] to implement.

In grid-connected mode, it is necessary to control power flow between the PV and the utility. To accomplish this, it is necessary to conduct this mode with the current controller scheme to ensure high power tracking, as it is not sufficient to rely only on the power control mode [34].

Therefore, the current control strategy of the PWM-VSI system is one of the most important aspects of the modern power electronics converters. There are two main categories for current controllers: nonlinear controllers based on closed loop current type PWM, and linear controllers based on open loop voltage type PWM. Both categories of controllers utilize the inner current feedback loop. In the nonlinear controller, hysteresis current control (HCC) is commonly used for three-phase grid-connected VSI systems. The HCC compensates the current error and generates PWM signals with acceptable dynamic response. While the current is controlled independently with a control delay, zero voltage vectors cannot be generated, resulting in a large current ripple with high total harmonic distortion (THD). The linear current controller based space vector PWM (SVPWM) is an adequate

controller, which compensates the current error either by the proportional-integral (PI) regulator or predictive control algorithm while the compensation and PWM generation can be done separately. This controller yields an excellent steady-state response, low current ripple, and a high quality sinusoidal waveform. In addition, the SVPWM can help to improve the controller behaviour because it has favourable features such as constant switching frequency, optimum switching pattern and excellent DC-link voltage utilization [35]. However, only HCC based controller is used for model simulation.

4.3 SYSTEM CONFIGURATION

Figure 4.2 shows the schematic diagram of SPV power generating system interconnected to grid. It consists of solar PV panel, maximum power point tracking (MPPT) controller with dc-dc boost converter, a three leg VSC, varying consumer loads and utility grid. The dc-dc boost converter is used to boost the voltage level of SPV to feed the power to the dc link. Acceptable power quality standards are to be maintained while integrating renewable energy sources to the electric grid.

The grid interconnected SPV power generating system considered as a two stage grid connected converter. As shown in Fig. 4.2, two stages are shown. The first stage consists of DC-DC converter with maximum power point tracking (MPPT) so that SPV extracts maximum power using MPPT algorithm. The second stage is DC-AC converter i.e. insulated gate bipolar transistor (IGBT) based voltage source converter (VSC). The basic control for VSC is to utilize entire power generated from SPV power source, provide necessary compensation and achieve load balancing. Both the DC-DC & DC-AC converters should operate independently.

In this system, the dc link voltage of SPV and VSC is 800V and to regulate the dc link voltage, a dedicated dc voltage PI controller is used. Ripple filter for the proposed system consists of capacitor connected in delta. The system is controlled in a way to compensate reactive power for voltage regulation, power factor improvement, load balancing and harmonics elimination. The control algorithm is developed to evacuate all the generated power from SPV generating system.

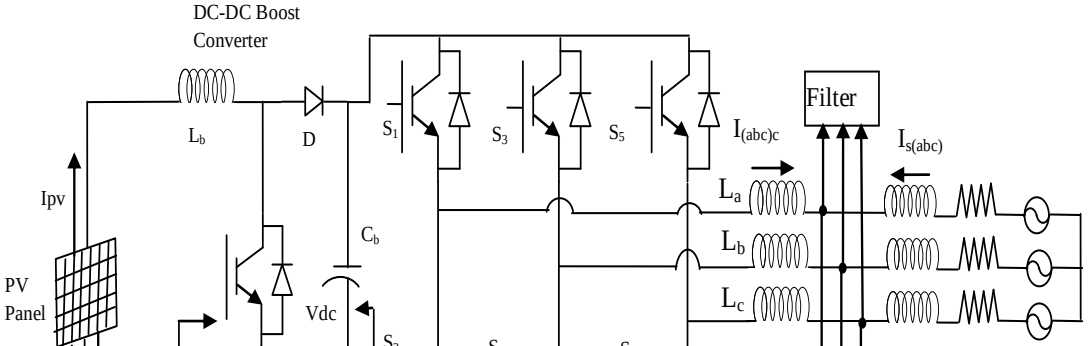

Figure 4.2: Schematic diagram of grid connected SPV system using SRFT control algorithm

4.4 DESIGN & SELECTION OF COMPONENTS:

4.4.1 Selection of DC link Capacitor voltage

The DC link capacitor voltage of VSC is given by e4.1quation

$$V_{dc} = \frac{(2\sqrt{2}V_{LL})}{\sqrt{3}\,m} \tag{4.1}$$

Where V_{LL} is the line to line voltage, and m is modulation index. It can be inferred that the dc link voltage should be greater than twice of the peak of the phase voltage of the system. For the system considered under investigation, DC link voltage is selected as 800V for modulation index of 0.9 and V_{LL} is 415 volt.

4.4.2 Design & Selection of DC link Capacitor

Three different criteria used to select and design DC link capacitor only. DC link capacitor design value could be based on dc-dc boost converter. This is already discussed in boost converter design in previous chapter. The value of dc link capacitor based on this method is calculated to be 350μF. The other two criteria are based on ripple current and energy conservation principle, discussed below.

4.4.2.1 DC link Capacitor based on Ripple Current

The value of DC link capacitor is given by equation 4.2 for load balancing of the consumer loads by VSC

$$C_d = \frac{I_d}{2 * \omega * V_{dcripple}} \tag{4.2}$$

where I_d is the dc link current, ω is angular frequency and $V_{dcripple}$ is 5% of the dc link voltage of VSC. The value of dc link current is calculated under when one phase load removal i.e. 2/3 I_d or 33% of load current is reduced by removing one phase of load. The value of dc link capacitor based on ripple current method is calculated as 1200μF.

4.4.2.2 DC link Capacitor based on Energy Conservation Principle

The design of DC link capacitor (C_d) of VSC depends upon the instantaneous energy available to the VSC at the time of transient. Based on the principle of energy conservation principle, the value of DC capacitor is given below as [12]

$$\frac{1}{2}C_d\left[V_{dc}^2 - V_{dc1}^2\right] = 3V\alpha It \tag{4.3}$$

where V is the phase voltage, I is the phase current, t is the time by which dc link voltage is to be recovered, V_{dc} is the reference DC link voltage and V_{dc1} is the minimum DC link voltage level of DC bus. Taking, V_{dc} = 800 V, V_{dc1} = 790 volt, α= 1.2, t=350 microsecond, the calculated value of C_d is obtained to be1500 μF.

4.4.3 Design of AC Inductors

The selection of ac inductance (L_{abc}) of VSC depends upon the different parameters like the ripple current Δi, switching frequency f_s, modulation index (m), dc link voltage (V_{dc}) and L_f is given by

$$L_f = \frac{\sqrt{3}\, mV_{dc}}{12hf_s\Delta i} \tag{4.4}$$

Taking, m =0.9 , h =1.2 , α= 1.2, t=350 microsecond.

4.5 CONTROL ALGORITHM

Different control algorithms are mentioned in literature like instantaneous reactive power theory (IRPT), synchronous reference frame theory (SRFT) etc. Synchronous reference frame theory (SRFT) is implemented in this chapter and it is used to control the SPV power generating system. Insulated gate bipolar transistor (IGBT) based VSC is used and the dc bus of SPV and VSC is controlled and maintained to a reference voltage in order to provide compensation for the load currents through SPV power.

4.5.1 Control of VSC

The synchronous reference frame theory (SRFT) control used is based on indirect current control. The references for three phase ac main (grid) currents are generated for the control of voltage source converter (VSC). The SRF theory is based on the approach of conversion of three phase components of load current into synchronously rotating d-q frame. The entire control is shown in Figure 4.2. The transformation equation used for abc to dq0 conversion is

$$\begin{bmatrix} i_{Lq} \\ i_{Ld} \\ i_{L0} \end{bmatrix} = \frac{2}{3}\begin{bmatrix} \cos\theta & \cos(\theta - 2\pi/3) & \cos(\theta + 2\pi/3) \\ \sin\theta & \sin(\theta - 2\pi/3) & (9)\text{.}n(\theta + 2\pi/3) \\ 1/2 & 1/2 & 1/2 \end{bmatrix}\begin{bmatrix} i_{La} \\ i_{Lb} \\ i_{Lc} \end{bmatrix} \quad (4.5)$$

where cosθ & sinθ are generated through three phase, phase locked loop (PLL) over source voltage (V_{sa}, V_{sb},V_{sc}). The dq component of current and voltage consists of average component (dc component) and oscillating component (harmonic component).

4.5.2 Control for Unity Power Factor Operation

For the operation of grid connected system in unity power factor mode, the control algorithm is developed on the basis that the utility grid must supply direct axis component of load current as well as active component of current required to regulate the DC bus voltage to the reference level and feed VSC losses (i_{loss}). The dedicated dc voltage PI controller regulates the dc bus voltage to desired reference level and provides the active power transfer for compensation of VSC losses. The value of current required to compensate the losses is given as [13]

$$i_w(k) = i_w(k-1) + K_{pd}\left(v_{de}(k) - v_{de}(k-1)\right) + K_{id}\left(v_{de}(k)\right) \quad (4.6)$$

where $v_{de}(k) = v^*_{dc}(k) - v_{dc}(k)$

is the error in between reference voltage and measured voltage at the dc link. K_{pd}& K_{id} are proportional and integral gains of the PI controller.

The reference current generated for ‘d’ component of grid current is given as

$$i^*_d = i_{ddc} + i_{loss} \quad (4.7)$$

4.2.3Control for Zero Voltage Regulation Mode of Operation

For zero voltage regulation at point of common coupling (PCC) of the proposed system, it is considered that the PV must deliver the quadrature axis current component (i_q) of load current and the ac mains (grid) should deliver remaining part of direct axis current component (i_d) of load current which is not supplied by PV system. An additional PI controller is used to regulate the voltage at the point of PCC. The input for this controller is the error signal generated due to the difference of measured PCC voltage (V_t) and the reference voltage (V^*_t). The output of the PI controller is considered to be quadrature component of current (I^*_q).

The amplitude of PCC voltage is given by the equation ()

$$V_t = \left(\frac{2}{3}\right)^{\frac{1}{2}}(v^2_{sa} + v^2_{sb} + v^2_{sc})^{1/2} \quad (4.8)$$

The reactive power component of current generated through PI controller by the difference of measured voltage at PCC (V_t) and the reference voltage of PCC (V_t^*) is given as

$$i_{qr}(k) = i_{qr}(k-1) + K_{pq}\left(v_{te}(k) - v_{te}(k-1)\right) + K_{iq}\left(v_{te}(k)\right) \quad (4.9)$$

where $v_{te}(k) = v_t^*(k) - v_t(k)$

is the error between reference voltage of PCC & measured voltage at PCC. K_{pd}& K_{id} are the proportional and integral gains of PCC voltage PI controller.

The reference current generated for the grid is given as

$$i_q^* = i_{qdc} - i_{qr} \quad (4.10)$$

The reference for the ac mains grid is now calculated in terms of abc components using inverse Park's transformation given as

$$\begin{bmatrix} i_a^* \\ i_b^* \\ i_c^* \end{bmatrix} = \begin{bmatrix} \cos\theta & \sin\theta & 1 \\ \cos(\theta - 2\pi/3) & \sin(\theta - 2\pi/3) & 1 \\ \cos(\theta + 2\pi/3) & \sin(\theta + 2\pi/3) & 1 \end{bmatrix} \begin{bmatrix} i_d^* \\ i_q^* \\ i_0^* \end{bmatrix} \quad (4.11)$$

4.5 MATLAB/Simulik MODEL:

MATLAB/Simulink model of grid connected solar photovoltaic system is shown in Figure 4.3. The model consists of three phase AC grid/source, solar PV system, filter, load, subsystem block of control algorithm, P-Q measurement block for measuring active and reactive power, subsystem block of scopes and power-gui block

IGBT based VSC is shown in Figure 4.3 to couple solar PV system to the grid. The model is developed using MATLAB/Simulink to demonstrate the operation of grid connected SPV system.

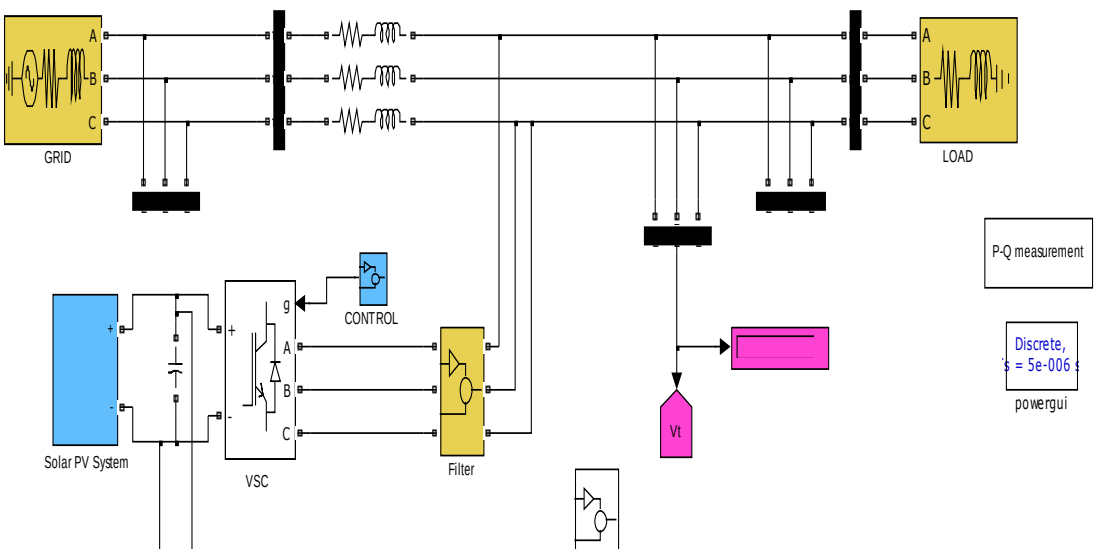

4.7 RESULTS AND DISCUSSIONS

Results are obtained for unity power factor operation (UPF) and zero voltage regulation (ZVR) using SRF theory. Simulation results under different load conditions, varying irradiance for both unity power factor correction and zero voltage regulation are discussed. Performance of the grid connected SPV power generating system is depicted in terms of grid voltage (V_s), DC bus voltage (V_{dc}), AC grid currents, (I_s), load currents (I_{load}), the active power supplied from /to grid (P), the reactive power (Q), solar PV current (I_{pv}), solar PV voltage (V_{pv}), PCC currents (I_{pcc}), PCC voltage (V_{pcc}), and terminal voltage at PCC (V_t).

4.7.1 For Unity Power Factor (UPF) operation

For unity power factor operation, the grid voltage (V_s) and grid current (I_s) are maintained at unity power factor under different conditions throughout. THD of supply currents is maintained as per IEEE-519 standards [38].

4.7.1.1 Performance of the system under linear load condition

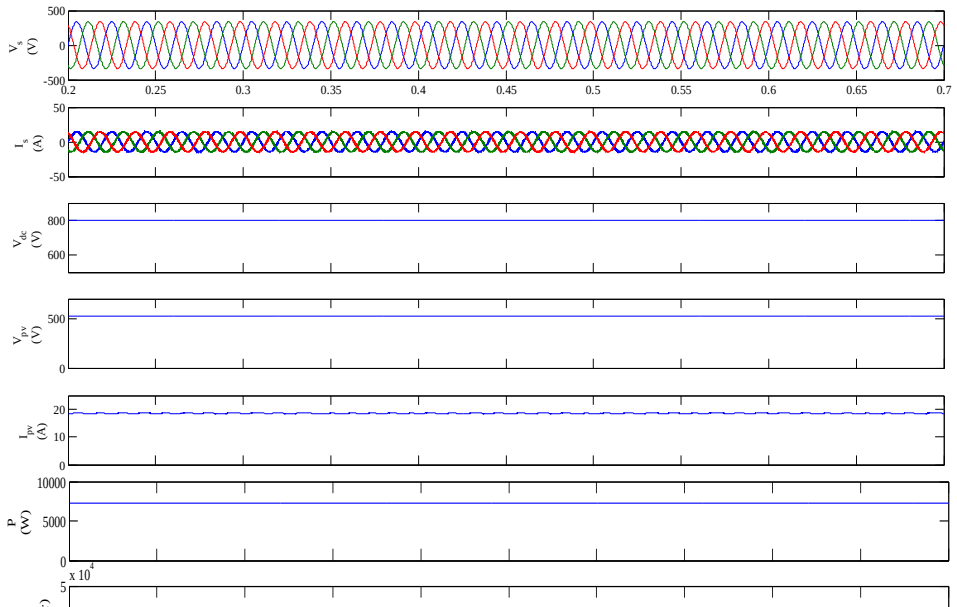

Figure 4.4a: Performance of system at linear load for unity power factor

Performance of the grid interfaced SPV power generating system under linear load of 15 kVA at lagging PF of 0.8 for UPF in a distribution system is illustrated in Fig. 4.4a. V_{dc} is maintained at the desired reference level of 800 V and the entire PV power is evacuated. The overall reactive power of load is supplied by the SPV and a portion of total load real power according its capacity and the connected load rating. The remaining active power is supplied by the grid (if required) and UPF is achieved and maintained for V_s & I_s.

Fig. 4.4b shows the waveform and harmonic spectrum for PCC current (I_{pcc}), grid/source current (I_s) and PCC voltage (V_{pcc}). THD is maintained well within the limits 5% according to the IEEE-519 standards.

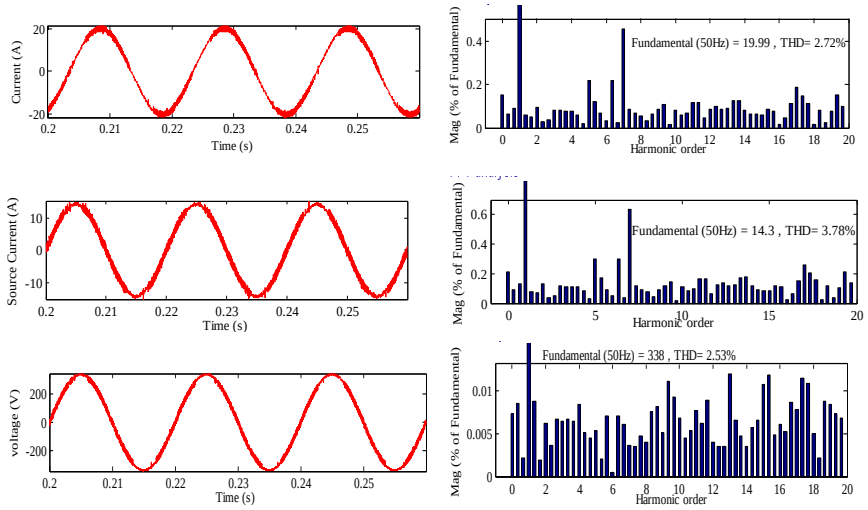

Figure 4.4b: Waveform and harmonic spectrum for I_{pcc}, I_s, V_{pcc}

4.4.1.2 Performance of the system for linear load with varying irradiance condition

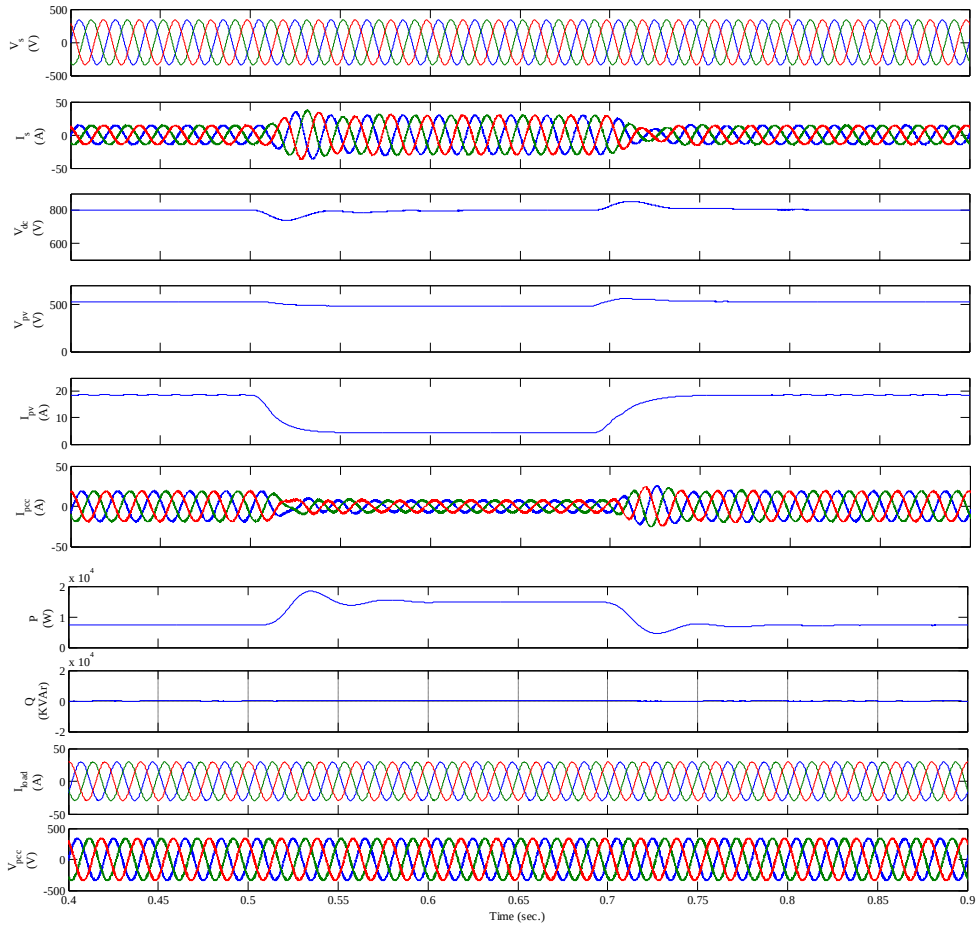

Figure 4.5: Performance of system at linear load for unity power factor under varying irradiance

Next, the performance of the grid interfaced SPV power generating system for linear load of 15 kVA at lagging pf 0.8 under varying irradiance condition is studied for UPF. The results are illustrated in Fig. 4.5. Irradiance is varied from 1000 kW/m^2 to 200 kW/m^2 at t=0.5 sec. and the MPP is tracked for new irradiance by MPPT-boost converter. V_{dc} is maintained at the desired reference level of 800 V and the entire PV power is evacuated. It is observed that the entire reactive power of load is supplied by the SPV. SPV also feeds the real power upto its capacity. remaining active power of kW is supplied by the grid as the connected load has a requirement of kw . UPF is achieved and maintained for V_s & I_s. In this case, it is observed that as the irradiance is reduced from 1000 kW/m^2 to 200 kW/m^2 , the short circuit current of PV is also reduced. Hence, the power generated by the PV array for new irradiance level is lesser than before. Therefore, some of the reactive power may need to be supplied by grid as the SPV is supplying nearly 20% of the initial power supplied. Since, the grid

is supplying reactive power also, the power factor is not exactly unity under low irradiance of 200 kW/m^2. At t=0.7 sec. irradiance is changed to 1000 kW/m^2 and then UPF is achieved again. It is also observed that if the irradiance level does not vary too much from the standard operating value of 1000 kW/m^2, the UPF between supply voltage and current can be maintained.

Performance of the grid interfaced SPV power generating system for linear load of 15 kVA at lagging pf of 0.8 under linear load varying condition for UPF in a distribution system is illustrated in Fig. 4.6a. The load is varied from 15 kVA to 20 kVA at t=0.3 sec. It is observed that the load current (I_{load}) is increased and accordingly grid current (I_s) has to increase to meet the load demand. V_{dc} is regulated by the controller at the desired reference level of 800 V and the PV power is evacuated. The overall reactive power of load is supplied by the SPV. UPF is achieved and maintained for V_s & I_s. Therefore real power is shared by grid and SPV but the reactive power is supplied by SPV solely. At t=0.5 sec the load is switched from 20kVA to 15kVA and again the dc link is maintained and PCC current (I_{pcc}) and PCC voltage (V_{pcc}) is also maintained.
Fig. 4.6b shows the waveform and harmonic spectrum for PCC current (I_{pcc}), grid/source current (I_s) and PCC voltage (V_{pcc}). THD is maintained under linear load varying condition for UPF in a distribution system well within the limits 5% according to the IEEE-519 standards. THD shown is calculated at t=0.3 sec., the time of load variation

4.4.1.3Performance of the system for linear load varying condition

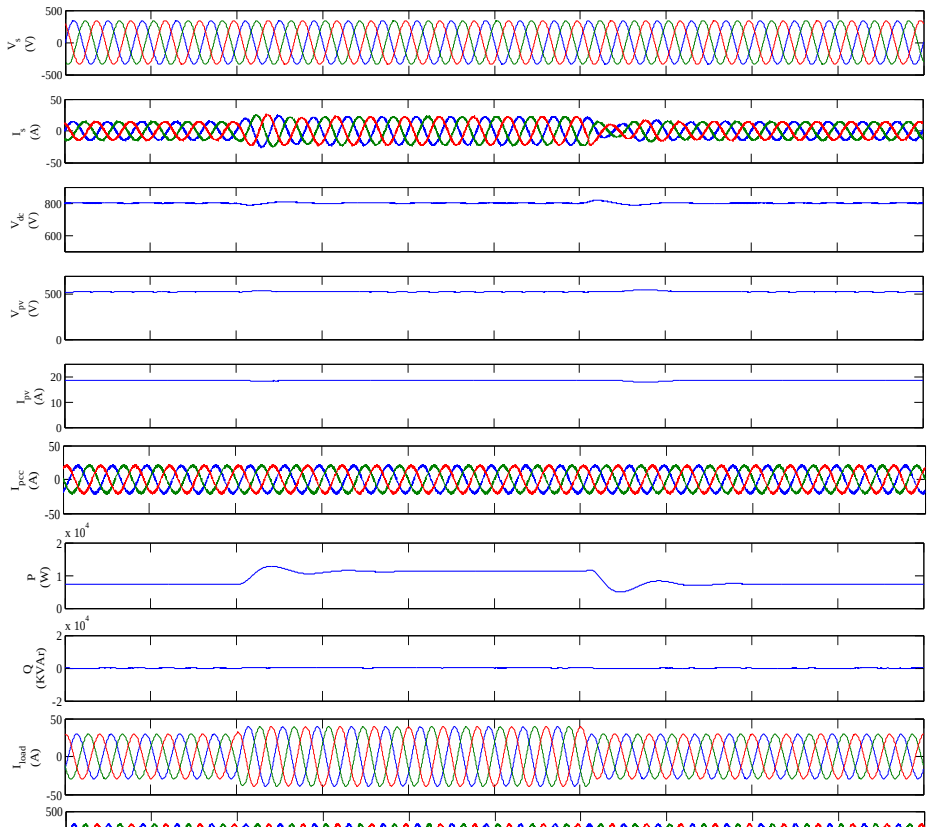

Figure 4.6a: Performance of system for unity power factor under varying linear load

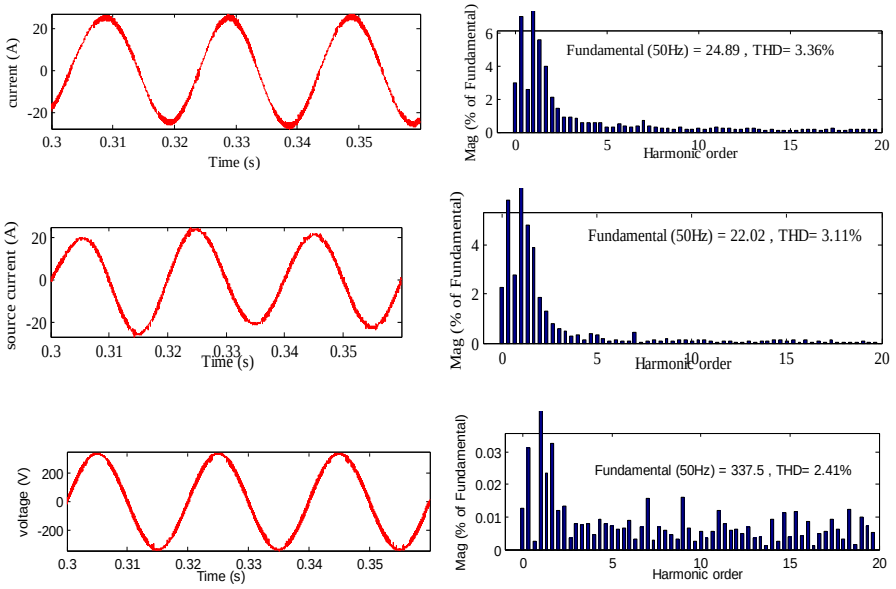

Figure 4.6b: Waveform and harmonic spectrum for I_{pcc}, I_s and V_{pcc} under varying linear load

4.4.1.4Performance of the system for unbalanced linear load condition

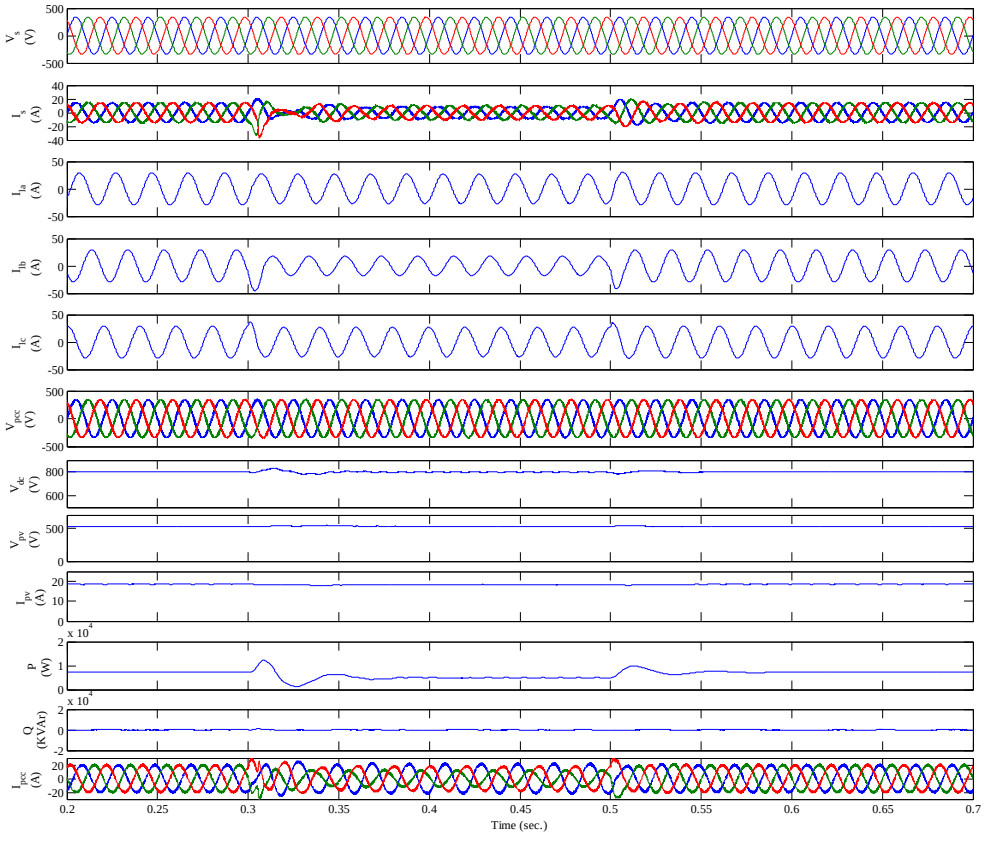

Figure 4.7a: Performance of system for unity power factor and load balancing under unbalanced linear load

Performance of the grid interfaced SPV system for linear load of 15 kVA at lagging PF of 0.8 under unbalanced linear load condition is illustrated in Fig. 4.7a. The load is switched to unbalanced condition at t=0.3 sec. At t=0.3 sec, one phase of the load is switched from 15 kVA to 7.5 kVA and other two phases remain loaded with 15 kVA. The load current is still balanced by the PCC current (I_{pcc}) supplied by SPV and compensation is provided by the PCC current (I_{pcc}) supplied by SPV and I_{pcc} become distorted. The overall load current, hence power required by the load is decreased and therefore the power supplied by the grid is reduced. V_{dc} is maintained at the desired reference level of 800 V and the PV power is evacuated. The overall reactive power of load is supplied by the SPV and also the real power upto its capacity and remaining active power is supplied by the grid and UPF is achieved and maintained for V_s & I_s. At t=0.5 sec. the load is switched to the balanced condition.

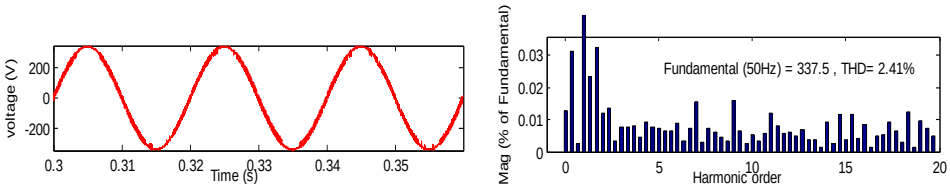

Figure 4.7b: Waveform and harmonic spectrum for V_{pcc} under varying linear load

Fig. 4.7b shows the waveform and harmonic spectrum for PCC voltage (V_{pcc}). THD is maintained under linear load varying condition for UPF in a distribution system well within the limits of 5% according to the IEEE-519 standards. THD shown is calculated at t=0.3 sec. i.e. at the time of unbalancing of load.

4.4.1.5 Performance of the system for non-linear load condition

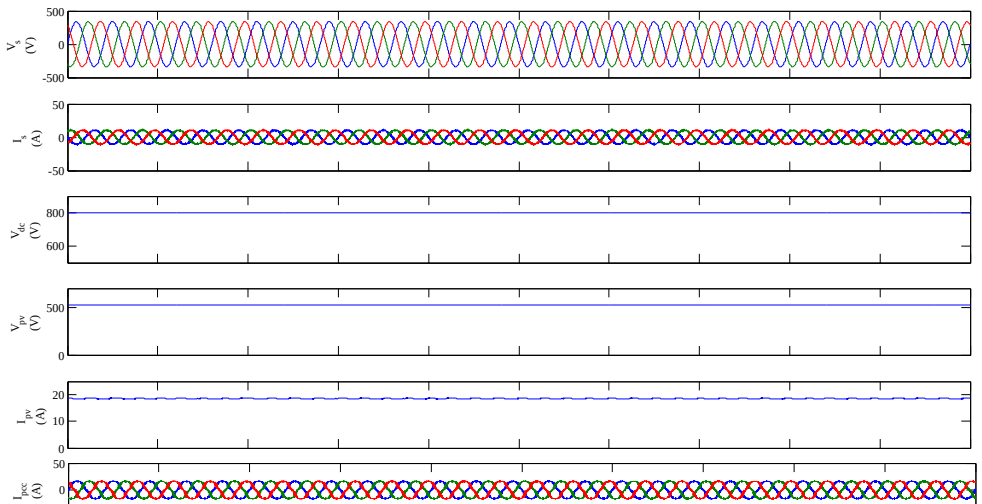

Performance of the grid interfaced SPV power generating system for non-linear load of 25Ω and 300mH is illustrated in Fig. 4.8a. V_{dc} is regulated at the desired reference level of 800 V with the help of PI controller and the PV power is evacuated. The overall reactive power of load is supplied by the SPV and also the real power upto its capacity and remaining active power is supplied by the grid and UPF is achieved and maintained for V_s & I_s. The compensation provided by the VSC-SPV and therefore THD of load current is improved.

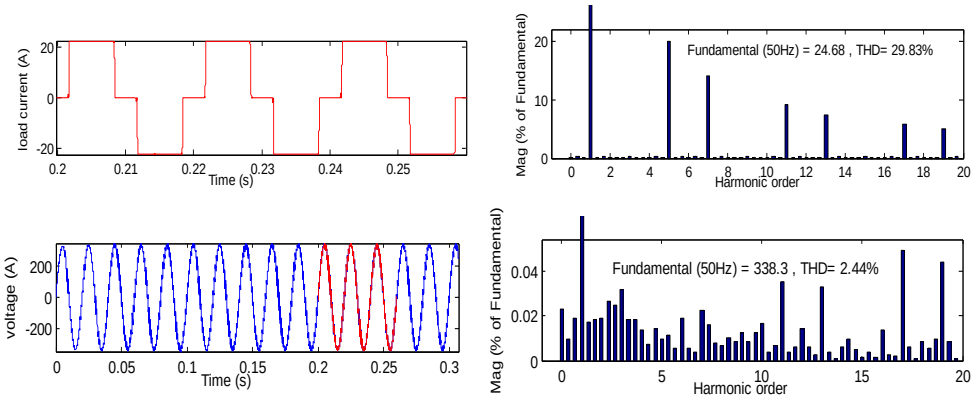

Figure 4.8b: Waveform and harmonic spectrum for I_{load} and V_{pcc} under non-linear load

Fig. 4.8b shows the waveform and harmonic spectrum for load current (I_{load}) and PCC voltage (V_{pcc}). THD is maintained well within the limits of 5% for V_{pcc} according to the IEEE-519 standards and THD of load current is improved by the compensation through PCC current (I_{pcc}).

Performance of the grid interfaced SPV power generating system for non-linear load of 25Ω and 300mH under unbalanced load condition for UPF in a distribution system is illustrated in Fig. 4.9a. It can be observed that the grid currents are in phase with

PCC voltages demonstrating unity power factor at AC mains. The load is been switched to unbalanced condition at at t=0.3 sec. The unbalancing in consumer loads is realized by removing the load on one phase at 0.3 sec. and further by removing load on other two phases at 0.45 sec,. V_{dc} is maintained at the desired reference level of 800 V and the PV power is evacuated. The overall reactive power of load is supplied by the SPV and also the real power upto its capacity and remaining active power is supplied by the grid and UPF is achieved and maintained for V_s & I_s. When the load is become unbalanced then the power required by the load will become less than the capacity of SPV and therefore the power is flowing into the grid. The sign of the power supplied by the grid will become negative and grid currents (I_s) will be in phase opposition to the grid voltage (V_s). PCC current provided the compensation for load current making the grid current balanced and improving the THD of load current. At t=0.45 all phases of the load is been removed and all the power from SPV is flowing into the grid and the sign of supplied power from grid is negative. At t=0.6 sec. the load is switched to the balanced condition.

4.4.1.6 Performance of the system for unbalanced non-linear load condition

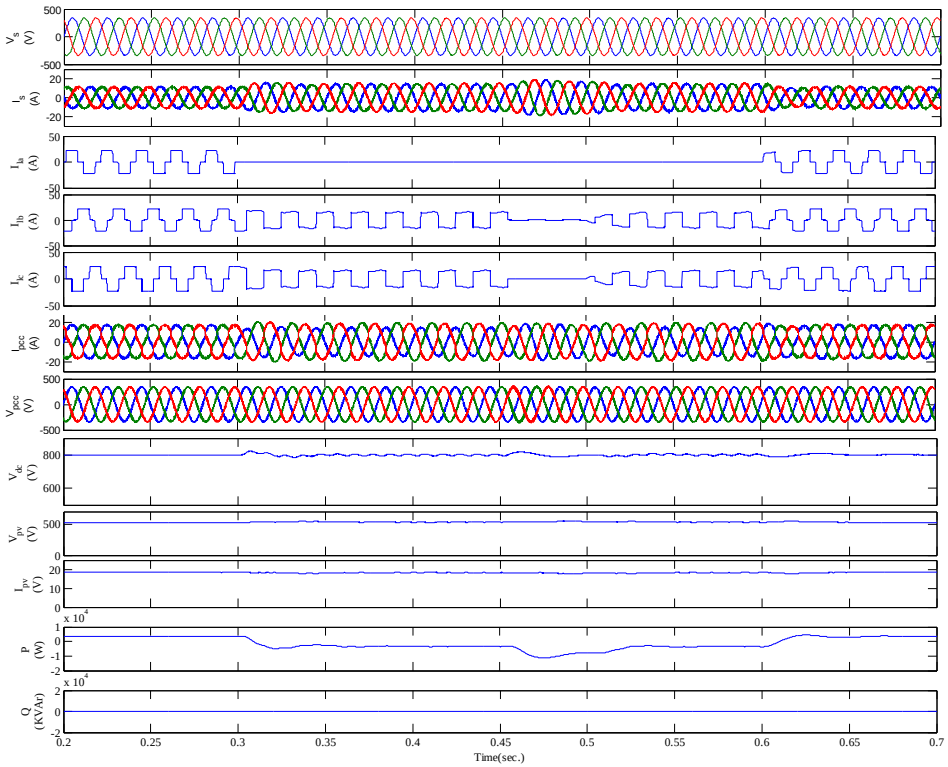

Figure 4.9a: Performance of system for unity power factor and load balancing under unbalanced non-linear load condition

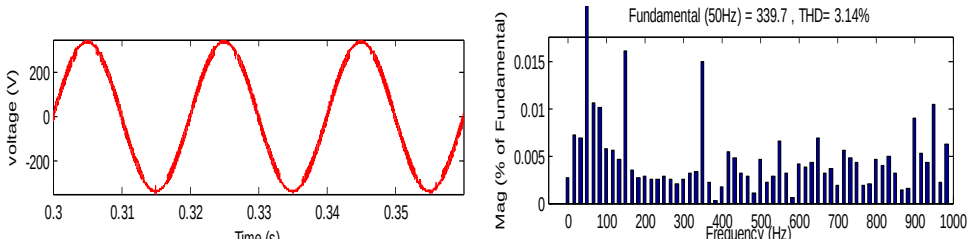

Figure 4.9b: Waveform and harmonic spectrum for V_{pcc} under unbalanced non-linear load

Fig. 4.9b shows the waveform and harmonic spectrum for PCC voltage (V_{pcc}). THD is maintained under linear load varying condition for UPF in a distribution system well within the limits of 5% according to the IEEE-519 standards. THD shown is calculated at t=0.3 sec. i.e. at the time of unbalancing of load.

4.7.2 For Zero Voltage Regulation (ZVR) operation

For zero voltage regulation operation (ZVR), the terminal voltage (V_t) of PCC voltage (V_{pcc}) is regulated to desired reference voltage level and zero voltage regulation is required under different conditions throughout and power quality is also maintained according to IEEE-519 standards.

4.7.2.1 Performance of the system under linear load condition

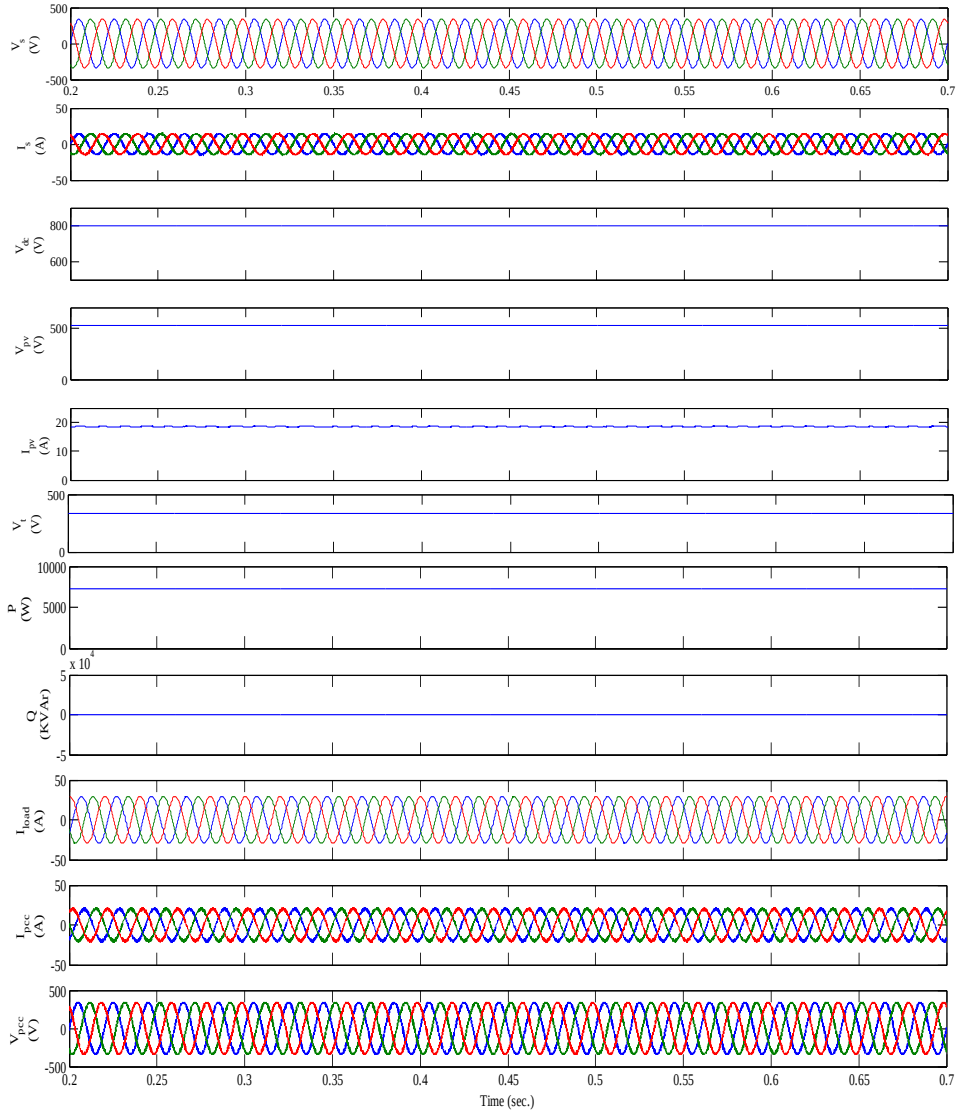

Figure 4.10a: Performance of system at linear load for zero voltage regulation

Performance of the grid interfaced SPV power generating system under linear load of 15 kVA at lagging PF of 0.8 for UPF in a distribution system is illustrated in Fig. 4.10a. V_{dc} is maintained at the desired reference level of 800 V and the PV power is evacuated. The overall reactive power of load is supplied by the SPV and also the real power upto its capacity and remaining active power is supplied by the grid and ZVR is achieved and maintained for V_t of PCC voltage (V_{pcc}).

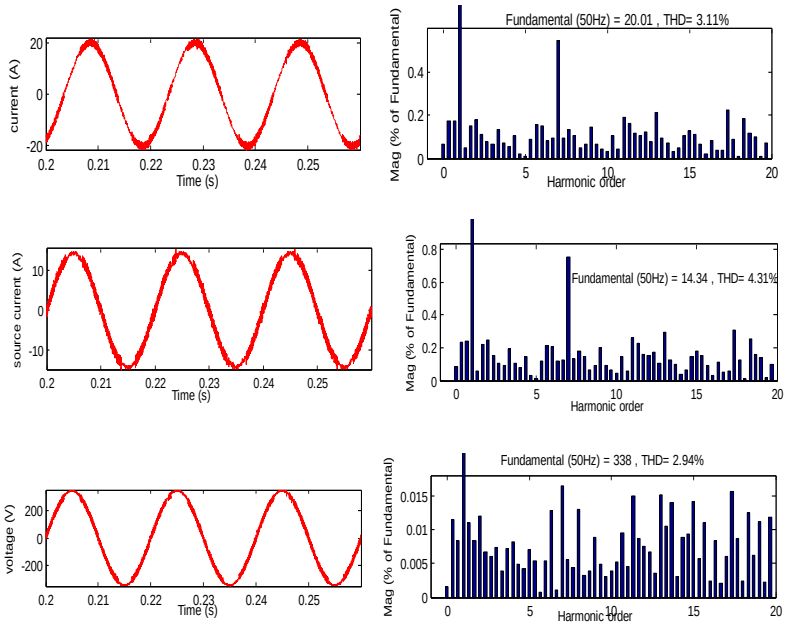

Figure 4.10b: Waveform and harmonic spectrum for I_{pcc}, I_s, V_{pcc}

Fig. 4.10b shows the waveform and harmonic spectrum for PCC current (I_{pcc}), source (grid) current (I_s) and PCC voltage (V_{pcc}). THD is maintained well within the limits 5% according to the IEEE-519 standards.

Performance of the grid interfaced SPV power generating system at linear load of 15 kVA at lagging PF of 0.8 under varying irradiance condition for zero voltage regulation in a distribution system is illustrated in Fig. 4.11. Irradiance is been varied from 1000 kW/m^2 to 200 kW/m^2 at t=0.5 sec. and the MPP is tracked for new irradiance by MPPT-boost converter. V_{dc} is maintained at the desired reference level of 800 V and the PV power is evacuated. The overall reactive power of load is supplied by the SPV and also the real power upto its capacity and remaining active power is supplied by the grid and ZVR is achieved and maintained for V_t of PCC

voltage (V_{pcc}). V_t is maintained at the desired reference level of 338V. In this case as the irradiance is reduced therefore the short circuit current of PV is also reduced and the power supplied by the PV array for new irradiance is less therefore some of the reactive power is also supplied by grid also. At t=0.7 sec. irradiance is changed to 1000 kW/m^2 and then ZVR is achieved again and also V_t and V_{dc} is also maintained to their reference value.

4.7.2.2 Performance of the system under varying irradiance condition for linear load:

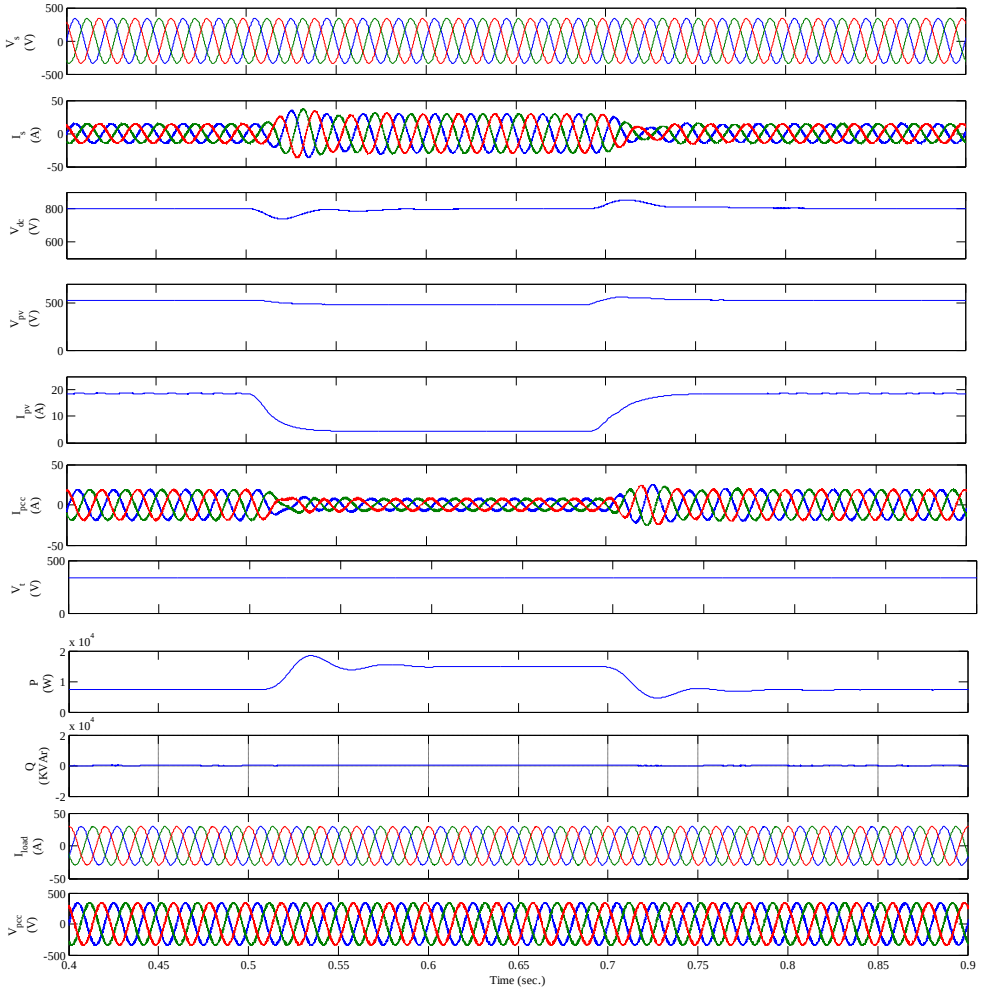

Figure 4.11: Performance of system for zero voltage regulation under varying irradiance at linear load

Performance of the grid interfaced SPV power generating system for linear load of 15 kVA at lagging PF of 0.8 under linear load varying condition for ZVR in a distribution system is illustrated in Fig. 4.12a. The load is been switched from 15 kVA to 20 kVA at t=0.3 sec and the load current (I_{load}) is increased and accordingly grid current (I_s) and then power supplied by grid (P) is been increased. V_{dc} is maintained at the desired reference level of 800 V and the PV power is evacuated.

The overall reactive power of load is supplied by the SPV and also the real power upto its capacity and remaining active power is supplied by the grid and ZVR is achieved and maintained for V_t of PCC voltage (V_{pcc}). Real power is shared by grid and SPV but the reactive power is supplied by SPV mainly. At t=0.5 sec the load is switched from 20kVA to 15kVA and again the

4.4.2.3Performance of the system for linear load varying condition

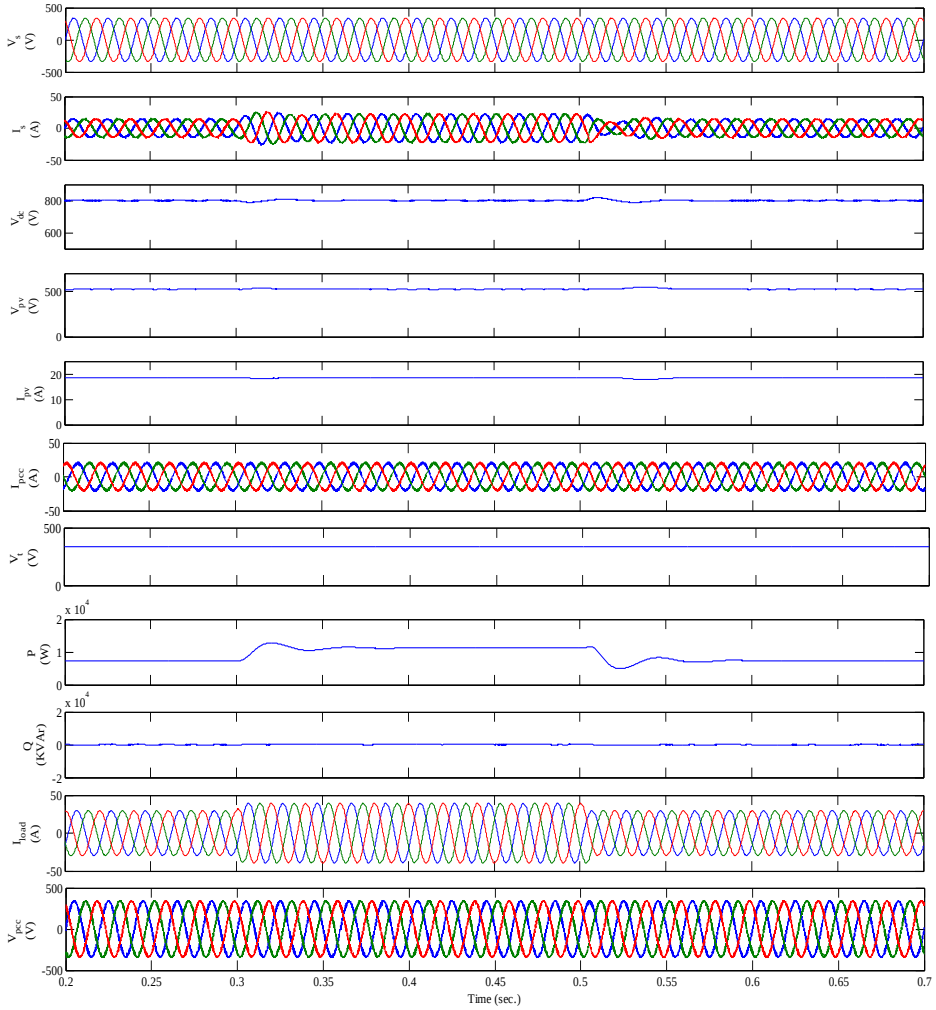

Figure 4.12a: Performance of system for zero voltage regulation under varying linear load

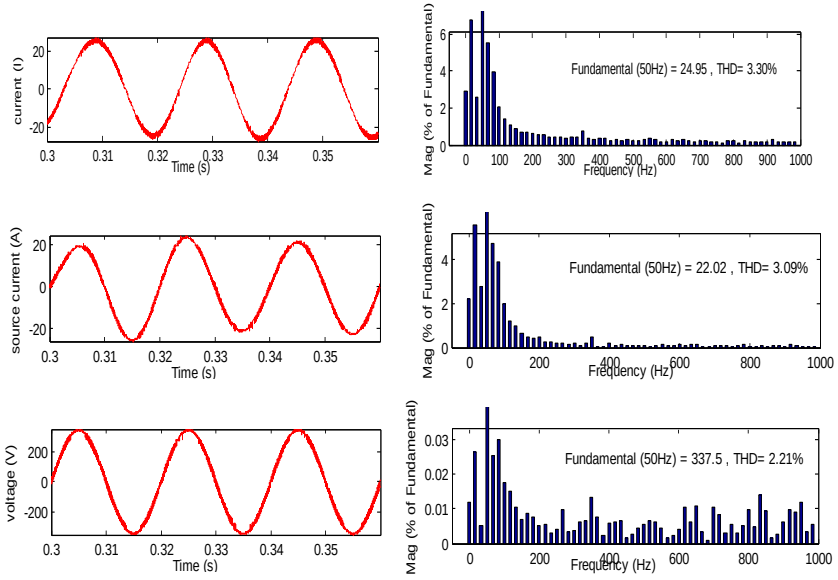

Figure 4.12b: Waveform and harmonic spectrum for I_{pcc}, I_s and V_{pcc} under varying linear load

dc link is maintained and PCC current (I_{pcc}), PCC voltage (V_{pcc}) and terminal voltage (V_t) is also maintained.

Fig. 4.6b shows the waveform and harmonic spectrum for PCC current (I_{pcc}), grid/source current (I_s) and PCC voltage (V_{pcc}). THD is maintained under linear load varying condition for ZVR in a distribution system well within the limits 5% according to the IEEE-519 standards. THD shown is calculated at t=0.3 sec. i.e. at the time of load variation.

4.4.2.4Performance of the system for unbalanced linear load condition

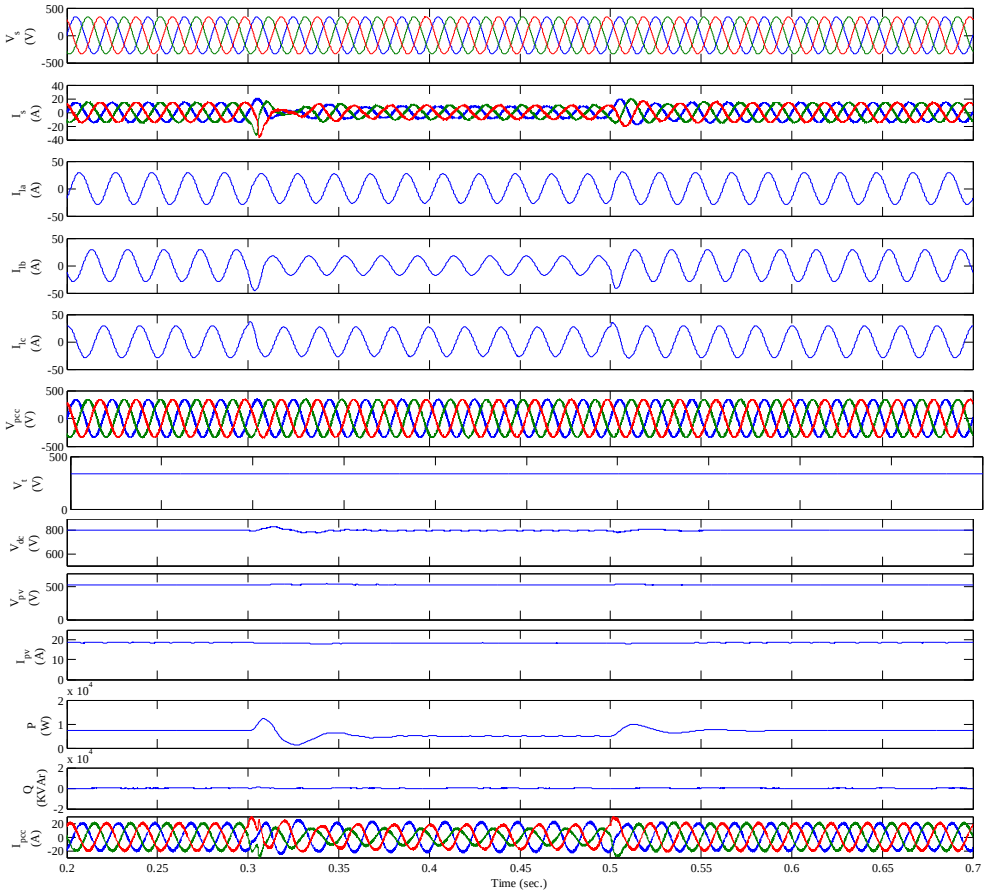

Figure 4.13a: Performance of system for zero voltage regulationand load balancing under unbalanced linear load

Performance of the grid interfaced SPV power generating system for linear load of 15 kVA at lagging PF of 0.8 under unbalanced linear load condition for ZVR in a distribution system is illustrated in Fig. 4.13a. The load is been switched to unbalanced condition at at t=0.3 sec. At t=0.3 sec, one phase of the load is switched from 15 kVA to 7.5 kVA and other two phases are loaded with 15 kVA. The load current is still balanced by the PCC current (I_{pcc}) supplied by SPV and compensation

is provided by the PCC current (I_{pcc}) supplied by SPV and I_{pcc} become distorted. The overall load current is decreased, hence power required by the load is decreased and therefore the power supplied by the grid is reduced. V_{dc} is maintained at the desired reference level of 800 V and the PV power is evacuated. The overall reactive power of load is supplied by the SPV and also the real power upto its capacity and remaining active power is supplied by the grid and ZVR is achieved and maintained for terminal voltage V_t of PCC voltage (V_{pcc}). At t=0.5 sec. the load is switched to the balanced condition. The terminal voltage (V_t) is regulated to its reference value of 338 V throughout the simulation.

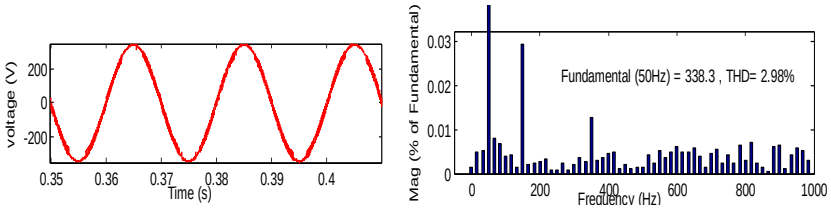

Figure 4.13b: Waveform and harmonic spectrum for V_{pcc} under varying linear load

Fig. 4.13b shows the waveform and harmonic spectrum for PCC voltage (V_{pcc}). THD is maintained under linear load varying condition for UPF in a distribution system well within the limits of 5% according to the IEEE-519 standards. THD shown is calculated at t=0.3 sec. i.e. at the time of unbalancing of load.

Performance of the grid interfaced SPV power generating system for non-linear load of 25Ω and 300mH balanced condition for ZVR in a distribution system is illustrated in Fig. 4.14a. V_{dc} & V_t is maintained at the desired reference level of 800 V and 338 V respectively and the PV power is evacuated. The overall reactive power of load is supplied by the SPV and also the real power upto its capacity and remaining active power is supplied by the grid and ZVR is achieved and maintained for terminal voltage V_t of PCC voltage (V_{pcc}). The compensation provided by the VSC-SPV and therefore THD of load current is improved.

4.4.2.5 Performance of the system for non-linear load condition

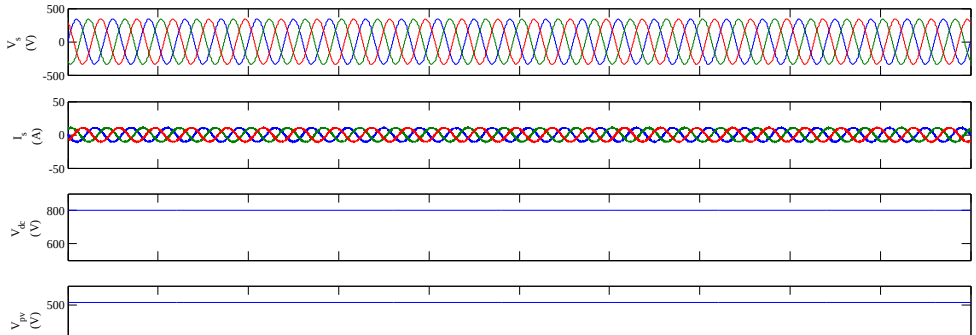

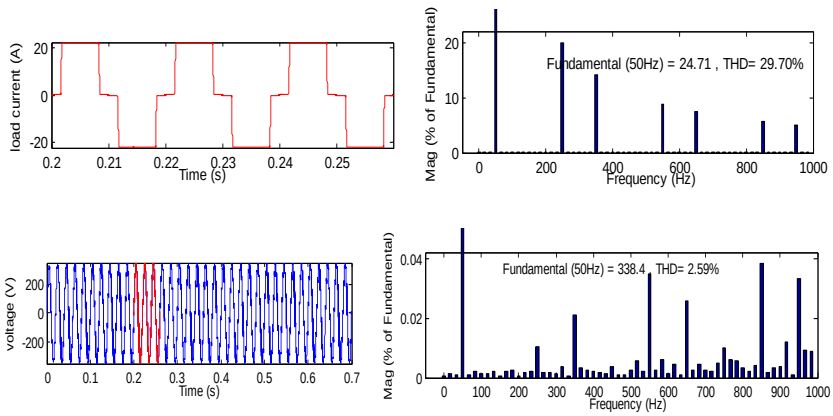

Figure 4.14b: Waveform and harmonic spectrum for I_{load} and V_{pcc} under non-linear load

Performance of the grid interfaced SPV power generating system for non-linear load of 25Ω and 300mH under unbalanced load condition for ZVR in a distribution system is illustrated in Fig. 4.9a. It can be observed that the terminal voltage (V_t) of PCC voltage (V_{pcc}) is regulated at reference level of 338 V & therefore PCC voltage demonstrating

4.4.2.6 Performance of the system for unbalanced non-linear load condition

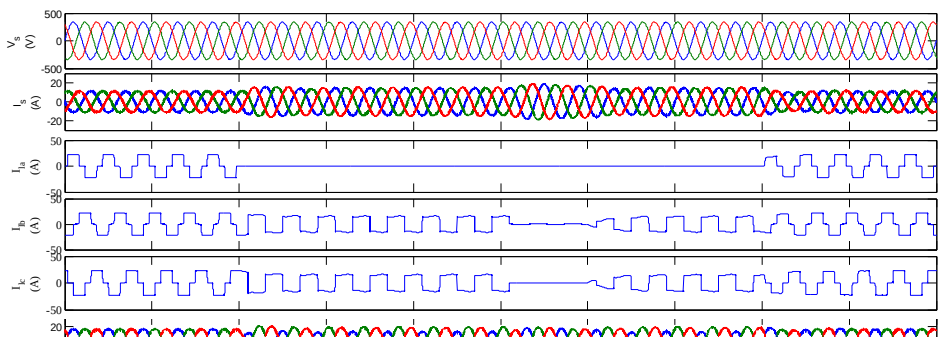

Figure 4.15a: Performance of system for zero voltage regulation and load balancing under unbalanced non-linear

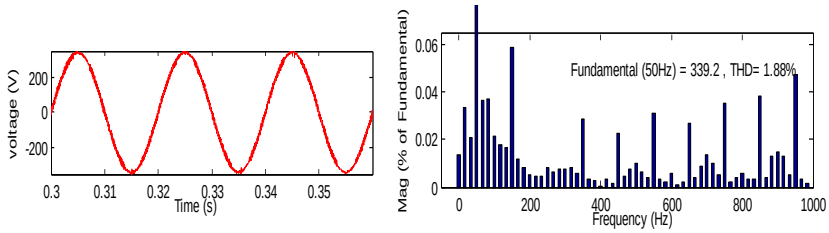

Figure 4.15b: Waveform and harmonic spectrum for V_{pcc} under unbalanced non-linear load

zero voltage regulation at PCC. The load is been switched to unbalanced condition at at t=0.3 sec. The unbalancing in consumer loads is realized by removing the load on one phase at 0.3 sec. and further by removing load on other two phases at 0.45 sec,. V_{dc} is maintained at the desired reference level of 800 V and the PV power is evacuated. The overall reactive power of load is supplied by the SPV and also the real power upto its capacity and remaining active power is supplied by the grid and for terminal voltage V_t of PCC voltage (V_{pcc}). When the load is become unbalanced then the power required by the load will become less than the capacity of SPV and therefore the power is flowing into the grid. The sign of the power supplied by the grid will become negative and grid currents (I_s) will be in phase opposition to the grid voltage (V_s). PCC current provided the compensation for load current making the grid current balanced and improving the THD of load current. At t=0.45 all phases of the load is been removed and all the power from SPV is flowing into the grid and the sign of supplied power from grid is negative. At t=0.6 sec. the load is switched to the balanced condition and terminal voltage (V_t) is regulated at reference obtaining ZVR.

Fig. 4.15b shows the waveform and harmonic spectrum for PCC voltage (V_{pcc}). THD is maintained under linear load varying condition for UPF in a distribution system well within the limits of 5% according to the IEEE-519 standards. THD shown is calculated at t=0.3 sec. i.e. at the time of unbalancing of load.

4.6 CONCLUSION:

The grid interconnected SPV power generating system performance is investigated and analyzed successfully under different conditions like load variation for linear load at lagging power factor load and load unbalancing condition for linear and non-linear loads in two different modes: unity power factor (UPF) and zero voltage regulation (ZVR) . Selection and design of components for grid coupling of SPV system is designed. The DC bus voltage (V_{dc}) and terminal voltage (V_t) for PCC voltage maintained at desired reference level for different conditions along with harmonics elimination and load balancing. The desired results were obtained successfully and total harmonic distortion (THD) is maintained according to IEEE-519 standards for PCC voltage (V_{pcc}) and PCC current (I_{pcc}).

CHAPTER 5

GRID CONNECTED SOLAR PHOTOVOLTAIC (SPV) SYSTEM USING POWER BALANCE THEORY ALGORITHM

5.1 GENERAL

In the last chapter, the grid connected photovoltaic (PV) system is controlled using synchronous reference frame theory (SRFT) based algorithm and results for different conditions are obtained. In this chapter, the grid connected SPV power generating system is controlled using power balance theory (PBT) or unit template method. Results for different loading conditions and linear/ nonlinear loads are presented in this chapter.

5.2 CONTROL ALGORITHM

Different control algorithms are mentioned in literature [36, 37] such as instantaneous reactive power theory (IRPT), synchronous reference frame theory (SRFT) etc. Synchronous reference frame theory (SRFT) is used to control the SPV power generating system in the previous chapter. Power balance theory (PBT) control algorithm is used here and the algorithm is depicted in Fig. 5.1. Insulated gate bipolar transistor (IGBT) based VSC is used to couple the PV system to the grid. The dc bus of VSC is controlled and maintained to a reference voltage in order to provide compensation for the load currents through SPV power. The generation of unit templates is discussed.

5.2.1 Generation of In phase Unit templates of Reference Grid Currents

The use of power balance theory is based on the generation of active power components of grid currents, which are computed using system voltages and load currents. One PI controller is realised over dc bus voltage controller. The unit in-phase templates (u_{sa}, u_{sb}, u_{sc}) are calculated from the three phase voltages (v_{sa}, v_{sb}, v_{sc}) as

$$u_{sa} = \frac{v_{sa}}{V_t}, u_{sb} = \frac{v_{sb}}{V_t}, u_{sc} = \frac{v_{sc}}{V_t} \tag{5.1}$$

where V_t is amplitude of three phase PCC voltage & calculated as

$$V_t = \left(\frac{2}{3}\right)^{\frac{1}{2}} (v^2_{sa} + v^2_{sb} + v^2_{sc})^{1/2} \tag{5.2}$$

The output of the PI controller ω

$$i_w(k) = i_w(k-1) + K_{pd}\left(v_{de}(k) - v_{de}(k-1)\right) + K_{id}\left(v_{de}(k)\right) \tag{5.3}$$

regulate the dc bus voltage of VSC in terms of current given by

where $v_{de}(k) = v^{*}_{dc}(k) - v_{dc}(k)$

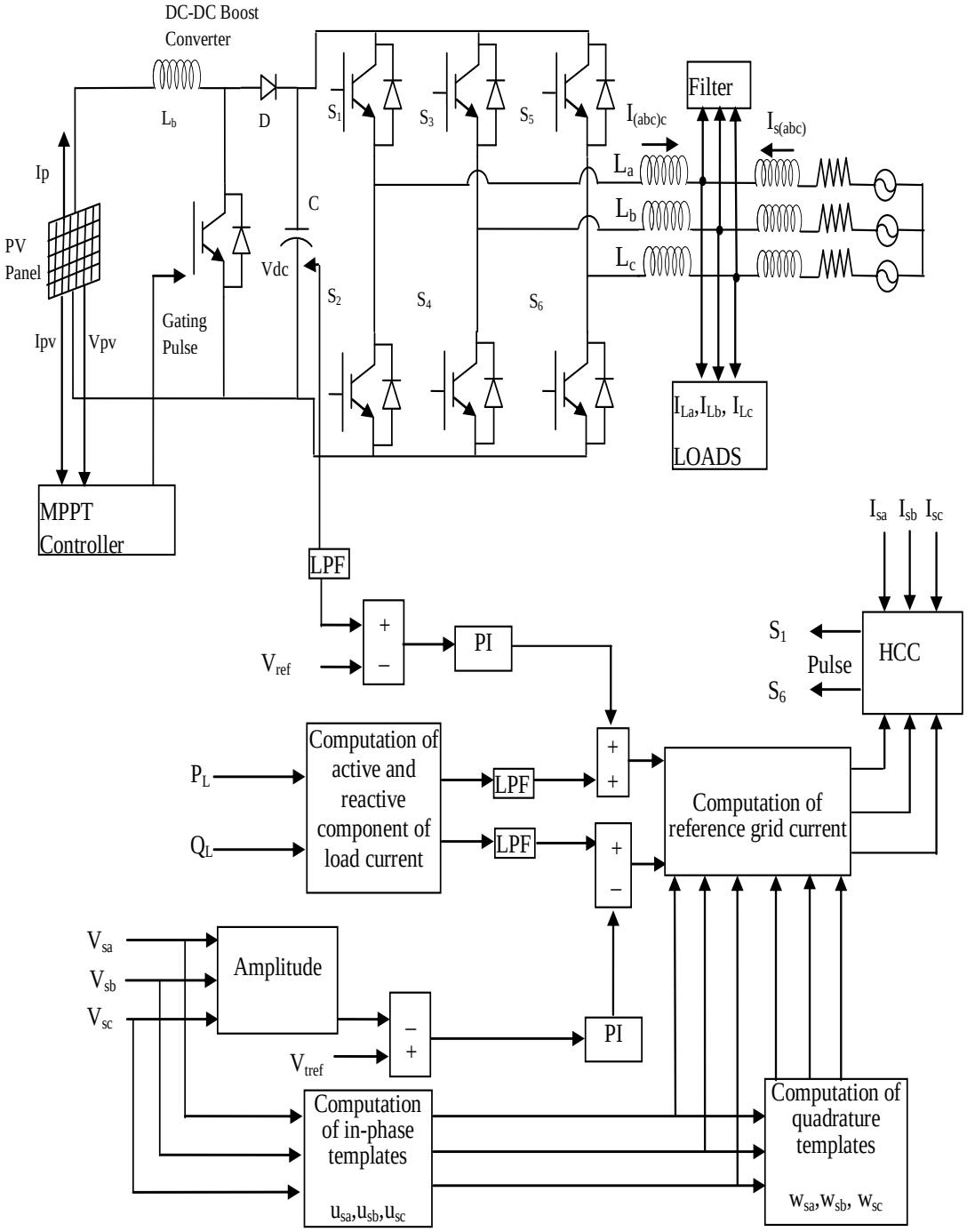

Figure 5.1: Schematic diagram of grid connected SPV system using PBT control algorithm

The error in between reference voltage and measured voltage of dc link is compared for consecutive samples and regulated to be zero. K_{pd}& K_{id} are proportional and

integral gain of the PI controller. The reference current generated for 'd' component of grid current is given as

$$i_d^* = i_{Ld} + i_{lossd} \tag{5.4}$$

where i^*_d grid current reference for d component, i_{Ld} is the d component of load current and i_{lossd} is the d component of current for loss at dc link.

Active power components of reference grid currents are

$$i^*_{sad} = i^*_d * u_{sa},\ i^*_{sbd} = i^*_d * u_{sb},\ i^*_{scd} = i^*_d * u_{sc} \tag{5.5}$$

5.2.2 Generation of Quadrature Unit templates of Reference Grid Currents: Reactive power component or quadrature component of grid currents are responsible for voltage regulation. If the load is of lagging nature, then impedance drop is taken care by supplying small leading reactive power to the grid & vice versa for leading power factor load. The flow of power is controlled by realising a second PI controller over the terminal voltage. The input for the controller is the error signal generated by the difference of measured voltage at PCC (V_t) and the reference voltage (V^*_t). The output of this PI controller is taken as quadrature component of current (I^*_q).

The unit vectors in quadrature with phase voltages is given by

$$\frac{u_c - u_b}{\sqrt{3}} = w_a \tag{5.6}$$

$$\frac{u_a}{\sqrt{2}} + \frac{u_b - u_c}{\sqrt{6}} = w_b \tag{5.7}$$

$$\frac{u_b - u_c}{\sqrt{6}} - \frac{u_a}{\sqrt{2}} = w_c \tag{5.8}$$

The reactive power component of current generated through PI controller by the difference of amplitude of measured voltage at PCC (V_t) and the reference voltage of PCC (V_t^*) is given as

$$i_{qr}(k) = i_{qr}(k-1) + K_{pq}\big(v_{te}(k) - v_{te}(k-1)\big) + K_{iq}\,(v_{te}(k)) \tag{5.9}$$

where $v_{te}(k) = v_t^*(k) - v_t(k)$

The error between reference and measured voltage at PCC. K_{pd} & K_{id} are the proportional and integral gains of PCC voltage PI controller. The reference current generated in terms of q components is given as

$$i_q^* = i_{Lq} - i_{tq} \tag{5.10}$$

where i^*_q grid current reference for q component, i_{Lq} is the q component of load current and i_{tq} is the q component of current corresponding to terminal voltage.

Rective power components of reference grid currents are

$$i^*_{saq} = i^*_q * w_{sa},\ i^*_{sbq} = i^*_q * w_{sb},\ i^*_{scq} = i^*_q * w_{sc} \tag{5.11}$$

5.2.3 Reference Grid Currents

The reference for the ac mains grid is computed from the sum of respective active and reactive power components of reference grid currents for all the three phases. These are represented in Eq 5.12

$$i^*_{sa} = i^*_{sad} + i^*_{saq}, i^*_{sb} = i^*_{sbd} + i^*_{sbq}, i^*_{sc} = i^*_{scd} + i^*_{scq} \tag{5.12}$$

The generated reference currents are compared with the sensed grid currents and six switching pulses are generated by hysteresis current controller to control VSC. The next section discusses the performance and results of the system with power balance control algorithm.

5.3 RESULTS AND DISCUSSIONS

Results are obtained for unity power factor operation (UPF) and zero voltage regulation (ZVR) under different load conditions, varying irradiance for both these modes. Performance of the grid connected SPV power generating system is depicted in terms of grid voltage (V_s), DC bus voltage (V_{dc}), AC grid currents, (I_s), load currents (I_{load}), the active power from /to grid (P), the reactive power (Q), solar PV current (I_{pv}), solar PV voltage (V_{pv}), PCC currents (I_{pcc}), PCC voltage (V_{pcc}), and terminal voltage at PCC (V_t).

5.3.1 For Unity Power Factor (UPF) operation

For unity power factor operation, the grid voltage (V_s) and grid current (I_s) are maintained at unity power factor. The results are verified under different conditions to ascertain if power quality standards can be met according to IEEE-519 standards [38].

5.3.1.1 Performance of the system under linear load condition

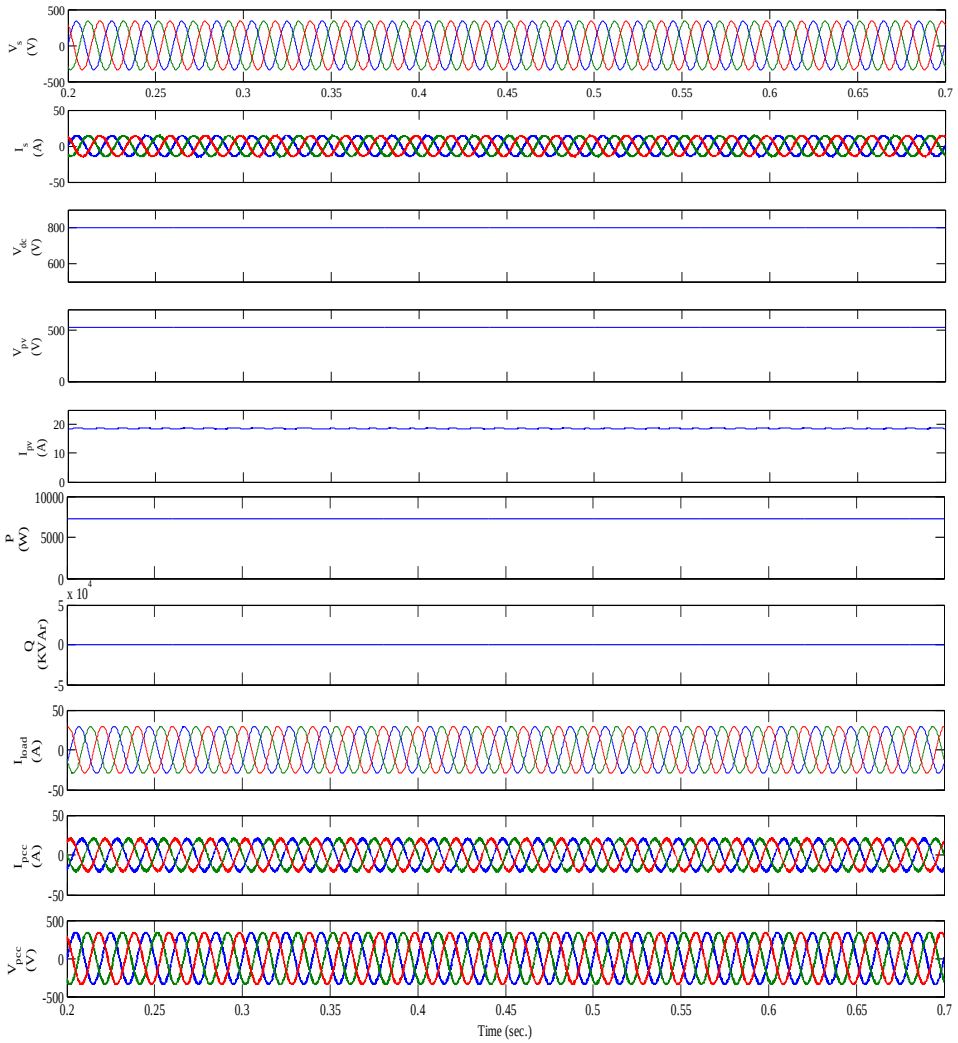

Figure 5.2a: Performance of system at linear load for unity power factor

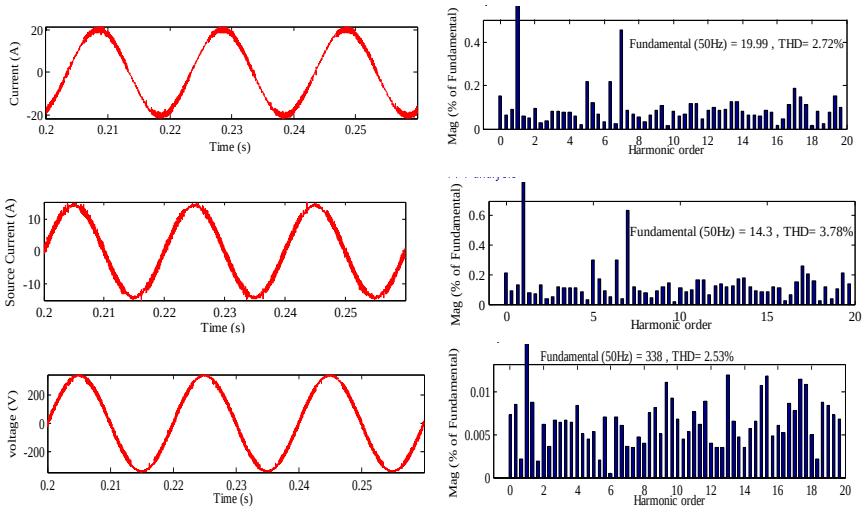

Figure 5.2b: Waveform and harmonic spectrum for I_{pcc}, I_s, V_{pcc}

Performance of the grid interfaced SPV power generating system under linear load of 15 kVA at lagging pf of 0.8 for UPF in Fig. 5.2a. V_{dc} is maintained at the desired reference level of 800 V and the PV power is evacuated. The system is so controlled that the overall reactive power of load is supplied by the SPV. SPV feeds the real power also upto its capacity/ rating and remaining active power is supplied by the grid. It is observed from the figure that UPF is achieved and maintained for V_s & I_s.

Fig. 5.2b shows the waveform and harmonic spectrum for PCC current (I_{pcc}), grid/source current (I_s) and PCC voltage (V_{pcc}). THD is maintained well within the limits 5% according to the IEEE-519 standards.

5.3.1.2 Performance of the system for linear load with varying irradiance condition

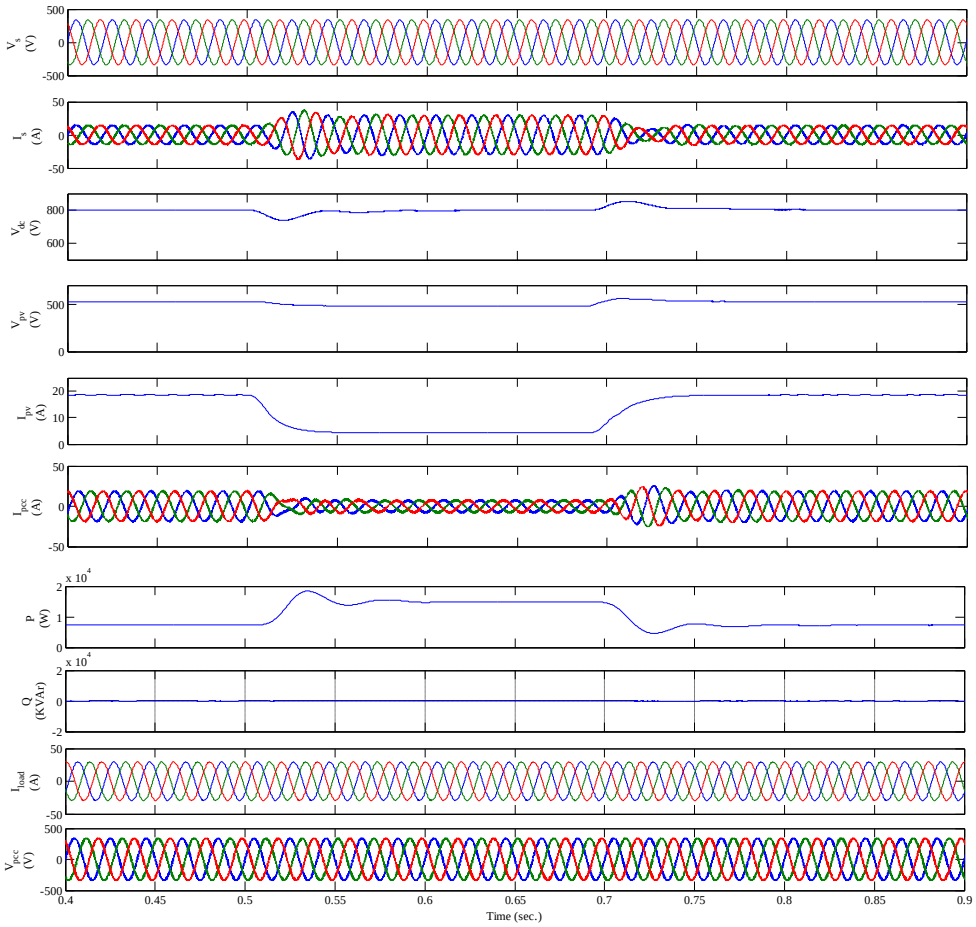

Figure 5.3: Performance of system at linear load for unity power factor under varying irradiance

Performance of the grid interfaced SPV power generating system for linear load of 15 kVA at lagging PF of 0.8 under varying irradiance condition for UPF in a distribution system is illustrated in Fig. 5.3. Irradiance is varied from 1000 kW/m^2 to 200 kW/m^2

at t=0.5 sec. and the MPP is tracked for new irradiance by MPPT-boost converter. V_{dc} is maintained at the desired reference level of 800 V and the PV power is evacuated. The overall reactive power of load is supplied by the SPV and also the real power upto its capacity. The remaining active power is supplied by the grid and UPF is achieved and maintained for V_s & I_s. In this case as the irradiance is reduced, so the power supplied by the PV array for new irradiance is less. Therefore, some of the reactive power is also supplied by grid hence, the power factor is not exactly unity under low irradiance of 200 kW/m^2. At t=0.7 sec. irradiance is changed to 1000 kW/m^2 and then UPF is achieved again.

5.3.1.3Performance of the system for linear load varying condition

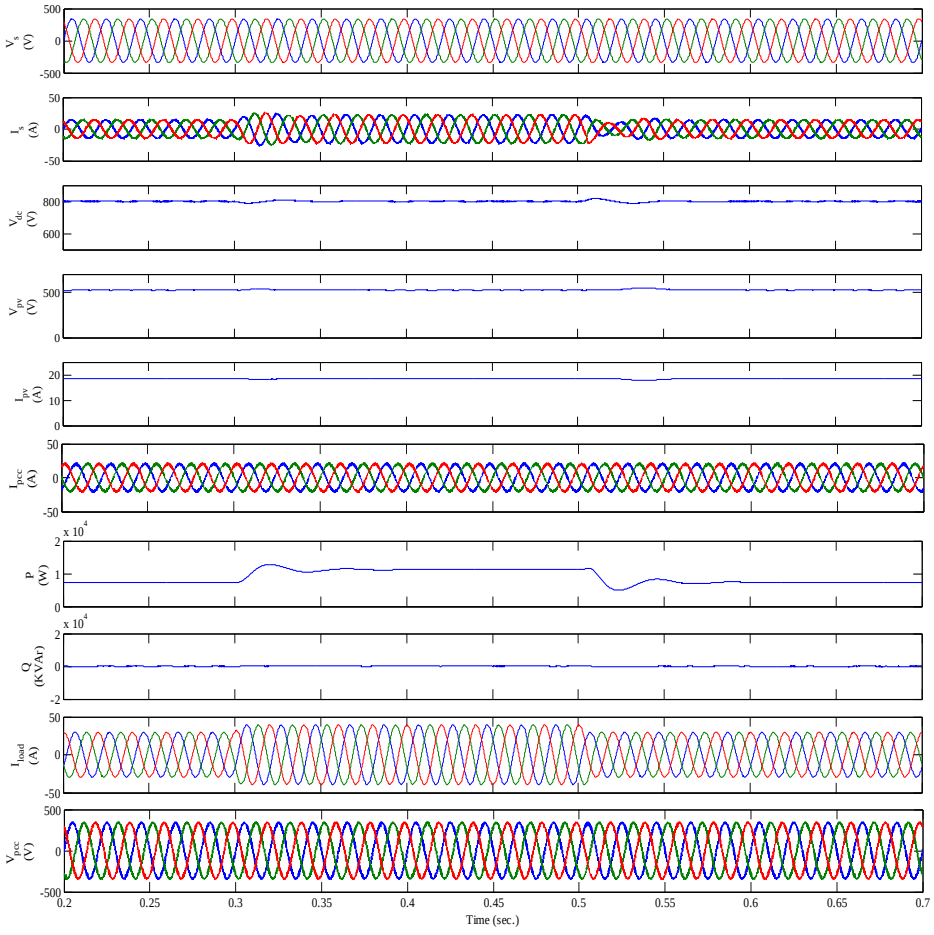

Figure 5.4a: Performance of system for unity power factor under varying linear load

Performance of the grid interfaced SPV power generating system for linear load of 15 kVA at lagging PF of 0.8 under linear load varying condition for UPF in a distribution system is illustrated in Fig. 5.4a. The load is switched from 15 kVA to 20 kVA at t=0.3 sec and the load current (I_{load}) is increased and accordingly grid current

(I_s) and the power supplied by grid (P) is observed to increase. However, V_{dc} is maintained at the desired reference level of 800 V with the PI controller. The entire PV power is evacuated. The overall reactive power of load is supplied by the SPV and also the maximum real power what it can supply. The remaining active power is supplied by the grid and UPF is achieved and maintained for V_s & I_s. Therefore real power is shared by grid. It is noted that the entire reactive power of the load is supplied by SPV solely. At t=0.5 sec, the load is switched back from 20kVA to 15kVA. It is observed that under these dynamic load changes, the dc link is regulated.

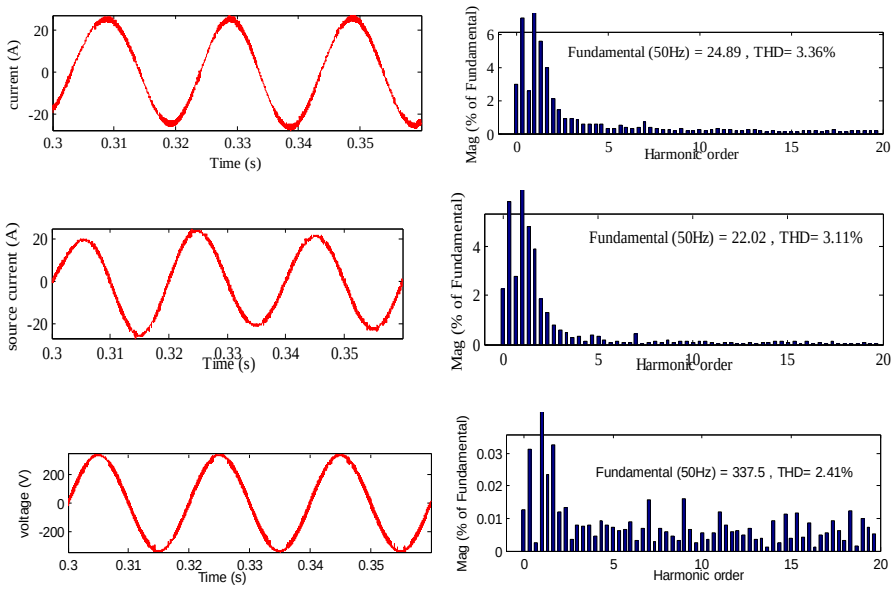

Figure 5.4b: Waveform and harmonic spectrum for I_{pcc}, I_s and V_{pcc} under varying linear load

Fig. 5.4b shows the waveform and harmonic spectrum for PCC current (I_{pcc}), grid/source current (I_s) and PCC voltage (V_{pcc}). THD is maintained under linear load varying condition for UPF in a distribution system well within the limits 5% according to the IEEE-519 standards. THD shown is calculated at t=0.3 sec. i.e. at the time of load variation.

Performance of the grid interfaced SPV power generating system for linear load of 15 kVA at lagging PF of 0.8 with unbalanced linear loads are illustrated in Fig. 5.5a. The load is switched to unbalanced condition at t=0.3 sec. At t=0.3 sec, one phase of the load is switched from 15 kVA to 7.5 kVA and other two phases remain loaded with 15 kVA, 0.8pf. The grid current is still balanced and the PCC current (I_{pcc}) supplied by SPV provides the necessary compensation. Thus, I_{pcc} is also observed as distorted. When the load demand decreases, the load current is also less, therefore the power

5.3.1.4Performance of the system for unbalanced linear load condition

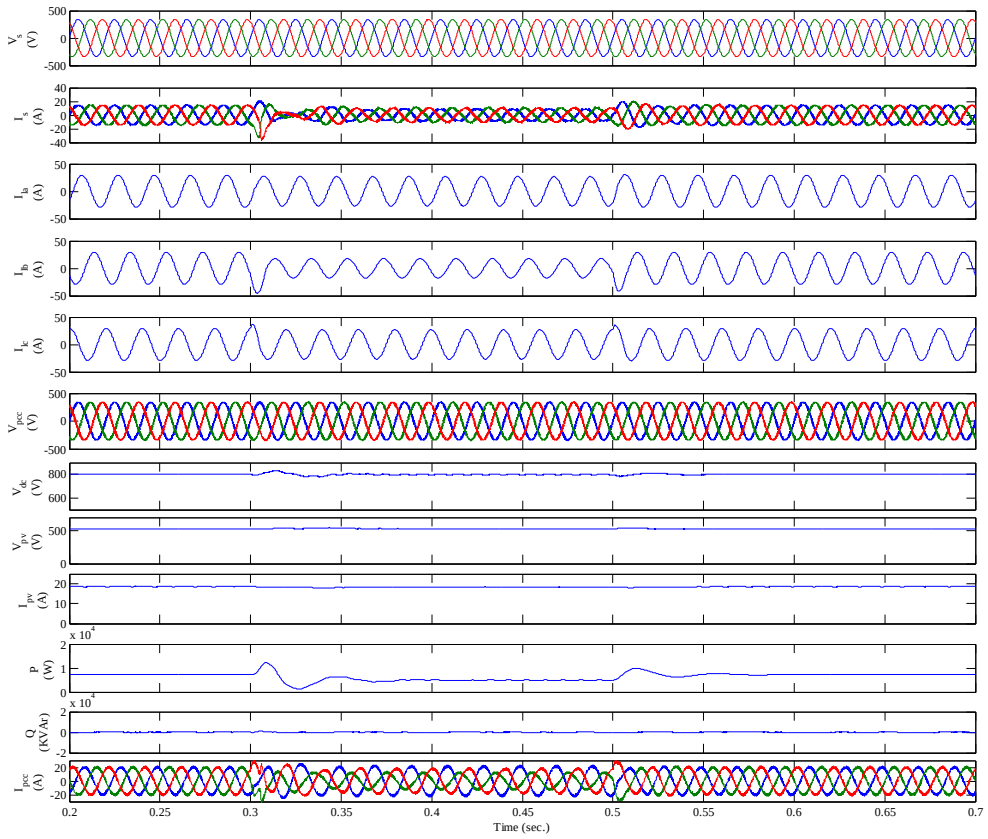

Figure 5.5a: Performance of system for unity power factor and load balancing under unbalanced linear load

supplied by the grid is reduced. V_{dc} is maintained at the desired reference level of 800 V and the PV power is evacuated. UPF is achieved and maintained for V_s & I_s. At t=0.5 sec. the load is switched to the balanced condition as before.

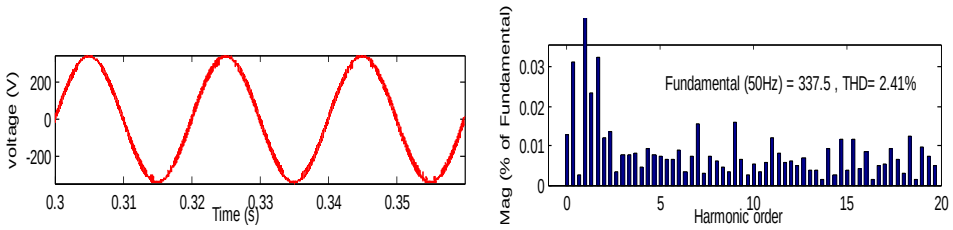

Figure 5.5b: Waveform and harmonic spectrum for V_{pcc} under varying linear load

Fig. 5.5b shows the waveform and harmonic spectrum for PCC voltage (V_{pcc}). THD is maintained to 2.41% under linear load varying condition for UPF in the system. It is observed to be well within the limits of 5% according to the IEEE-519 standards.

5.3.1.5 Performance of the system for non-linear load condition

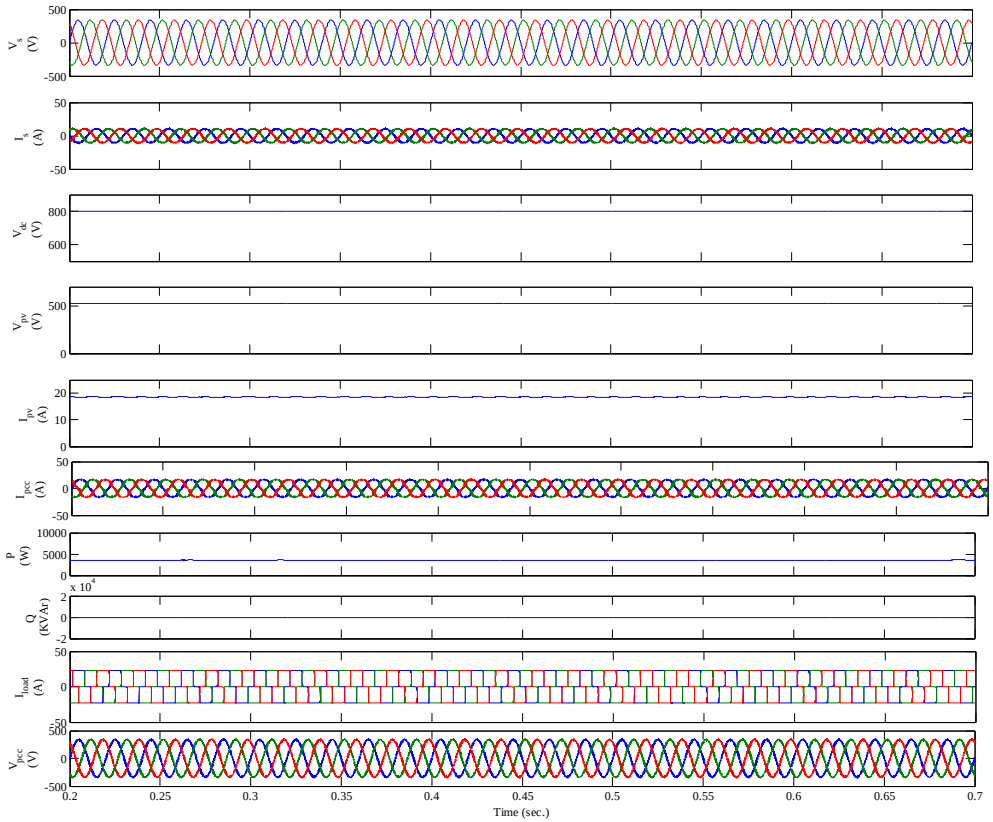

Figure 5.6a: Performance of system for unity power factor under non-linear load condition

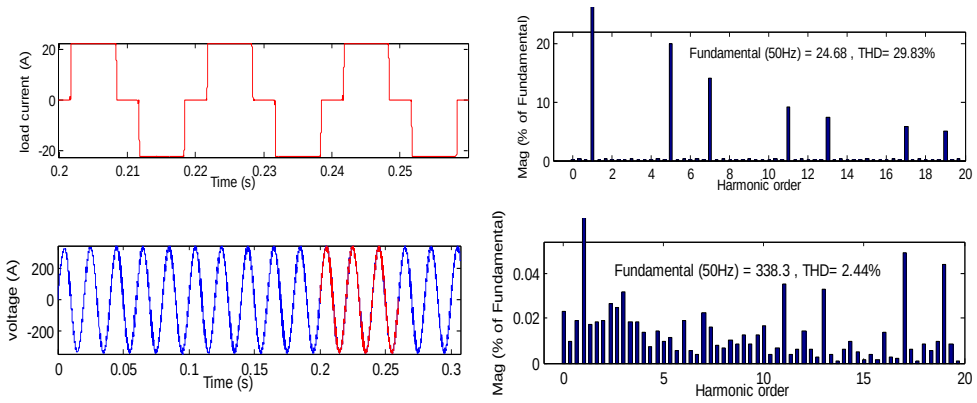

Figure 5.6b: Waveform and harmonic spectrum for I_{load} and V_{pcc} under non-linear load

Performance of the grid interfaced SPV power generating system for non-linear load of 25Ω and 300mH balanced condition for UPF in a distribution system is illustrated in Fig. 5.6a. V_{dc} is maintained at the desired reference level of 800 V and the PV power is evacuated. The entire reactive power of load is supplied by the SPV. SPV also supplies the real power upto its capacity. If the system load demand is higher, the remaining active power is supplied by the grid. UPF is achieved and maintained for V_s & I_s. The compensation is provided by the VSC-SPV and therefore THD of current is improved.

Fig. 5.6b shows the waveform and harmonic spectrum for load current (I_{load}) and PCC voltage (V_{pcc}). THD is maintained well within the limits of 5% for V_{pcc} according to the IEEE-519 standards and THD of load current is 29.83%.

Performance of the grid interfaced SPV power generating system for non-linear load of 25Ω and 300mH under unbalanced load condition for UPF in a distribution system is illustrated in Fig. 5.7a. It can be observed that the grid currents are in phase with PCC voltages demonstrating unity power factor at AC mains. The load is switched to unbalanced condition at t=0.3 sec by removing the load on one phase and further by removing load on other two phases at 0.45 sec. V_{dc} is maintained at the desired reference level of 800 V by the controller. The PV power is evacuated. The overall reactive power of load is supplied by the SPV and and remaining active power is supplied by the grid and UPF is achieved and maintained for V_s & I_s. Even when the load becomes unbalanced, the grid current remains balanced. The THD of ac supply current is improved. At t=0.45sec, all phases of the load are removed and it is observed that all the power generated from SPV is flowing into the grid. This is confirmed from the sign of supplied power from grid which is seen to be negative. At t=0.6 sec. the load is switched back to the balanced condition.

Fig. 5.7b shows the waveform and harmonic spectrum for PCC voltage (V_{pcc}). THD is maintained under linear load varying condition for UPF in a distribution system well within the limits of 5% according to the IEEE-519 standards. THD shown is calculated at t=0.3 sec. i.e. at the time of unbalancing of load

5.3.1.6 Performance of the system for unbalanced non-linear load condition

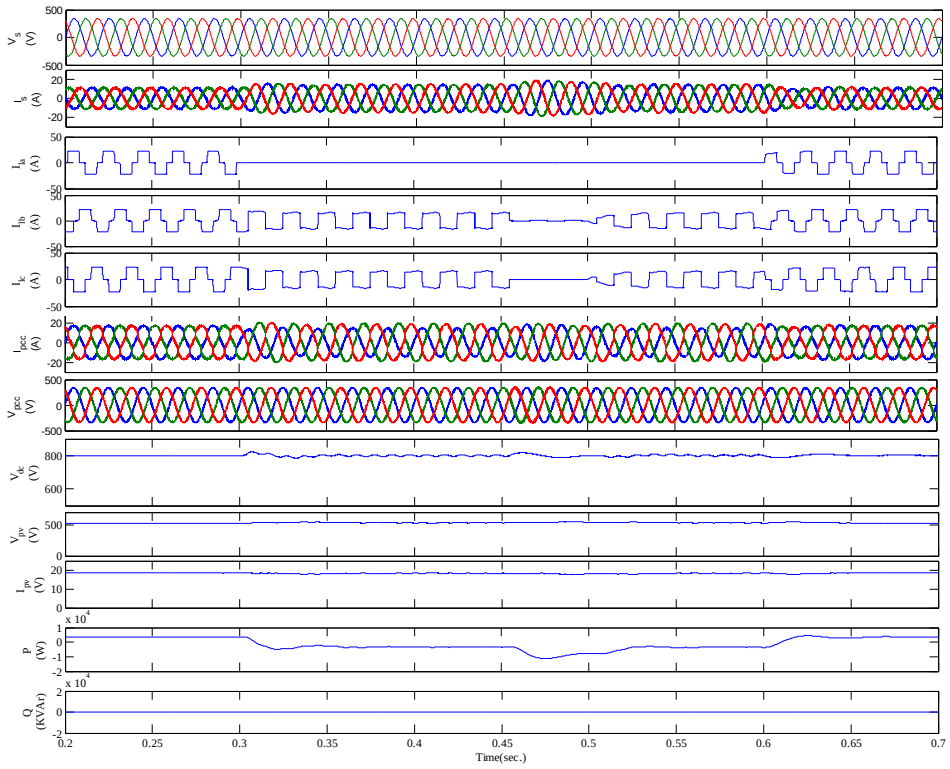

Figure 5.7a: Performance of system for unity power factor and load balancing under unbalanced non-linear load condition

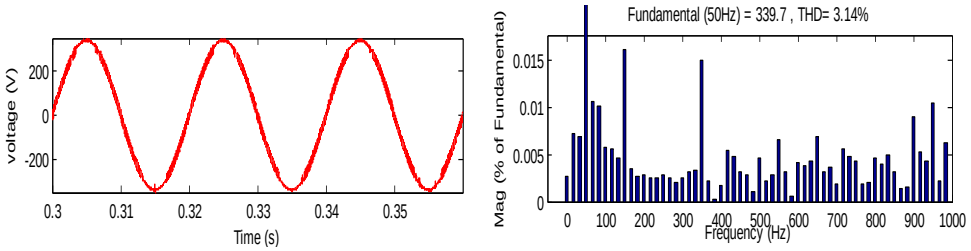

Figure 5.7b: Waveform and harmonic spectrum for V_{pcc} under unbalanced non-linear load

5.3.2 For Zero Voltage Regulation (ZVR) operation

For zero voltage regulation operation (ZVR), the terminal voltage (V_t) of PCC voltage (V_{pcc}) is regulated to desired reference voltage level. Power quality is also improved according to IEEE-519 standards. Different load conditions are discussed below.

5.3.2.1 Performance of the system under linear load condition

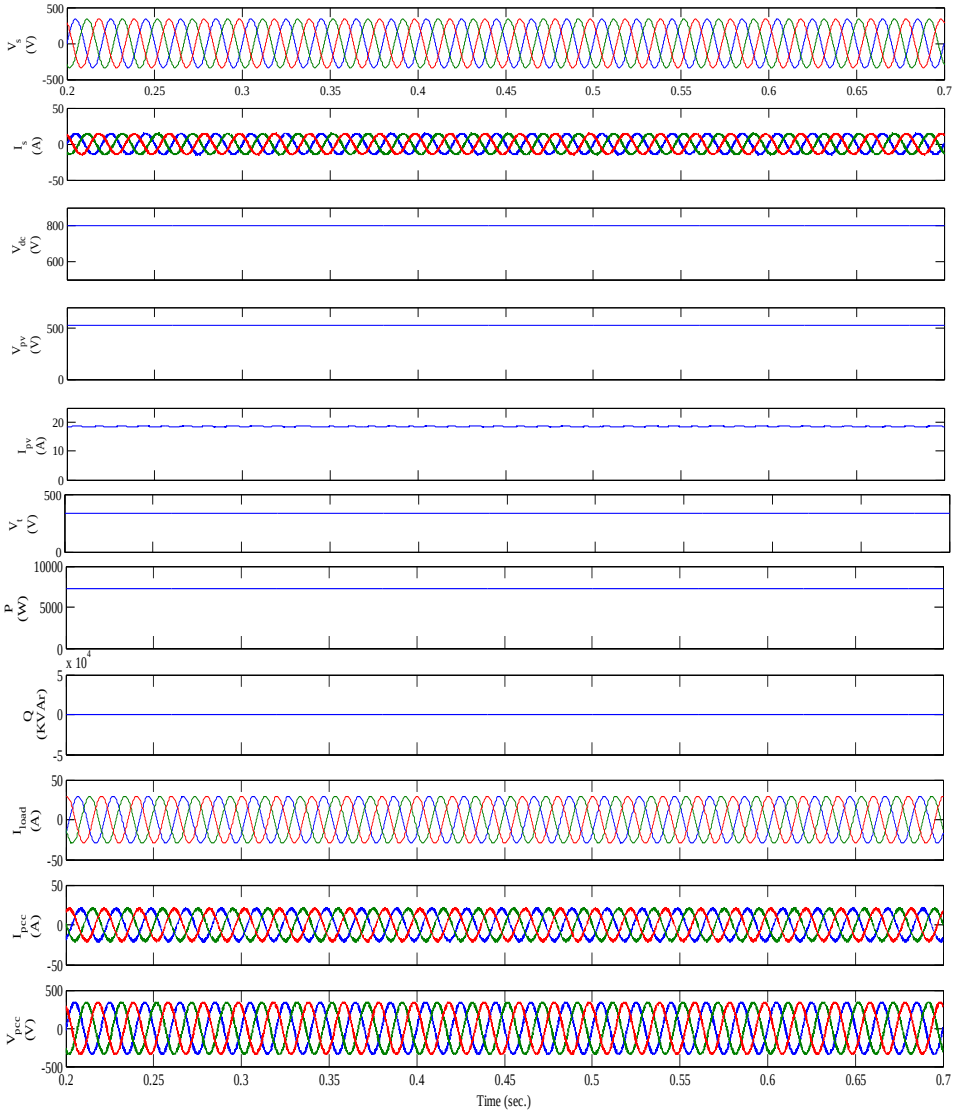

Figure 5.8a: Performance of system at linear load for zero voltage regulation

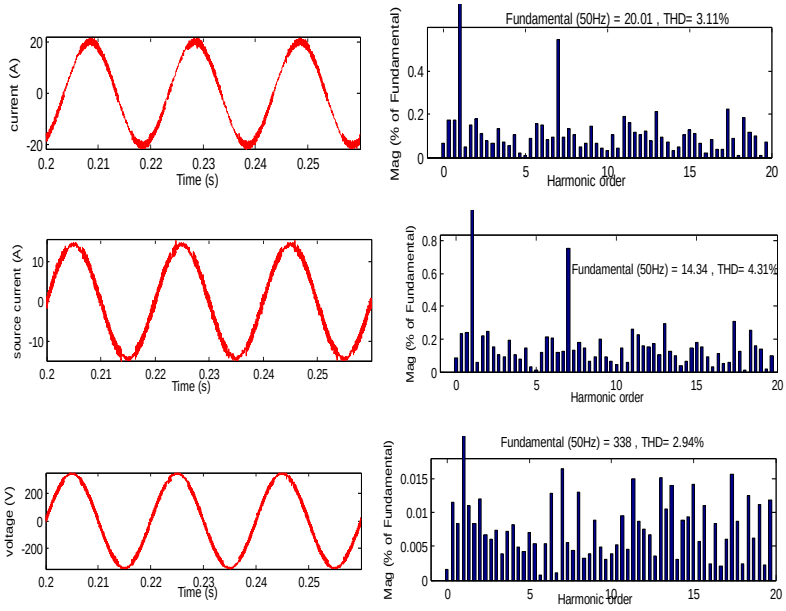

Figure 5.8b: Waveform and harmonic spectrum for I_{pcc}, I_s, V_{pcc}

Performance of the grid interfaced SPV power generating system under linear load of 15 kVA at lagging PF of 0.8 for ZVR is illustrated in Fig. 5.8a. V_{dc} is maintained at the desired reference level of 800 V and the PV power is evacuated. The overall reactive power of load is supplied by the SPV and partial real power of load is met by SPV. The remaining active power still needed by load is supplied by the grid and ZVR is achieved and maintained for V_t of PCC voltage (V_{pcc}).

Fig. 5.8b shows the waveform and harmonic spectrum for PCC current (I_{pcc}), source (grid) current (I_s) and PCC voltage (V_{pcc}). THD is maintained well within the limits 5% according to the IEEE-519 standards.

Performance of the grid interfaced SPV power generating system at linear load of 15 kVA at lagging pf of 0.8 under varying irradiance condition for zero voltage regulation is illustrated in Fig. 5.9. Irradiance is been varied from 1000 kW/m^2 to 200 kW/m^2 at t=0.5 sec. and the MPP is tracked for new irradiance by MPPT-boost converter. V_{dc} is maintained at the desired reference level of 800 V and the PV power is evacuated. The entire reactive power of load is supplied by the SPV. ZVR is achieved and maintained for V_t of PCC voltage (V_{pcc}). V_t is maintained at the desired reference level of 338V. In this case as the irradiance is reduced, the power supplied by the PV array for new irradiance is less. Hence, some of the reactive power is also supplied by grid also. At t=0.7 sec, irradiance is changed back to 1000 kW/m^2 and then ZVR is achieved again. It is found that both V_t and V_{dc} are maintained to their reference value.

5.3.2.2 Performance of the system under varying irradiance condition for linear load:

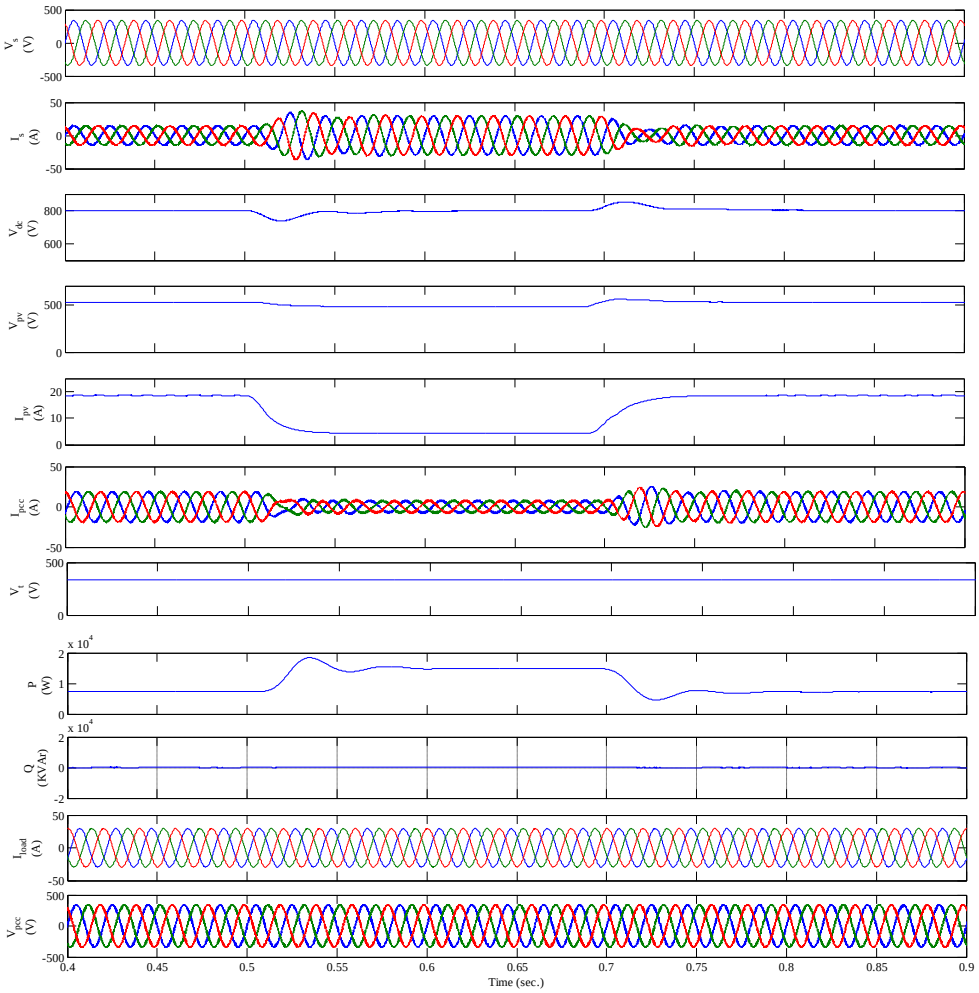

Figure 5.9: Performance of system for zero voltage regulation under varying irradiance at linear load

Performance of the grid interfaced SPV power generating system for linear load of 15 kVA at lagging PF of 0.8 under linear load varying condition for ZVR in a distribution system is illustrated in Fig. 5.10a. The load is switched from 15 kVA to 20 kVA, 0.8pf at t=0.3 sec and the load current (I_{load}) is increased and accordingly grid current (I_s) and then power supplied by grid (P) is increased. V_{dc} is maintained at the desired reference level of 800 V and the PV power is evacuated. ZVR is achieved and maintained for V_t of PCC voltage (V_{pcc}). Real power is shared by grid and SPV but the reactive power is supplied by SPV mainly. At t=0.5 sec, the load is switched from 20kVA to 15kVA, 0.8pf lag. The dc link and terminal voltage is maintained using both the controllers.

5.3.2.3 Performance of the system for linear load varying condition

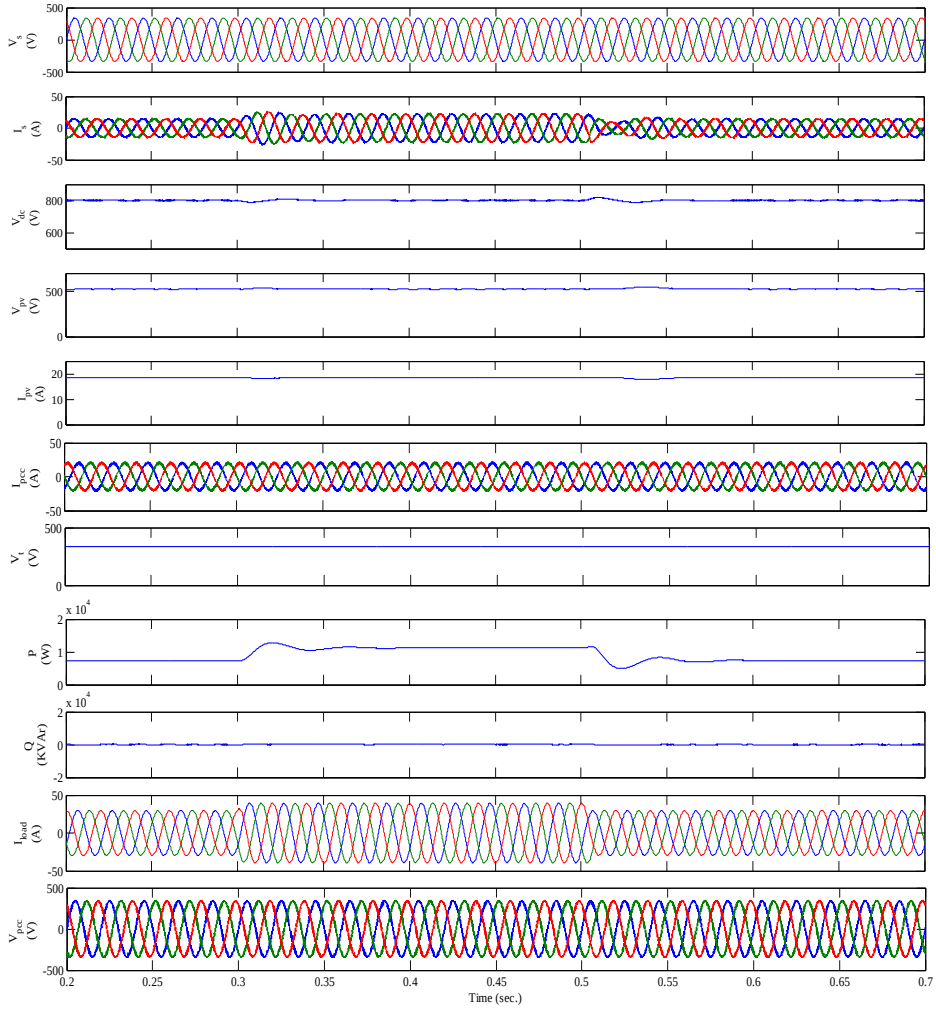

Figure 5.10a: Performance of system for zero voltage regulation under varying linear load

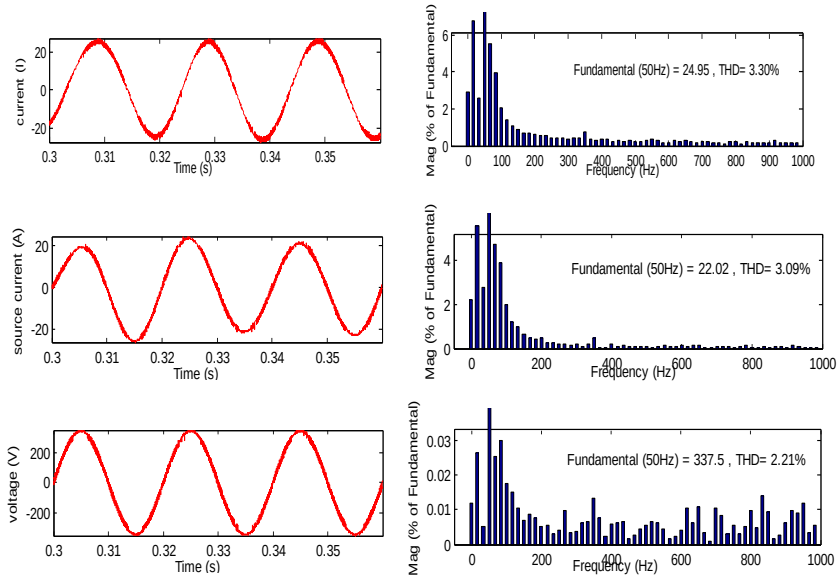

Figure 5.10b: Waveform and harmonic spectrum for I_{pcc}, I_s and V_{pcc} under varying linear load

Fig. 5.10b shows the waveform and harmonic spectrum for PCC current (I_{pcc}), grid/source current (I_s) and PCC voltage (V_{pcc}). THD is maintained under linear load varying condition for ZVR in a distribution system. For I_{pcc}, I_s and V_{pcc} , it is observed that IEEE-519 standards are met. THD shown is calculated at t=0.3 sec. i.e. at the time of load variation.

5.3.2.4Performance of the system for unbalanced linear load condition

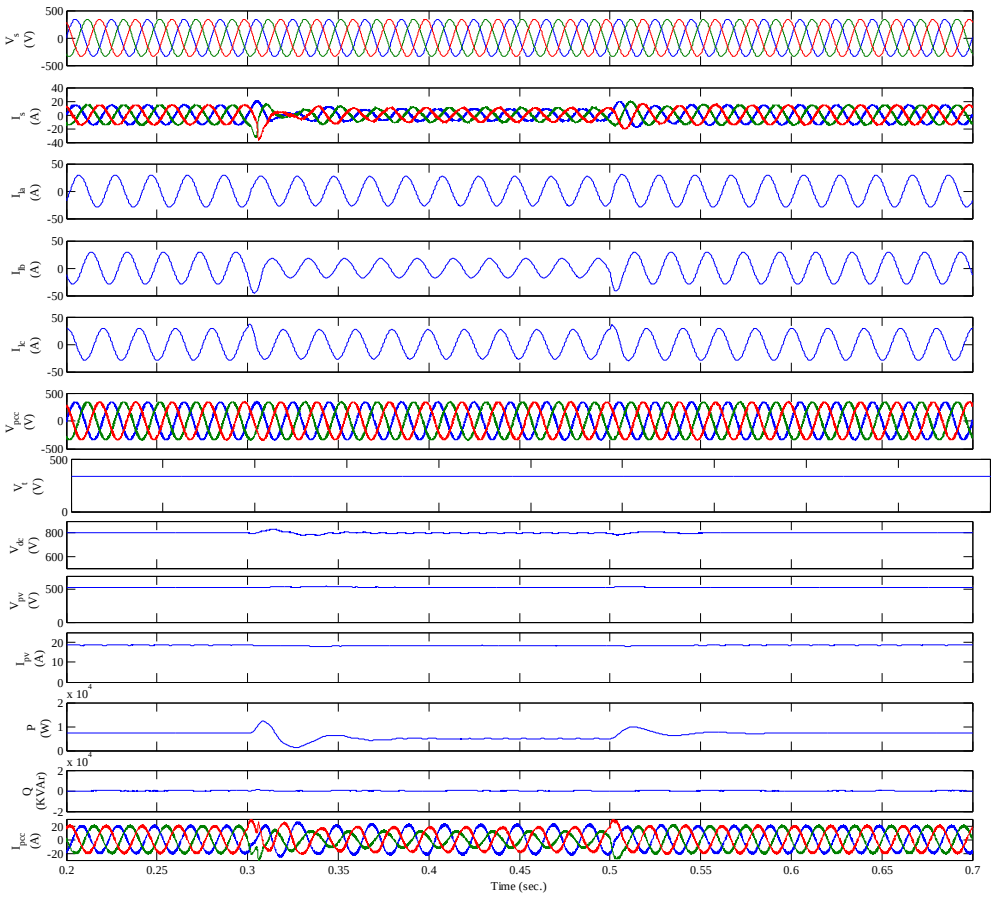

Figure 5.11a: Performance of system for zero voltage regulation and load balancing under unbalanced linear load

Performance of the grid interfaced SPV power generating system for linear load of 15 kVA at lagging pf of 0.8 under unbalanced linear load condition for ZVR in a distribution system is illustrated in Fig. 5.11a. The load is been switched to unbalanced load condition in one of the phases from 15 kVA to 7.5 kVA at t=0.3sec. The load current is still balanced by the PCC current (I_{pcc}) supplied by SPV and compensation is provided by the PCC current (I_{pcc}) supplied by SPV; thus I_{pcc} becomes distorted. V_{dc} is maintained at the desired reference level of 800 V and the PV power is evacuated. ZVR is achieved and maintained for terminal voltage V_t of

PCC voltage (V_{pcc}). At t=0.5 sec. the load is switched to the balanced condition. The terminal voltage (V_t) is regulated to its reference value of 338 V throughout the simulation.

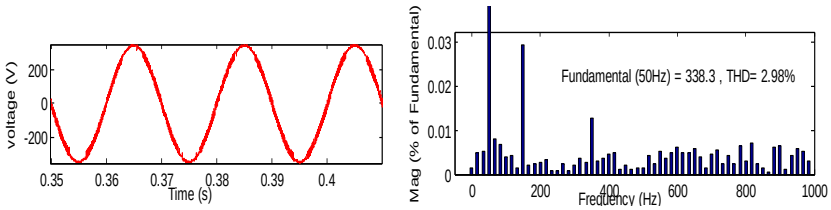

Figure 5.11b: Waveform and harmonic spectrum for V_{pcc} under varying linear load

Fig. 5.11b shows the waveform and harmonic spectrum for PCC voltage (V_{pcc}). THD is maintained under varying linear load varying condition for this case also. THD shown is calculated at t=0.3 sec. i.e. at the time of unbalancing of load.

5.3.1.5 Performance of the system for non-linear load condition

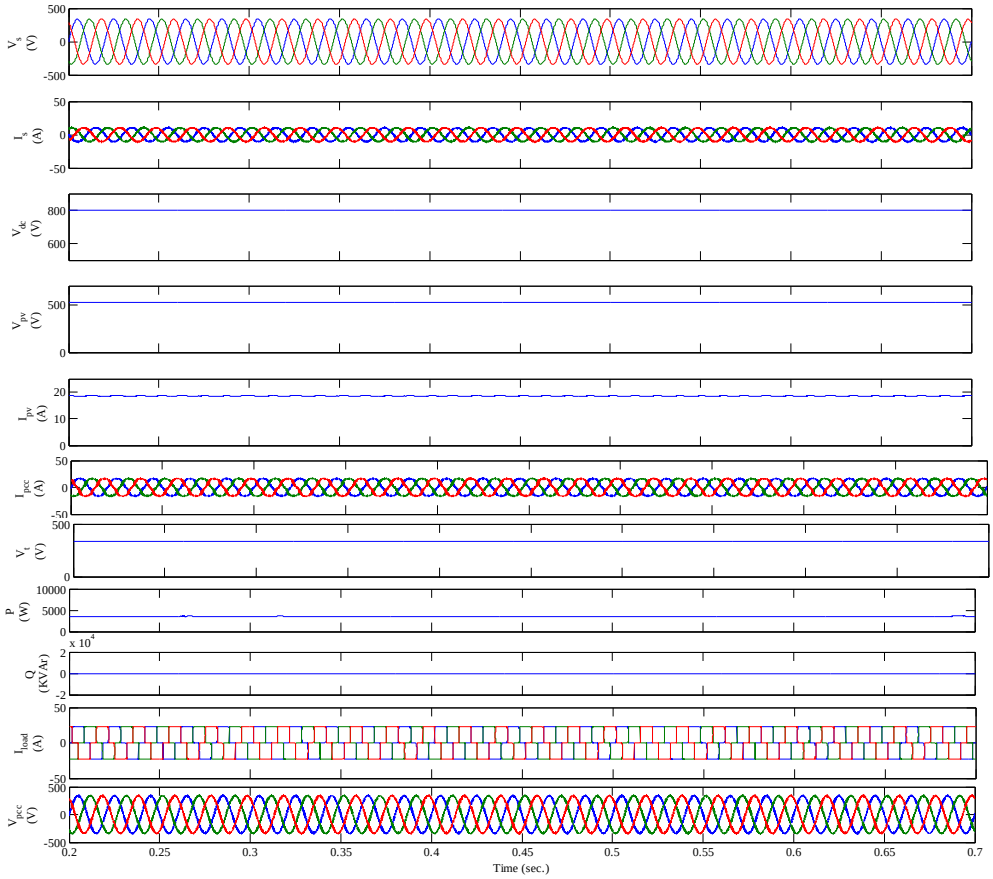

Figure 5.12a: Performance of system for zero voltage regulation under non-linear load condition

Performance of the grid interfaced SPV power generating system for non-linear load of 25Ω and 300mH balanced condition for ZVR in a distribution system is illustrated in Fig. 5.12a. V_{dc} & V_t are maintained at the desired reference level of 800 V and 338

V respectively and the PV power is evacuated. The overall reactive power of load is supplied by the SPV and the grid. ZVR is achieved and maintained for terminal voltage V_t of PCC voltage (V_{pcc}). The compensation provided by the VSC-SPV.

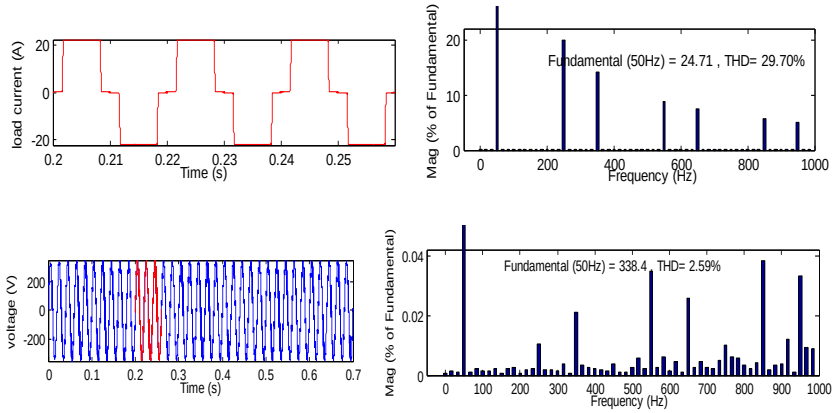

Figure 5.12b: Waveform and harmonic spectrum for I_{load} and V_{pcc} under non-linear load

Fig. 5.12b shows the waveform and harmonic spectrum for I_{load} and V_{pcc}.The THD of load current is 29.7% while the THD of grid current is regulated to a value less than 5% level as stipulated by IEEE- 519 standards as shown in Fig 5.12b.

5.3.1.6 Performance of the system for unbalanced non-linear load condition

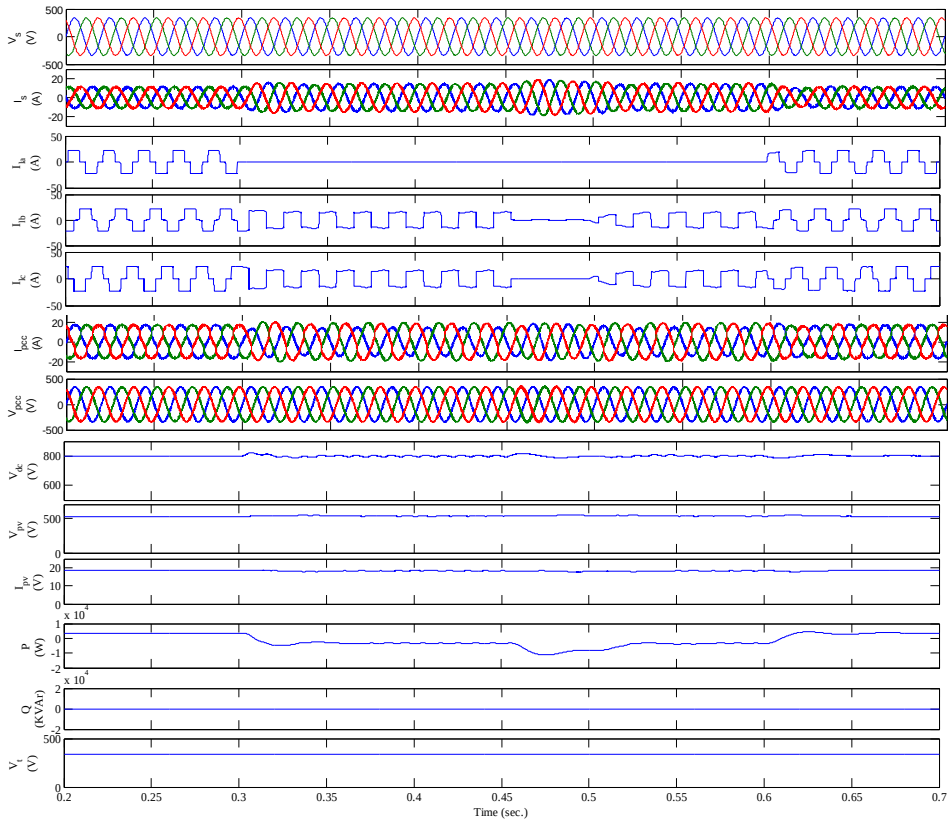

Figure 5.13a: Performance of system for zero voltage regulation and load balancing under unbalanced non-linear load condition

Performance of the grid interfaced SPV power generating system for non-linear load of 25Ω and 300mH under unbalanced load condition for ZVR in a distribution system is illustrated in Fig. 5.13a. It can be observed that the terminal voltage (V_t) of PCC voltage (V_{pcc}) is regulated at reference level of 338 V. The load is switched to unbalanced condition at t=0.3 sec, and at 0.45 sec. V_{dc} is maintained at the desired reference level of 800 V and the PV power is evacuated. The overall reactive power of load is supplied by the SPV and also the real power upto its capacity. The remaining active power is supplied by the grid and also power for maintaining terminal voltage V_t of PCC voltage (V_{pcc}) to reference value. When the load becomes unbalanced, still the controllers regulate the dc link voltage and ac terminal voltage. At t=0.6 sec, the load is switched back to the initial balanced condition and terminal voltage (V_t) is regulated at reference obtaining ZVR.

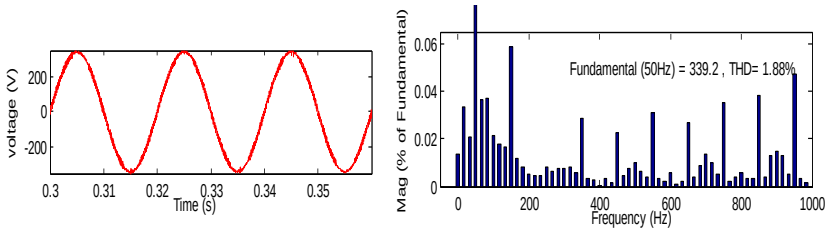

Figure 5.15b: Waveform and harmonic spectrum for V_{pcc} under unbalanced non-linear load

Fig. 5.13b shows the waveform and harmonic spectrum for PCC voltage (V_{pcc}). THD is maintained under linear load varying condition for ZVR in a distribution system well within the limits of 5% according to the IEEE-519 standards. THD shown is calculated at t=0.3 sec. i.e. at the time of unbalancing of load.

5.3 CONCLUSION:

The grid interconnected SPV power generating system performance is investigated and analyzed for different conditions like solar irradiance variation, load variation for linear lagging power factor load, balanced load condition for linear and non-linear load, variable irradiance, varying linear load and load unbalancing condition for linear and non-linear load. Two different modes- unity power factor (UPF) and zero voltage regulation (ZVR) are discussed in detail. The DC bus voltage (V_{dc}) and PCC voltage (V_{pcc}) can be both maintained at desired levels by suitable tuning of controller parameters. Various load conditions are varied and the controllers work well for all dynamic load changes. The power balance algorithm based on in phase and quadrature templates works well both both UPF and ZVR. In the UPF operation, the

reactive power supplied by the grid is zero. UPF is maintained for linear and non-linear load conditions. The terminal voltage (V_t) of PCC voltage (V_{pcc}) is maintained at its reference value using a second PI controller. Total harmonic distortion (THD) in grid currents for all cases is maintained less than 5% according to IEEE-519. A SPV based on power balance theory can be suitably controlled to achieve UPF and ZVR modes.

CHAPTER-6

CONCLUSION

The characteristics of PV have been successfully obtained for different conditions of irradiation and temperature levels. Incremental conductance and P&O algorithm of MPPT is modelled and simulated. The maximum power point (MPP) of PV array voltage and current is achieved and so the maximum power is obtained using boost converter. Constant power is maintained at the input and output side of the converter with slight variation due to switching losses and irrespective of the load change. The grid interconnected solar photovoltaic system (SPV) system performance is investigated and analyzed successfully for different conditions like load variation for linear lagging power factor load and load unbalancing for linear and non-linear load. Unity power factor (UPF) for ac mains (grid) voltage and current and zero voltage regulation (ZVR) for terminal voltage of PCC voltage is achieved using synchronous reference frame theory (SRFT) and power balance theory (PBT) algorithm. The DC bus voltage and terminal voltage of PCC voltage maintained at desired level for different conditions along with harmonics elimination and load balancing.

CHAPTER-7

FUTURE SCOPE OF WORK

In this work it is shown that Solar photovoltaic system (SPV) is connected to grid using two algorithms under different loading conditions. The work can be expanded in the following area

1) Solar photovoltaic system modelled considering partial shedding condition.

2) Use of other MPPT techniques to track MPP point for the condition of rapid varying parameter of PV.

3) DC-dc converters in isolated will be used to protect our system and also other dc-dc converter topologies can be used.

4) Various control algorithms for grid connected PV system control can be implemented.

5) Storage system can also be used in grid connected mode.

6) Islanding detection and Islanding mode of operation of PV with storage capacity can also be studied and implemented.

REFERENCES

[1] RNE 21 (2011) "Renewables 2011" , Global status report, pp. 17,18.

[2] Global Market Outlook-2016.

[3] Grid connected solar power in India, Ministry of New and Renewable energy (MNRE),Government of India (GoI).

[4] Press information bureau, Government of India (GoI), Ministry of Renewable energy (MNRE).

[5] Gilbert M. Masters, "Renewable and efficient electric power system", John Wiley & sons, 2004, ISBN 0-471-28060-7.

[6] A. Goetzberger and V. U. Hoffmann, "Photovoltaic solar energy generation", Springer, 2005,

ISBN 3-540-23676-7.

[7] Frank Jackson, "Planning and installing Photovoltaic system, a guide for installers, architects and engineers", Earthscan, Second edition, ISBN-13: 978-1-84407-442-6.

[8] Roger A. Messenger, "Jerry Ventre "Photovoltaics system engineering", CRC press, Second edition, 2004, ISBN 0-8493-1793-2.

[9] P. A. Lynn, "Electricity from sunlight: An introduction to photovoltaic", John Wiley & sons, 2010, p238.

[10] Larry Partain, "Solar cells & their applications", Second edition, John Wiley & sons, 2010, ISBN 978-0-470-44633-1

[11] T. Markvart, Solar electricity, John Wiley & sons, 2000, p. 280.

[12] M.G. Villalva, J.R. Gazoli and E. Ruppert F., " Modelling and Circuit-Based Simulation of Photovoltaic Arrays", *Brazilian Journal Power Electronics*, vol.14, no.1, pp. 35-45, ISSN 1414-8862, 2009.

[13] T. Salmi, M. Bouzguenda, A. Gastli and A. Masmoudi, "MATLAB/Simulink Based Modelling of Solar Photovoltaic Cell", *International Journal of Renewable Energy Research*, Tarak Salmi et al., vol.2, no.2, 2012.

[14] Trishan Eshram and Patrick L. Chapman, "Comparison of Photovoltaic Array Maximum Power Point Techniques", *IEEE Transaction on Energy Conversion*, vol.22, no.2, pp. 439-449, June 2007.

[15] Jung-Woo Baek, Jae-Sub Ko, Jung-Sik Choi, Sung-Jun Kang and Dong-Hwa Chung, " Development of novel MPPT algorithm of PV system considering radiation variation", International Conference on Control, Automation and Systems 2010 , Oct. 27-30, 2010, KINTEX, Gyeonggi-do, Korea

[16] Ahmad Al-Diab and Constantinos Sourkounis, "Variable Step Size P&O MPPT Algorithm for PV Systems", 2010, 12th International Conference on Optimization of Electrical and Electronic Equipment, OPTIM 2010

[17] C. Zhang, D. Zhao, J. Wang and G. Chen, "A modified MPPT method with variable perturbation step for photovoltaic system", in *Power Electronics and Motion Control Conference*, 2009, pp. 2096-2099.

[18] Ahmed K. Abdelsalam, Ahmed M. Massoud, Shehab Ahmed and Prasad N. Enjeti, "High- Performance Adaptive Perturb and Observe MPPT Technique for Photovoltaic-Based Microgrids"
IEEE Transactions on Power Electronics, vol. 26, no. 4, april 2011.

[19] D. Sera, T. Kerekes, R. Teodorescu and F. Blaabjerg, "Improved MPPT Algorithms for Rapidly Changing Environmental Conditions", in *Proc. 12th International Conference on Power Electronics and Motion Control*, 2006, pp. 1614-1619.

[20] D. Sera, T. Kerekes, R. Teodorescu and F. Blaabjerg, "Improved MPPT method for rapidly changing environmental conditions", in *Proc. IEEE International Symposium on Industrial Electronics*, 2006, vol. 2, pp. 1420-1425.

[21] M.Veerachary, T.Senjyu and K.Uezato, "Maximum power point tracking control of IDB converter supplied PV system", *IEE Proc -Electr Power Appl*, vol 148, no 6, november 2001.

[22] Phan Quoc Dzung, Le DinhKhoa, Hong Hee Lee, Le Minh Phuong and Nguyen Truong Dan Vu, "The New MPPT Algorithm using ANN-Based PV", *IFOST*, 2010.

[23] Subiyanto, A Mohamed and M A Hannan, "Maximum Power Point Tracking in Grid Connected PV System Using A Novel Fuzzy Logic Controller" , *Student Conference on Research and Development* (SCOReD), 16-18 Nov. 2009, UPM Serdang, Malaysia.

[24] Arun Kumar Verma, Bhim Singh and D.T Shahani, "Fuzzy-Logic Based MPPT Control of Grid Interfaced PV Generating System with Improved Power Quality".

[25] Timothy J. Ross, "Fuzzy Logic with Engineering Applications", John Wiley & sons, Third edition, 2010, ISBN: 978-0-470-74376-8.

[26] M.H Rashid, "Power Electronics Circuits, Design and Applications," Pearson Education, Third Edition, India, 2007.

[27] Ned Mohan, Tore M. Undeland and William P. Robbins, "Power electronics converters, applications, and design", Wiley India Press Pvt. Ltd., Third Edition, Reprint 2009

[28] Arun Verma, Bhim Singh, D.T.Sahani, "Power Balanced theory based Grid Interfaced Photovoltaic power generating system with Power Quality Improvedmennt at AC mains," in Proc. for *the IEEE International conference on Power Electronics, Drives and Energy systems*, 16-19 Dec, 2012

[29] Vishal Verma, Amritesh Kumar, "Grid coupled maximum power point tracked Photovoltaic system with selective Power Conditioning capability," in Proc. for *the IEEE International conference on Power and Energy (PECon)*, 2-5 Dec, 2012, Kota Kinabalu Subah, Malaysia.

[30] Farid Katiraei, Reza Iravani, Nikos Hatziargyriou and Aris Dimeas "Microgrid management Control and operation aspect of microgrids," *IEEE Power & Energy Magazine*, May/June 2008.

[31] Arun Verma, Bhim Singh, D.T.Sahani, " Grid Interfaced Photovoltaic power generating system with Power Quality Improvedmennt at AC mains," *IEEE ICSET*, 2012, Nepal.

[32] S.A.Azmi, G.P.Adam, Khaled H.Ahmed, Stephen J.Finney, Barry W. Williams, "Grid Interfacing of Multimegawatts Photovoltaic Inverters," *IEEE Transaction on Power Electronics*, vol.28, no.6, june2013

[33] H.El..Fadil and J.M.Gurrero, "Grid-connected of Photovoltaic Module using non-linear control,"*3rd IEEE International symposium on Power Electronics for Distributed Generation system (PEDG)*, 2012.

[34] Waleed Al-Saedi , Stefan W. Lachowicz, Daryoush Habibi and Octavian Bass, "Power flow control in grid-connected micro-grid operation using Particle Swarm Optimization under variable load conditions", *ELSEVIER*, Electrical Power and Energy Systems 49 (2013), 76–85.

[35] Yong X, Jiamei D and Shuangbao M., " Power flow control of a distributed generation unit in micro-grid", *IEEE 6th international power electronics and motion control conference (IPEMC)*, 2009; 2009. p. 2122–5.

[36] Hirofumi Akagi, E. H. Watanabe and M.Aredes, "Instantaneous power theory and applications to power conditioning", Hoboken, NJ: Wiley, 2007.

[37] Arindam Ghosh and Gerard Ledwich, "Power quality enhancement using custom power devices", Springer, 2010.

[38] IEEE Recommended Practices and Requirements for Harmonics Control in Electric Power Systems, IEEE Standard 519, 1992.

APPENDIX

A. Parameters for 10 kWatt Solar Photovoltaic System

N = 1.3,

Number of series modules (N_s) = 10,

Number of parallel modules (N_p) = 4,

Series Resistance = 0.037998 ohms,

Parallel Series Resistance = 953.5 ohms,

Voltage at Pmax = 54.6*10 volt,

Current at Pmax = 4.7*4 amps.

B. Parameters for DC-DC Boost converter

Duty cycle (D) = 0.86,

Inductance (L) = 1.5 mH,

Capacitance (C) = 250 μF,

Switching frequency (fsw) = 10 kHz.

C. Parameters for VSC

DC bus voltage: 800V,

DC bus Capacitance: 1500μF,

AC inductor: L_a=L_b=L_c=1.1mH,

AC line voltage: 415V, 50Hz,

Switching frequency: 10KHz,

Modulation index: 0.9,

Line impedance: Rs=.05Ω, Ls=1mH,

Linear load: 15 kVA,

Non-linear load: Three phase bridge rectifier with R = 25 Ω and L = 300 mH.